

IDENTIFICATION OF HEAVY METAL TRANSPORTERS

A Dissertation

Presented to the Faculty of the Graduate School

of Cornell University

In Partial Fulfillment of the Requirements for the Degree of

Doctor of Philosophy

by

ZHIYANG ZHAI

August 2011

© 2011 ZHIYANG ZHAI  
ALL RIGHTS RESERVED

## IDENTIFICATION OF HEAVY METAL TRANSPORTERS

ZHIYANG ZHAI, Ph. D.

Cornell University 2011

Increased release of heavy metals of geogenic and anthropogenic origin has led to generation of multiple polluted sites in the USA and across the world that are waiting for efficient clean-up technologies. Phytoremediation uses plants to mitigate these types of environmental problems, and provides a cost-efficient and environmentally friendly alternative to existing remediation solutions. Application of phytoremediation relies on the understanding of mechanisms of heavy metal detoxification in plants. As one of the most important heavy metal detoxification mechanisms, the phytochelatin dependent pathway plays an essential role in detoxification and sequestration of heavy metals in plants, fungi and some nematodes. While the mechanism of phytochelatin biosynthesis has been well established, proteins mediating transport of phytochelatins and/or heavy metal phytochelatin complexes have eluded definition. My PhD research led to the following findings: firstly, it was found that *Arabidopsis* Oligopeptide Transporter 3 (OPT3) mediates transport of cadmium and contributes to shoot accumulation of glutathione and phytochelatins. Secondly, in collaboration with three other research groups, it was shown that an ATP-binding cassette transporter of *Schizosaccharomyces pombe*, Abc2, is the long-sought phytochelatin transporter on the vacuolar membrane. Identification of such transporter(s) greatly improves the understanding of heavy metal detoxification

mechanisms and provides promising bioengineering target(s) for phytoremediation applications. Thirdly, an efficient reverse genetic method was developed to study the function of genes of interest through RNA interference in plant protoplasts. The protocol has been developed for *Arabidopsis thaliana*; however, since protoplasts can be isolated from different tissues and different plant species, direct transfer of synthetic double stranded RNA into protoplasts can be employed as a gene-silencing tool to study tissue specific processes in a variety of species, and can be adapted to a high-throughput format.

## BIOGRAPHICAL SKETCH

### EDUCATION

Cornell University	Crop Science	Ph.D.	2011
Sun Yat-Sen University, China	Plant Biology	M.S.	2003
Henan Normal University, China	Biotechnology	B.S.	2000

### EXPERIENCE/APPOINTMENTS

Research Fellow, Root Biology Center of South China Agricultural University

06/2005-06/2007

Engineer, Guangzhou Landscape Gardening Institute 07/2003-07/2005

### PUBLICATIONS

1. **Zhai Z**, et al. (2011) *Arabidopsis thaliana* oligopeptide transporter 3 mediates long-distance root-to-shoot transport of cadmium. *Manuscript in preparation*.
2. Jung HI, **Zhai Z** and Vatamaniuk OK (2011). Direct Transfer of Synthetic Double-Stranded RNA into Protoplasts of *Arabidopsis thaliana*. In Kodama, Hiroaki and Komamine, Atsushi (Eds.), *RNAi and Plant Gene Function Analysis* (Vol.8) New York, U.S.A: Humana Press.
3. Mendoza-C ózatl DG, **Zhai Z**, Jobe TO, Akmakjian GZ, Song WY, Limbo O, Russell MR, Kozlovskyy VI, Martinoia E, Vatamaniuk OK, Russell P, Schroeder JI (2010). Tonoplast-localized Abc2 transporter mediates phytochelatin accumulation in vacuoles and confers cadmium tolerance. *J Biol Chem.*, 285(52):40416-26. Epub 2010 Oct 11.
4. **Zhai Z**, Jung HI, Vatamaniuk OK (2009). Isolation of protoplasts from tissues of 14-day-old seedlings of *Arabidopsis thaliana*. *J Vis Exp.*, 17;(30). pii: 1149. doi:

10.3791/1149.

5. **Zhai Z**, Sooksa-nguan T, Vatamaniuk OK (2009). Establishing RNA interference as a reverse-genetic approach for gene functional analysis in protoplasts. *Plant Physiology*, 149(2):642-52. Epub 2008 Nov 12.
6. **Zhai Z**, Wu Y, Engelmann F, Chen R, Zhao Y (2003). Genetic stability assessments of plantlets regenerated from cryopreserved *in vitro* cultured grape and kiwi shoot-tips using RAPD. *Cryo Letters*, 24(5):315-22.

## ACKNOWLEDGMENTS

I would like to thank Dr. Olena K. Vatamaniuk for her every-step instruction during my last four years' research and the opportunity of systematic and intense training in plant physiology, molecular biology and biochemistry. I appreciate her introduction of me into the American Society of Plant Biology. I greatly appreciate her support for my research ideas and tolerance to my different opinions during research discussion.

I also would like to thank Dr. Jian Hua, Dr. Leon Kochian and Dr. Klaas van Wijk for their constructive advice in my research, Dr. David Salt (Purdue University) and his lab members: Brett Lahner and John Danku for ICP-MS analyses of plant and yeast samples, Dr. Ha-il Jung (Vatamaniuk's lab) for the help in studies of subcellular localization of OPT3 in protoplasts and in generating transgenic plants, Sheena Gayomba (Vatamaniuk's lab) and Matt Milner (Kochian's lab) for helping with *S. cerevisiae* uptake studies, Zhilong Bao and Mingyue Gou (Hua's lab) for helping to produce *opt3-3cad1-3* double mutant and transgenic plants, Dr. Michael Scanlon and his lab member: Margaret Frank for helping to perform *A. thaliana* tissue sectioning, all my labmates in Vatamaniuk's lab: Anuj Sharma, Sarwat Ismail, and Sungjin Kim for support in my research, Dr. Walter Gassmann (University of Missouri) for kindly providing yeast ABC822 strain.

I particularly thank my wife Hui Liu for her help in the vertical plate assay, hydroponic experiments, grafting, genotyping, sample preparation, and HPLC.

This dissertation is dedicated to my dear wife Hui Liu and my dear parents for their consistent support and considerate love.



## TABLE OF CONTENTS

Biographical Sketch . . . . .	iii
Acknowledgements . . . . .	v
Dedication . . . . .	vi
Table of Contents . . . . .	vii
List of Figures . . . . .	ix
List of Tables . . . . .	xii
List of Abbreviations. . . . .	1
Reface . . . . .	2
References. . . . .	10
Chapter 1 <i>Arabidopsis thaliana</i> Oligopeptide Transporter 3 (OPT3) mediates root-to-shoot long-distance transport of cadmium . . . . .	15
Abstract. . . . .	15
Introduction . . . . .	16
Results. . . . .	19
Discussion. . . . .	36
Materials and Methods . . . . .	40
References. . . . .	46
Chapter 2 <i>Schizosaccharomyces pombe</i> Abc2 transporter mediates phytochelatin accumulation in vacuoles and confers cadmium tolerance. . . . .	54
Abstract. . . . .	54
Introduction. . . . .	54
Results and Discussion. . . . .	57

Materials and Methods. . . . .	.59
References. . . . .	.62

Chapter 3 Establishing RNA Interference as a Reverse-Genetic Approach for Gene

Functional Analysis in Protoplasts. . . . .	.65
Abstract . . . . .	65
Introduction . . . . .	66
Results. . . . .	70
Conclusion and Future perspective . . . . .	83
Materials and Methods . . . . .	87
References . . . . .	92

## LIST OF FIGURES

### Introduction

**Figure 1** PC dependent intracellular heavy metal detoxification in plants.

**Figure 2** Over-expression of *AtPCS1* in wild type *Arabidopsis* cannot increase tolerance to Cd.

### Chapter 1 *Arabidopsis thaliana* Oligopeptide Transporter 3 (OPT3) mediates root-to-shoot long-distance transport of cadmium.

**Figure 1.** Phylogenetic relationships between *A. thaliana* OPT family members.

**Figure 2.** Roots of seedlings of *OPT3* knockdown mutants, *opt3-2* and *opt3-3*, are sensitive to Cd.

**Figure 3.** Phenotype of wild-type and *opt3-3* plants.

**Figure 4.** Leaves of *opt3-3* mature plants are more tolerant to Cd.

**Figure 5.** Complementation of *opt3-3* mutant with genomic fragment containing *OPT3*.

**Figure 6.** Expression of *OPT3* is responsive to Cd.

**Figure 7.** Cd, Fe, PCs and GSH concentrations in leaves and roots of Col-0 and *opt3-3* without (-Cd) or with exposure to 25  $\mu$ M of Cd for 3 days (+Cd).

**Figure 8.** Cd, Fe, Cu, Zn and Mn concentrations in leaves and roots of Col-0 and *opt3-3* under normal hydroponic condition (-Cd) or with 3-day exposure of 25  $\mu$ M of Cd (+Cd) in hydroponic culture media.

**Figure 9.** Expression of *OPT3* in leaves is 10-fold higher than in roots.

**Figure 10.** Sensitivity of reciprocally grafted wild-type and *opt3-3* mutant to Cd.

**Figure 11.** Subcellular localization and tissue-specificity of *OPT3* expression.

**Figure 12.** Sensitivity of *opt3-3cad1-3* double mutant to different concentration of Cd.

**Figure 13.** Growth assay of ABC822 (*opt1Δ*) strain transformed with pYES3-*OPT3* (*OPT3*), pYES3-*OPT3(-N)* (*OPT3(-N)*), pYES3-*ScOPT1* (*ScOPT1*) or empty pYES3 (empty) construct.

**Figure 14.** Time course of [<sup>32</sup>S] GSH uptake by the ABC822 (*opt1Δ*) strain transformed with the empty pYES3 vector, the pYES3-*OPT3* or pYES3-*ScOPT1* construct in a uptake medium containing 100 μM [<sup>32</sup>S]GSH.

**Figure 15.** Cd sensitivity assay of ABC822 strain (*Δopt1* mutant) transformed with empty pYES3 or pYES3-*OPT3* construct on SC media supplemented with 100 μM of Cd.

**Figure 16.** <sup>109</sup>Cd uptake by the ABC822 (*opt1Δ*) strain transformed with the empty pYES3 empty vector or the pYES3-*OPT3* construct in uptake medium contained 25 μM of <sup>109</sup>Cd for 5 minutes.

**Figure 17.** The model of OPT3-mediated transport of Cd.

## **Chapter 2 *Schizosaccharomyces pombe* Abc2 transporter mediates phytochelatin accumulation in vacuoles and confers cadmium tolerance.**

**Figure 1.** PC accumulation in vacuoles was decreased in the *hmt1* mutant and abolished in the *abc1-4 hmt1* quintuple and the *abc2 hmt1* double mutant. Expression of Abc2 in the *abc1-4 hmt1* quintuple mutant restored the accumulation of PCs in vacuoles.

**Figure 2.** HMWCs in purified vacuoles from *S. pombe* wild type (A, open circles)

have an identical elution pattern compared with a HMWC standard synthesized *in vitro* (**B**). Vacuoles isolated from the *hmt1* mutant showed reduced content of HMWCs (**A**, *filled circles*) whereas no HMWCs were detected in purified vacuoles isolated from the *abc2 hmt1* double mutant (**A**, *open squares*).

### **Chapter 3 Establishing RNA Interference as a Reverse-Genetic Approach for Gene Functional Analysis in Protoplasts.**

**Figure 1.** Isolation of protoplasts from *Arabidopsis* seedlings.

**Figure 2.** The visualization of the efficiency of the transfection of protoplasts with the pSAT vector expressing nuclear-localized EGFP.

**Figure 3.** Silencing of the exogenous gene, *EGFP*, in protoplasts by RNAi.

**Figure 4.** Dose and time dependence of transient RNAi silencing of *PCSI* in protoplasts.

**Figure 5.** Simultaneous interference with the expression of *HXK1* and *HXK2* in protoplasts by RNAi.

**Figure 6.** Gene-specific interference with the expression of *HXK1* and *HXK2*.

**Figure 7.** Gene-specific and simultaneous interference with the expression of *HXK1* and *HXK2* using PCR-linked UTR regions as dsRNA templates.

**Figure 8.** RNAi silencing of *ECS1* in protoplasts interferes with the expression of *ECS1* RNA and polypeptide, and decreases the ability of protoplasts to accumulate GSH.

## LIST OF TABLES

### Chapter 1

**Table 1.** Root-to-leaf leaf partitioning of GSH, PCs, Cd, Fe, Cu, Zn, and Mn in Col-0 and *opt3-3* plants under normal growth condition (-Cd) or after 3-day exposure to 25  $\mu$ M of Cd in hydroponic culture media (+Cd).

**Table 2.** Primers used in this research.

### Chapter 2

**Table 1** *Schizosaccharomyces pombe* strains used in this study.

### Chapter 3

**Table 1.** Comparison of the relative abundance of transcripts in protoplasts after RNAi using different DNA templates.

**Table 2.** List of oligos that were used to amplify DNA templates for *in vitro* dsRNA synthesis.

**Table3.** List of oligos that were used for RT-PCR analyses.

## LIST OF ABBREVIATIONS

ABC	ATP-Binding Cassette
Cd	Cadmium
GSH	Glutathione
NA	Nicotianamine
OPT	Oligopeptide Transporter
PC	Phytochelatin
PCS	Phytochelatin Synthase
$\gamma$ -EC	$\gamma$ -Glutamine-cysteine
RNAi	RNA interference
WT	Wild type
MT	Metallothionein

## PREFACE

Although heavy metals (metallic chemical elements with a density greater than 5 g/cm<sup>3</sup>) are natural components of the Earth's crust, they have increasingly been released into the environment as industrial and consumer wastes (Lasat, 2002; Omichinski, 2007). High concentrations of heavy metals pose a serious environmental concern. In fact, cadmium (Cd), mercury (Hg), lead (Pb), and metalloid arsenic (As) are among the 10 most hazardous substances in the 2007 PRIORITY LIST of CERCLA (Comprehensive Environmental Response, Compensation, and Liability Act) (<http://www.atsdr.cdc.gov/cercla/index.html>). Traditional heavy metal remediation removes the contaminant material by physical or chemical means. In contrast, phytoremediation uses plants to mitigate environmental problems, emerging as a cost-efficient and environmentally friendly alternative to existing remediation solutions. However, developing plants for phytoremediation applications requires understanding of the fundamental molecular mechanisms that allow plants to absorb, detoxify, redistribute, and accumulate heavy metals.

Among existing metal detoxification mechanisms, the phytochelatin (PC)-dependent pathway plays an important role in heavy metal detoxification in plants, algae, nematodes (*e.g. Caenorhabditis elegans*), and fungi (*e.g. Schizosaccharomyces pombe*) (Grill et al., 1985; Mutoh and Hayashi, 1988; Hayashi et al., 1991; Clemens et al., 2001; Vatamaniuk et al., 2001). Although the precise mechanism of the biosynthesis of PCs in plant cells has been well established (Grill, 1989; Clemens et al., 1999; Ha et al., 1999; Vatamaniuk, 1999; Vatamaniuk et al., 2000; Vatamaniuk et



al., 2004; Romanyuk et al., 2006), the molecular machinery driving the transport of Cd-PC complexes as well as free Cd ions across plasma and vacuolar membranes is still not well understood.

The purpose of this research is to use *A. thaliana* and *S. pombe* as models for identifying transport proteins that are responsible for the vacuolar sequestration and long-distance transport of Cd and/or Cd-PC complexes. The ultimate goal of the research is to generate novel tools for phytoremediation applications and develop heavy metal-safe crops that contain negligible amount of non-essential heavy metals in edible organs when grown in a heavy metal polluted field.

### **Heavy metal toxicity and tolerance mechanisms in plants**

At the cellular level, the toxicity of heavy metals results from the displacement of endogenous co-factors (like zinc) from their cellular binding sites, thiol-capping of essential proteins, and promotion of the formation of reactive oxygen species (ROS) (Hall, 2002). In order to maintain the concentration of essential metals within physiological limits and to minimize the toxic effects of nonessential metals, plants have evolved a complex network of homeostatic mechanisms that control the uptake and detoxification of metals. For most of plants, basic metal tolerance mechanisms are ubiquitous and include chelation, compartmentalization, and elimination as well as ROS detoxification. Chelation involves binding of heavy metals by cellular ligands. It was found that cysteine-rich peptides and proteins: glutathione (GSH), phytochelatins (PCs) and metallothionein (MT), respectively, can chelate and detoxify heavy metals in plants, some fungi and certain nematodes (Cobbett and Goldsbrough, 2002).

Compartmentalization points to sequestration of ligand-heavy metal complexes or free ions into subcellular compartments. Elimination is the transport of ligand-heavy metal complexes or free ions out of cells. ROS detoxification involves either blocking ROS generation or neutralizing ROS. All of these mechanisms ensure that the concentration of toxic heavy metals in the cell is maintained below the threshold of toxicity.

### **The prominent role of phytochelatins**

Compared with MT, PCs are more important because loss-of-function of PC synthase (PCS) in *A. thaliana* makes plants extremely sensitive to cadmium as well as to other metals and metalloids (Howden et al., 1995), while *Arabidopsis* plants that lack MT1a and MT2b, two major MTs that are expressed in phloem, exhibit normal Cu and Cd tolerance (Guo et al., 2008).

PCs are small, metal-binding peptides with the general structure  $(\gamma\text{-Glu-Cys})_n\text{-Gly}$  ( $n=2\text{-}11$ ) (Kondo et al., 1984; Grill et al., 1985; Jackson et al., 1987). They have been found in virtually all plants, algae, certain fungi and the nematode *C. elegans* (Grill et al., 1985; Mutoh and Hayashi, 1988; Hayashi et al., 1991; Clemens, 2001; Vatamaniuk et al., 2001). PCs are synthesized from glutathione (GSH) and related thiols by PC synthases (PCS, *alias*  $\gamma$ -glutamylcysteine dipeptidyl transpeptidases (EC 2.3.2.15) that in the presence of heavy metals transfers  $\gamma$ -glutamylcysteinyl moiety from one molecule of GSH, or previously synthesized PCs, onto the N-terminus of GSH or PCs to generate polymers containing 2-11  $\gamma$ -Glu-Cys repeats, followed by C-terminus Gly (Grill, 1989; Vatamaniuk et al., 2000; Vatamaniuk et al., 2004). Once produced, PCs efficiently chelate Cd and other heavy metals and form the low-

molecular-weight cytosolic PC-Cd complexes, which are transported into the vacuole where the high-molecular-weight complexes are formed and stabilized by incorporation of inorganic  $S^{2-}$  (Ortiz et al., 1992; Speiser et al., 1992; Vande Weghe and Ow, 2001) (Figure 1).

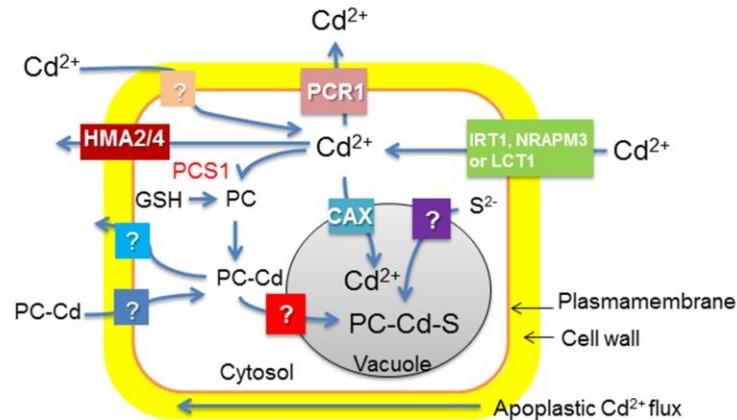


**Figure 1. Cadmium transport pathway in the plant cell.** In plants, Cd is taken up into the cell, presumably through the plasma membrane-localized iron transporters, IRT1, NRAMP3, or  $Ca^{2+}$  channel, LCT1 (Clemens et al., 1998; Thomine et al., 2000; Vert et al., 2002). In the cell, Cd promotes formation of different chain length phytochelatins (PCs) by PC synthase (PCS1)-mediated transpeptidation of GSH (Vatamaniuk et al., 2000; Vatamaniuk et al., 2004). PCs chelate cytosolic Cd and form low molecular weight complexes (Cd-PC). These complexes are sequestered into the vacuole by unknown transporter(s). In the vacuole, PCs are complexed with inorganic sulfide ( $S^{2-}$ ) to form stable high molecular weight complexes (PC-Cd-S). PC-Cd complex may also be transported across the plasma membrane via the activity of unidentified transporters. Free Cd ions can also be directly expelled by PCR1 (Song et al., 2004) or sequestered into the vacuole via the proton antiport activity of CAX-like proteins (Shigaki and Hirschi, 2000), or loaded into xylem by  $P_{IB}$ -Type ATPase, HMA2/4 (Wong and Cobbett, 2009), or re-absorbed from xylem. Question marks indicate unknown transporters. Besides the symplastic pathway of the Cd transport, Cd is also transported through the apoplastic pathway.

Beside vacuolar compartmentalization, PCs also facilitate long-distance transport of Cd. Research in *A. thaliana* has shown that PCs undergo the root-to-shoot long-distance transport (Gong et al., 2003). Further research from the same lab showed that

significant amount of PC<sub>2</sub> can be also transported from shoot to root in *A. thaliana* (Chen et al., 2006). In another species, *Brassica napus*, phloem plays a predominant role in long-distance transport of Cd as PC-Cd and glutathione-Cd complexes (Mendoza-Cozatl et al., 2008).

Considering the importance of the PC-dependent pathway for heavy metal detoxification, it was suggested as a tool for engineering plants for phytoremediation. The question is whether enhanced biosynthesis of PC would increase both tolerance and accumulation of heavy metals. The answer is yes, at least in yeast, the single cell eukaryote. Expression of *AtPCSI* (*A. thaliana* **PC** synthase) in *S. cerevisiae* cells significantly increases their tolerance and accumulation of Cd, As and Pb (Vatamaniuk, 1999). However, over-expression of *AtPCSI* in wild-type *Arabidopsis* did not increase tolerance to Cd even though it increased PC content at higher concentrations of Cd (Figure 2). This finding suggests that in higher plants, enhancing chelation of heavy metal is not sufficient for detoxification. We hypothesize that enhanced activity of PC-Cd transporters that facilitate the root-to-shoot translocation and vacuolar sequestration of Cd, is also needed for efficient heavy metal detoxification and accumulation in harvestable organs.

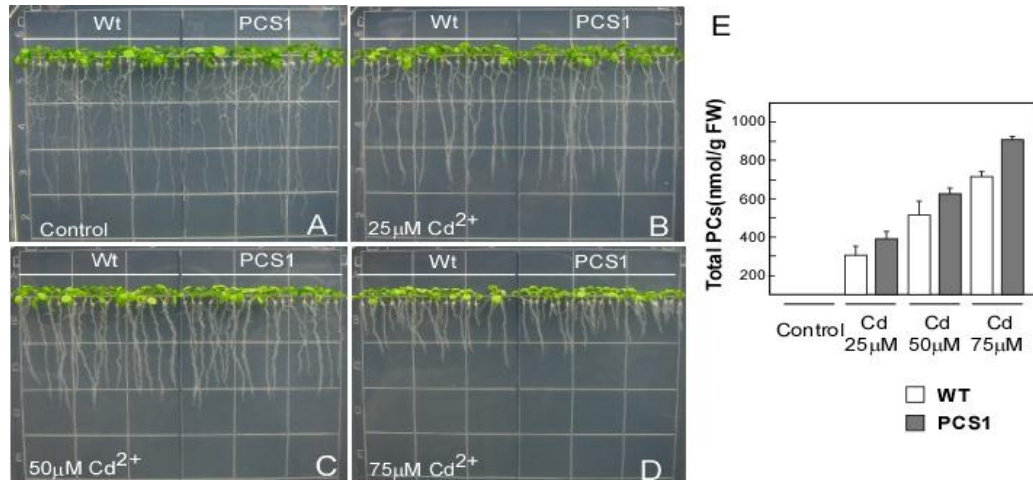


**Figure 2. Over-expression of *AtPCS1* in wild type *A. thaliana* does not increase tolerance to Cd.** A-D, wild-type (Wt) and *AtPCS1* overexpressing plants (PCS1) were grown vertically on 1/2 MS solid medium supplemented with the indicated concentrations of Cd; E, Reverse-phase (RP)-HPLC analysis of total PCs content in 10-day-old seedlings of wild-type (WT) and *AtPCS1* transgenic plants (PCS1) cultured at different concentrations of Cd. PC content was below detection limits in plants that grew in standard (without Cd) conditions.

### Transporters for Cd and Cd-PC complexes

It has been shown that in *A. thaliana* Cd can be taken up by a multi specific transporter of the ZIP family, IRT1 (Vert et al., 2002), while P-type ATPases HMA2 and HMA4 are involved in loading of Cd into xylem (Wong and Cobbett, 2009) (Fig. 1). However, how Cd is reabsorbed from xylem into leaves and which transporters are involved in either vacuolar sequestration or long-distance transport of heavy metal-PC complexes is not known (Fig. 1). We are particularly interested in Cd-PC transporters because in the whole process of Cd tolerance, PCs serve as both Cd detoxicants and carriers. It has been suggested that transport of PC-Cd complexes across the vacuolar membrane is mediated by ATP-binding cassette (ABC) transporter(s) (Salt and Rauser, 1995), while some members of the *A. thaliana* Oligopeptide Transporters family

(OPT) have been shown to mediate transport of GSH and PC<sub>2</sub> when expressed in a heterologous system (Bourbouloux et al., 2000; Osawa et al., 2006).

ABC transporters. Proteins are classified as ABC transporters based on the sequence homology and organization of their ATP-binding domain(s), also known as nucleotide-binding folds (NBFs). Each NBF encompasses approximately 200 amino acid residues and contains three defining sequence motifs. These are a Walker A box and Walker B box separated by approximately 120 amino acid residues, and an ABC signature (alias C) motif situated between the two Walker boxes (Rea, 2007). The functional protein typically contains two NBFs and two transmembrane domains (TMDs). The TMDs contain 6–11 membrane-spanning  $\alpha$ -helices and mediate translocation of molecules across the lipid bilayer (Rea, 2007). The NBFs are located in the cytoplasm and bind ATP and use the energy of ATP hydrolysis to drive the substrate transport across membrane (Rea, 2007). In *Schizosaccharomyces pombe*, HMT1, a half-molecule ABC transporter (comprising only one NBF and one TMD) had been long believed to be the Cd-PC transporter on the vacuolar membrane because: first, it is vacuolar membrane localized; second, *S. pombe hmt1* mutant cells are hypersensitive to Cd; third, vacuolar membrane enriched vesicles isolated from *S. pombe hmt1* mutant cells overexpressing SpHMT1 conferred Cd-PC transport *in vitro* (Ortiz, 1995). Although the *A. thaliana* genome encodes 129 ABC proteins, it lacks the HMT1 orthologue (Sanchez-Fernandez et al). Interestingly, orthologs of HMT1 are present in animals including *Drosophila* and humans, which do not possess PC synthase machinery. That raised the question that either HMTs' functions have diverged in different species or they function in metal detoxification by another

mechanism. Our genetic studies of CeHMT1, an SpHMT1 ortholog in *C. elegans*, and biochemical studies of HMT1 of *Drosophila* and *S. pombe*, showed that HMTs' function in Cd detoxification is conserved in different species, but that they are not *bona fide* Cd-PC transporters, and while they may mediate Cd-PC transport, they function in heavy metal tolerance by another unknown mechanism (Vatamaniuk et al 2005, Sooksa-nguan et al, 2009). Data from our lab were further complemented by that of our colleagues that showed that SpHMT1 confers Cd tolerance independently of PC synthase (Preveral, 2009). Therefore, the identity of vacuolar membrane Cd-PC transporter(s) in plants, *S. pombe* and *C. elegans* is unknown.

OPTs. *Arabidopsis* genome has 9 members of the oligopeptide transporters, OPT1-OPT9. OPT homologs have also been identified in yeast and other plant species. Members of the OPT family are predicted to have 12 to 14 transmembrane domains and contain two conserved motifs (NPG and KIPPR) (Koh et al., 2002). This family was named so because some members of this family were shown to transport oligopeptides *in vitro*. For example *Saccharomyces cerevisiae* OPT1 (ScOPT1) was shown to transport reduced GSH, oxidized GSH (GSSG), GSH conjugates and phytochelatins, PC<sub>2</sub> (Bourbouloux et al., 2000; Osawa et al., 2006).

Although substantial efforts have been made to isolate vacuolar Cd-PC transporters, their identity still remains unknown. Besides the enigma regarding vacuolar PC-Cd transporters, the identity of plasma membrane Cd and Cd-PC transporters that facilitate long-distance transport between different organs is unknown as well.

The goal of my PhD research was to identify vacuolar membrane and/or

plasma membrane localized Cd-PC transporters and other novel proteins involved in Cd transport using two model species: *A. thaliana* and *S. pombe*. In seeking novel, time-, labor- and cost-efficient approaches for identifying heavy metal-PC transporters, An RNA interference in protoplasts technique was developed as an alternative method for gene functional analysis.

## REFERENCES

- Bourbouloux A, Shahi P, Chakladar A, Delrot S, Bachhawat AH** (2000) Hgt1p, a high affinity glutathione transporter from the yeast *Saccharomyces cerevisiae*. *Journal of Biological Chemistry* **275**: 13259-13265
- Chen A, Komives EA, Schroeder JI** (2006) An improved grafting technique for mature *Arabidopsis* plants demonstrates long-distance shoot-to-root transport of phytochelatin in *Arabidopsis*. *Plant physiology* **141**: 108-120
- Clemens S, Antosiewicz DM, Ward JM, Schachtman DP, Schroeder JI** (1998) The plant cDNA LCT1 mediates the uptake of calcium and cadmium in yeast. *Proceedings of the National Academy of Sciences of the United States of America* **95**: 12043
- Clemens S, Kim EJ, Neumann D, Schroeder JI** (1999) Tolerance to toxic metals by a gene family of phytochelatin synthases from plants and yeast. *Embo J* **18**: 3325-3333
- Clemens S, Schroeder J, Degenkolb T** (2001) *Caenorhabditis elegans* expresses a functional phytochelatin synthase. *Eur J Biochem.* **268**: 3640-3643
- Clemens S, Schroeder, J. I., Degenkolb, T.** (2001) *Caenorhabditis elegans* expresses a functional phytochelatin synthase. *Eur J Biochem* **268**: 3640-3643
- Cobbett C, Goldsbrough P** (2002) Phytochelatin and metallothioneins: roles in heavy metal detoxification and homeostasis. *Plant Biology* **53**: 159-182



- Gong JM, Lee DA, Schroeder JI** (2003) Long-distance root-to-shoot transport of phytochelatins and cadmium in Arabidopsis. Proceedings of the National Academy of Sciences of the United States of America **100**: 10118-10123
- Grill E, Löffler, S., Winnacker, E. L., Zenk, M. H.** (1989) Phytochelatins, the heavy-metal-binding peptides of plants, are synthesized from glutathione by a specific gamma-glutamylcysteine dipeptidyl transpeptidase (phytochelatin synthase). Proc Natl Acad Sci U S A **86**: 6838-6842
- Grill E, Winnacker EL, Zenk MH** (1985) Phytochelatins - the Principal Heavy-Metal Complexing Peptides of Higher-Plants. Science **230**: 674-676
- Grill E, Winnacker EL, Zenk MH** (1985) Phytochelatins: The Principal Heavy-Metal Complexing Peptides of Higher Plants. Science **230**: 674-676
- Guo WJ, Meenam M, Goldsbrough PB** (2008) Examining the specific contributions of individual Arabidopsis metallothioneins to copper distribution and metal tolerance. Plant Physiology **146**: 1697-1706
- Ha SB, Smith AP, Howden R, Dietrich WM, Bugg S, O'Connell MJ, Goldsbrough PB, Cobbett CS** (1999) Phytochelatin synthase genes from Arabidopsis and the yeast Schizosaccharomyces pombe. Plant Cell **11**: 1153-1163
- Hall JL** (2002) Cellular mechanisms for heavy metal detoxification and tolerance. Journal of Experimental Botany **53**: 1-11
- Hayashi Y, Isobe M, Mutoh N, Nakagawa CW, Kawabata M** (1991) Cadystins: small metal-binding peptides. Methods Enzymol **205**: 348-358
- Howden R, Goldsbrough PB, Andersen CR, Cobbett CS** (1995) Cadmium-Sensitive, Cad1 Mutants of Arabidopsis-Thaliana Are Phytochelatin Deficient. Plant Physiology **107**: 1059-1066
- Jackson PJ, Unkefer CJ, Doolen JA, Watt K, Robinson NJ** (1987) Poly(Gamma-Glutamylcysteinyl)Glycine - Its Role in Cadmium Resistance in Plant-Cells.

Proceedings of the National Academy of Sciences of the United States of America **84**: 6619-6623

**Koh S, Wiles AM, Sharp JS, Naider FR, Becker JM, Stacey G** (2002) An oligopeptide transporter gene family in Arabidopsis. *Plant Physiology* **128**: 21-29

**Kondo N, Imai K, Isobe M, Goto T, Murasugi A, Wadanakagawa C, Hayashi Y** (1984) Cadystin-a and Cadystin-B, Major Unit Peptides Comprising Cadmium Binding Peptides Induced in a Fission Yeast ----- Separation, Revision of Structures and Synthesis. *Tetrahedron Letters* **25**: 3869-3872

**Lasat MM** (2002) Phytoextraction of toxic metals. *J. Environ. Qual.* **31**: 109-120

**Mendoza-Cozatl DG, Butko E, Springer F, Torpey JW, Komives EA, Kehr J, Schroeder JI** (2008) Identification of high levels of phytochelatin, glutathione and cadmium in the phloem sap of Brassica napus. A role for thiol-peptides in the long-distance transport of cadmium and the effect of cadmium on iron translocation. *Plant Journal* **54**: 249-259

**Mutoh N, Hayashi Y** (1988) Isolation of mutants of *Schizosaccharomyces pombe* unable to synthesize cadystin, small cadmium-binding peptides. *Biochem. Biophys. Res. Commun.* **151**: 32-39

**Omichinski JG** (2007) Toward methylmercury bioremediation. *Science* **317**: 205-206

**Ortiz DF, Kreppel L, Speiser DM, Scheel G, McDonald G, Ow DW** (1992) Heavy metal tolerance in the fission yeast requires an ATP-binding cassette-type vacuolar membrane transporter. *EMBO J.* **11**: 3491-3499

**Ortiz DF, Ruscitti, T., McCue, K.F., Ow, D. W.** (1995) Transport of Metal-binding Peptides by HMT1, A Fission Yeast ABC-type Vacuolar Membrane Protein. *J. Biol. Chem.* **270**: 4721-4728

**Osawa H, Stacey G, Gassmann W** (2006) ScOPT1 and AtOPT4 function as proton-coupled oligopeptide transporters with broad but distinct substrate specificities. *Biochemical Journal* **393**: 267-275

**Preveral S, Gayet, L., Moldes, C., Hoffmann, J., Mounicou, S., Gruet, A.,**

**Reynaud, F., Lobinski, R., Verbavatz, J. M., Vavasseur, A., Forestier, C.** (2009) A common highly-conserved cadmium detoxification mechanism from bacteria to humans. Heavy metal tolerance conferred by the ABC transporter SpHMT1 requires glutathione but not metal-chelating phytochelatin peptides. *J Biol Chem*: 4936-4943

**Rea PA** (2007) Plant ATP-binding cassette transporters. *Annu Rev Plant Biol* **58**: 347-375

**Romanyuk ND, Rigden DJ, Vatamaniuk OK, Lang A, Cahoon RE, Jez JM, Rea PA** (2006) Mutagenic definition of a papain-like catalytic triad, sufficiency of the N-terminal domain for single-site core catalytic enzyme acylation, and C-terminal domain for augmentative metal activation of a eukaryotic phytochelatin synthase. *Plant Physiol* **141**: 858-869

**Salt DE, Rauser WE** (1995) MgATP-Dependent Transport of Phytochelatin Across the Tonoplast of Oat Roots. *Plant Physiol* **107**: 1293-1301

**Shigaki T, Hirschi K** (2000) Characterization of CAX-like genes in plants: implications for functional diversity. *Gene* **257**: 291-298

**Song WY, Martinoia E, Lee J, Kim D, Kim DY, Vogt E, Shim D, Choi KS, Hwang I, Lee Y** (2004) A novel family of cys-rich membrane proteins mediates cadmium resistance in Arabidopsis. *Plant Physiology* **135**: 1027-1039

**Sooksa-Nguan T, Yakubov B, Kozlovskyy VI, Barkume CM, Howe KJ, Thannhauser TW, Rutzke MA, Hart JJ, Kochian LV, Rea PA, Vatamaniuk OK** (2009) Drosophila ABC transporter, DmHMT-1, confers tolerance to cadmium. DmHMT-1 and its yeast homolog, SpHMT-1, are not essential for vacuolar phytochelatin sequestration. *J Biol Chem* **284**: 354-362

**Speiser DM, Ortiz DF, Kreppel L, Scheel G, McDonald G, Ow DW** (1992) Purine biosynthetic genes are required for cadmium tolerance in *Schizosaccharomyces pombe*. *Mol Cell Biol* **12**: 5301-5310

**Thomine S, Wang R, Ward JM, Crawford NM, Schroeder JI** (2000) Cadmium and iron transport by members of a plant metal transporter family in Arabidopsis with homology to Nramp genes. *Proceedings of the National*

Academy of Sciences of the United States of America **97**: 4991-4996

**Vande Weghe JG, Ow DW** (2001) Accumulation of metal-binding peptides in fission yeast requires hmt2+. *Mol Microbiol* **42**: 29-36

**Vatamaniuk OK, Bucher EA, Ward JT, Rea PA** (2001) A new pathway for heavy metal detoxification in animals. Phytochelatin synthase is required for cadmium tolerance in *Caenorhabditis elegans*. *J Biol Chem* **276**: 20817-20820

**Vatamaniuk OK, Bucher EA, Ward JT, Rea PA** (2001) A new pathway for heavy metal detoxification in animals. Phytochelatin synthase is required for cadmium tolerance in *Caenorhabditis elegans*. *J Biol Chem* **276**: 20817-20820

**Vatamaniuk OK, Mari S, Lang A, Chalasani S, Demkiv LO, Rea PA** (2004) Phytochelatin synthase, a dipeptidyltransferase that undergoes multisite acylation with gamma-glutamylcysteine during catalysis: stoichiometric and site-directed mutagenic analysis of *Arabidopsis thaliana* PCS1-catalyzed phytochelatin synthesis. *J Biol Chem* **279**: 22449-22460

**Vatamaniuk OK, Mari S, Lu YP, Rea PA** (2000) Mechanism of heavy metal ion activation of phytochelatin (PC) synthase: blocked thiols are sufficient for PC synthase-catalyzed transpeptidation of glutathione and related thiol peptides. *J Biol Chem* **275**: 31451-31459

**Vatamaniuk OK, Mari S., Lu, Y. P., Rea, P. A.** (1999) AtPCS1, a phytochelatin synthase from *Arabidopsis*: isolation and in vitro reconstitution. *Proc Natl Acad Sci U S A* **96**: 7110-7115

**Vert G, Grotz N, Dedaldechamp F, Gaymard F, Guerinot ML, Briat JF, Curie C** (2002) IRT1, an *Arabidopsis* transporter essential for iron uptake from the soil and for plant growth. *The Plant Cell Online* **14**: 1223-1233

**Wong CKE, Cobbett CS** (2009) HMA P-type ATPases are the major mechanism for root-to-shoot Cd translocation in *Arabidopsis thaliana*. *New Phytologist* **181**: 71-78

## CHAPTER 1

### *Arabidopsis thaliana* Oligopeptide Transporter 3 (OPT3) Mediates Long-distance Root-to-shoot Transport of Cadmium

Zhiyang Zhai et al. *Manuscript in preparation.*

#### ABSTRACT

Long-distance transport of heavy metals from root to shoot is an important part of metal homeostasis in plants. While it was shown that cadmium (Cd) and its complexes with the thiol-rich oligopeptides, phytochelatins (PCs), undergo long-distance transport in *A. thaliana*, the specific plasma membrane-localized transporters responsible for loading and re-absorption of Cd and/or Cd-PC from the xylem, are not known. Here we found that a member of the oligopeptide transporter family (OPT) in *A. thaliana*, OPT3, plays a significant role in root-to-shoot translocation of cadmium (Cd). We showed that roots of the Cd-grown *A. thaliana* OPT3 knockdown (*opt3-3*) mutant are more sensitive to Cd while its leaves are more tolerant to Cd than corresponding tissues of Cd-grown wild-type *A. thaliana*. Also, leaves of the Cd-cultured *opt3-3* plants accumulate less, but roots accumulate more Cd, PCs and glutathione (GSH) than corresponding tissues in wild-type plants. Reciprocal grafting experiments with *opt3-3* and wild-type plants revealed that Cd sensitivity of leaves of the grafted plants is determined by the OPT3 function in shoots, not in roots. We also showed that *OPT3* is expressed in the xylem parenchyma in the petioles and leaves and that the corresponding polypeptide resides on the plasma membrane. Consistent

with the role of OPT3 in Cd transport, its expression in the *Δopt1* mutant of *S. cerevisiae* increases its Cd sensitivity and facilitates Cd, but not GSH uptake *in vitro*. Studies of the relationship between *OPT3* and *PCSI*, encoding PC synthase, showed that *OPT3* and *PCSI* do not act in a simple linear heavy metal tolerance pathway. Based on the above, we conclude that OPT3 contributes to Cd accumulation in leaves by re-absorbing Cd from xylem. This is the first OPT with demonstrable function in ion transport and the first transporter with shown function in re-absorbing Cd ions from xylem into leaves.

## INTRODUCTION

Heavy metals are defined as metals that have density of more than  $5 \text{ g cm}^{-3}$ . Some heavy metals (*e.g.* iron [Fe], copper [Cu]) are micronutrients, but are toxic in excess. Nonessential heavy metals (*e.g.* cadmium [Cd], mercury [Hg] and lead [Pb]) are potentially toxic even at low concentrations (Waalkes, 2000; Waisberg, 2003). At the cellular level, the toxicity of heavy metals results from the displacement of endogenous co-factors (*e.g.* Cu and zinc [Zn]) from their cellular binding sites, thiol-capping of essential proteins, and promotion of the formation of reactive oxygen species (ROS) (Stadtman, 1990).

In order to maintain the concentration of essential metals within physiological limits and to minimize the detrimental effects of nonessential metals, plants have evolved a network of mechanisms that control the uptake, accumulation, transport and detoxification of metals (Clemens, 2001). In case of Cd exposure, Cd is taken up into the cell presumably through the plasma membrane-localized iron transporters, IRT1,

NRAMP3 or Ca<sup>2+</sup> channel, LCT1 (Clemens et al., 1998; Thomine et al., 2000; Vert et al., 2002). In the cell, Cd promotes formation of different chain length phytochelatins (PCs) by PC synthase (PCS1)-mediated transpeptidation of GSH (Grill, 1989; Howden et al., 1995; Clemens et al., 1999; Ha et al., 1999; Vatamaniuk, 1999; Vatamaniuk et al., 2000; Vatamaniuk et al., 2004; Romanyuk et al., 2006). PCs chelate cytosolic Cd and form low molecular weight complexes (Cd-PC). These complexes are sequestered into the vacuole. It was recently shown that *S. pombe* Abc2 mediates phytochelatin accumulation in vacuoles (Mendoza-Cozatl et al., 2010). Its homologs in plants, ABCC1 and ABCC2, mediate transport of arsenite [As(III)]-PC<sub>2</sub> into vacuoles (Song et al., 2010). In the vacuole, PCs are complexed with inorganic sulfide (S<sup>2-</sup>) to form stable high molecular weight complexes (Cd-PC-S) (Ortiz et al., 1992; Speiser et al., 1992; Vande Weghe and Ow, 2001). Cd ions can also be removed by PCR1 (Plant Cadmium Resistance 1) (Song et al., 2004) or sequestered into the vacuole via proton antiport activity of CAX-like proteins (Shigaki and Hirschi, 2000). Besides cellular elimination and compartmentalization, Cd-chelator and free Cd ions are also transported through the vascular system, taking part in long-distance transport. Research in *Arabidopsis* has shown that PCs undergo long-distance root-to-shoot transport (Gong et al., 2003). Further research from the same lab showed that PCs can be also transported from shoots to roots in *A. thaliana* (Chen et al., 2006). In another species, *Brassica napus*, phloem plays a predominant role in long-distance transport of Cd as Cd-PC and Cd-GSH complexes (Mendoza-Cozatl et al., 2008). To date, only HMA2 and HMA4 were shown to play a role in root-to-shoot translocation of Cd, presumably by xylem loading in roots (Wong and Cobbett, 2009). Other transporters

mediating long-distance transport of Cd-PC complexes or free Cd ions are still unknown.

In this regard, some members of the oligopeptide transporter family (OPT) have been shown to transport PCs and GSH when heterologously expressed in yeast or oocytes. Nine members of the oligopeptide transporter family (OPT) exist in the *Arabidopsis* genome (Fig. 1). OPT homologs have also been identified in other plants and in yeast, but not in animals.

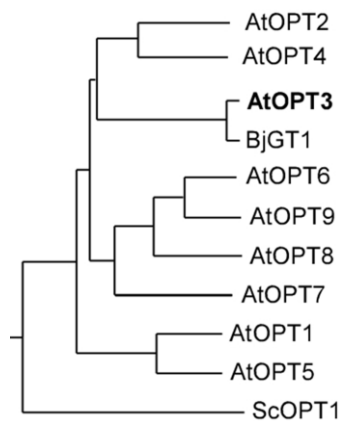


**Figure 1.** Phylogenetic relationships between *A. thaliana* OPT family members. Also shown OPT homologs from *Saccharomyces cerevisiae* (ScOPT1) and *Brassica juncea* (BjGT1). Accession numbers are as follows: AtOPT1, At5g55930; AtOPT2, At1g09930; AtOPT3, At4g16370; AtOPT4, At5g64410; AtOPT5, At4g26590; AtOPT6, At4g27730; AtOPT7, At4g10770; AtOPT8, At5g53520; AtOPT9, At5g53510; ScOPT1, Z49487; BjGT1, CAD91127.1.

Members of the OPT family are predicted to have 12 to 14 transmembrane domains and contain two conserved motifs (NPG and KIPPR)(Koh et al., 2002). Studies in a heterologous system, *Saccharomyces cerevisiae* auxotroph mutants, indicated that some members of the *A. thaliana* OPT family transport synthetic tetrapeptides (KLLG, KLGL) or penta-peptides (KLLLG, YGGFL ) (Koh et al., 2002). *S. cerevisiae* OPT1 (ScOPT1) was also shown to transport reduced GSH, oxidized GSH (GSSG), GSH conjugates and phytochelatins, PC<sub>2</sub> (Bourbouloux et al., 2000; Osawa et al., 2006). Heterologous expression of either BjGT1, an OPT homolog from Indian mustard (*Brassica juncea*), OsGT1, an ScOPT1 homolog from rice (*Oryza sativa*), or



AtOPT6 (from *A. thaliana*), in a  $\Delta opt1$  yeast mutant (yeast deletion line ABC 822), restored its growth on medium with GSH as the only sulfur source, indicating that they were all able to mediate influx of GSH (Bogs et al., 2003; Cagnac et al., 2004; Zhang et al., 2004).

Interestingly, recent evidence implicates OPTs in ion homeostasis. For example, mRNA expression of *AtOPT2* and *AtOPT3* is induced by mineral deficiencies, and heterologously expressed *AtOPT3* restores Fe, Cu and Mn accumulation defects in *S. cerevisiae* transport mutants (Wintz et al., 2003). Null mutation of *AtOPT3* causes embryo lethality presumably due to a defect in Fe movement to developing seeds (Stacey et al., 2002; Stacey et al., 2008). However, it remains unknown how OPTs function in ion homeostasis *in planta*, what are *in vivo* substrates of OPTs and whether they are involved in toxic metal homeostasis.

In this study, we found that OPT3 is a plasma membrane-localized transporter that functions in xylem parenchyma cells and facilitates reabsorption of Cd from xylem into foliar tissues. While OPTs have been implicated in transport of oligopeptides, our findings show that at least some OPT family members can directly mediate transport of ions and in this way are involved in ion homeostasis in plants.

## RESULTS

**OPT3 is involved in Cd tolerance.** Two T-DNA insertion mutant lines for *OPT3* were isolated and designated as *opt3-2* and *opt3-3* (to maintain consistency between Stacey et al., 2008 and our studies). Both, *opt3-2* and *opt3-3* were knockdown mutants each with a T-DNA inserted in the 5'UTR of *OPT3*, which resulted in more than 90%

reduction in *OPT3* expression in both mutant lines (Fig. 2a and c). Seedling growth analyses showed that germination and growth of *opt3-2* and *opt3-3* were similar to *A. thaliana* wild-type (Col-0) plants on half-strength Murashige and Skoog (½ MS) solid medium without Cd supplementation (Fig. 2b and d). However, when germinated and grown for 8 days on ½ MS supplemented with 20 μM of CdCl<sub>2</sub>, lengths of primary roots of *opt3-2* and *opt3-3* were only 50% of that of Col-0 plants (Fig. 2b and d). Since *opt3-2* and *opt3-3* alleles exhibited a similar Cd-sensitivity phenotype and fold-decrease in the level of *OPT3* transcript, we used the *opt3-3* mutant allele for subsequent studies.

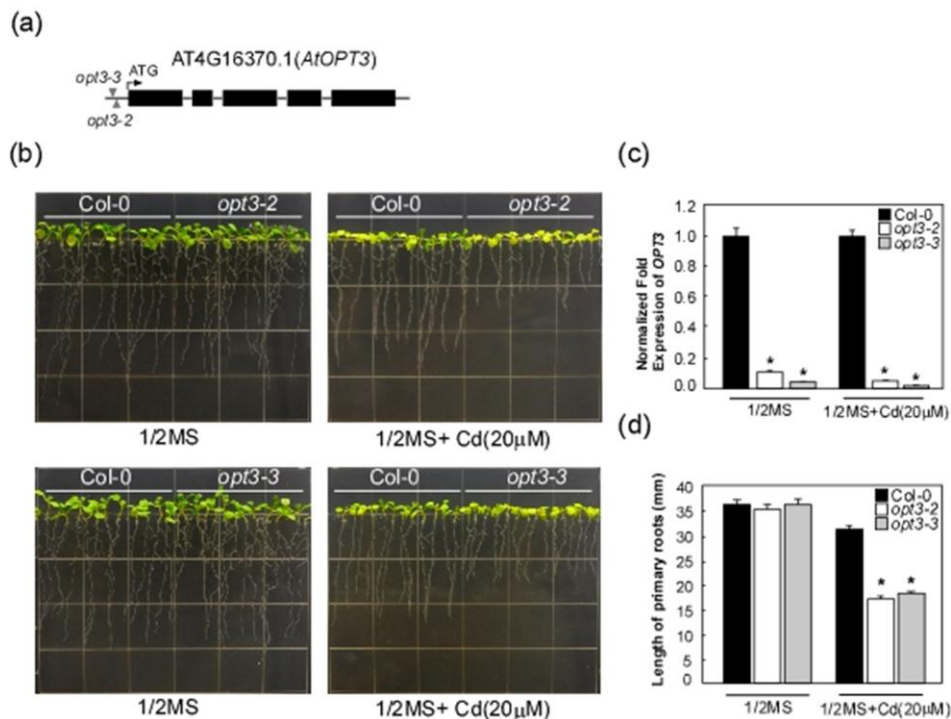


**Figure 2.** Roots of seedlings of *OPT3* knockdown mutants, *opt3-2* and *opt3-3*, are sensitive to Cd. **(a)** T-DNA insertion sites in both *opt3-2* and *opt3-3* alleles are located in 5' untranslated region (UTR) of *OPT3*. **(b)** Seeds of wild type of *A. thaliana* (Col-0) and *opt3-2* and *opt3-3* mutants (*opt3-2* and *opt3-3*, respectively) germinated and grew vertically on ½ MS without (1/2MS) or with 20 μM of CdCl<sub>2</sub> [1/2MS + Cd (20 μM)] for 8 days. **(c)** Transcript abundance of *OPT3* in wild-type (Col-0) and *opt3-2* and *opt3-3* alleles (*opt3-3* and *opt3-3*) grown as described in (b). *OPT3* expression was

quantified by qRT-PCR. Shown are mean  $\pm$  SE; n=3; asterisks [\*] indicate statistically significant differences ( $p < 0.001$ ), *opt3-2* or *opt3-3* vs. Col-0. **(d)** Lengths of primary roots of wild-type (Col-0) and *opt3-2* and *opt3-3* seedlings (*opt3-2* and *opt3-3*) germinated and grown on 1/2 MS plates without (1/2 MS) or with indicated concentration of CdCl<sub>2</sub> [1/2MS + Cd (20  $\mu$ M)]. Shown are mean  $\pm$  SE; n=30; asterisks [\*] indicate statistically significant differences ( $p < 0.001$ ) *opt3-2* or *opt3-3* vs. Col-0.

We also analyzed Cd sensitivity of hydroponically-cultured mature plants.

Consistent with previous observations (Stacey et al., 2008), *opt3-3* mutant plants were smaller and developed some necrotic lesions in cotyledons and relatively older leaves when cultured under normal growth (without Cd) condition (Fig. 3 and Fig. 4). After exposure to Cd for 4 days, leaves of wild-type plants showed symptoms of Cd toxicity: wilting and vein chlorosis, while leaves of *opt3-3* did not show any perceptible symptoms of Cd toxicity (Fig. 4).

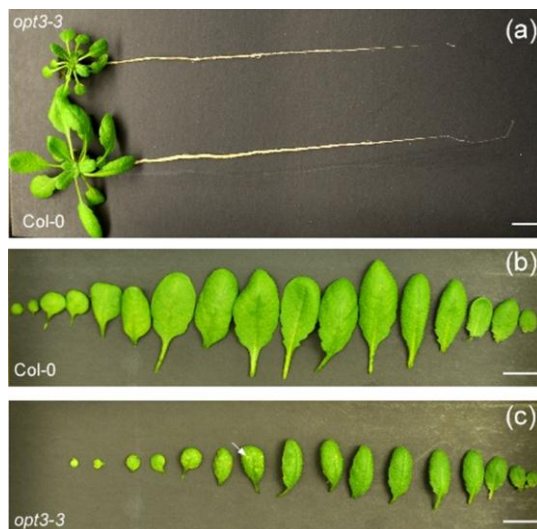


**Figure 3.** Phenotype of wild-type (Col-0) and *OPT3* mutant (*opt3-3*) plants. Col-0 and *opt3-3* were grown in standard hydroponic condition to early bolting phase (~30 days old). **(a)** Individual Col-0 and *opt3-3* plants. **(b)** Individual leaves of Col-0 plant, from youngest (left) to oldest (right). **(c)** Individual leaves of *opt3-3* plant from youngest (left) to oldest (right). White arrow indicates necrotic lesion. Bar = 1cm.



**Figure 4.** Leaves of *opt3-3* mature plants are more tolerant to Cd. After 4 days of exposure to 25  $\mu\text{M}$   $\text{CdCl}_2$ , leaves of Col-0 (Control) plants at early bolting stage showed symptom of Cd toxicity: wilting, vein chlorosis while leaves of *opt3-3* (*opt3-3*) at same positions did not show perceptible symptom of Cd toxicity.

To ensure that this result was due to a loss of OPT3, we complemented *opt3-3* mutant with the *OPT3*-containing 6.8 kilo-base (kb) genomic fragment, and compared Cd sensitivity of the resulting transgenic line with the Col-0 and *opt3-3* mutant plants. We found that sensitivity of leaves of T2 transgenic plants was similar to Col-0, suggesting that observed Cd tolerance of *opt3-3* mutant leaves resulted solely from the *OPT3* knockdown (Fig. 5).

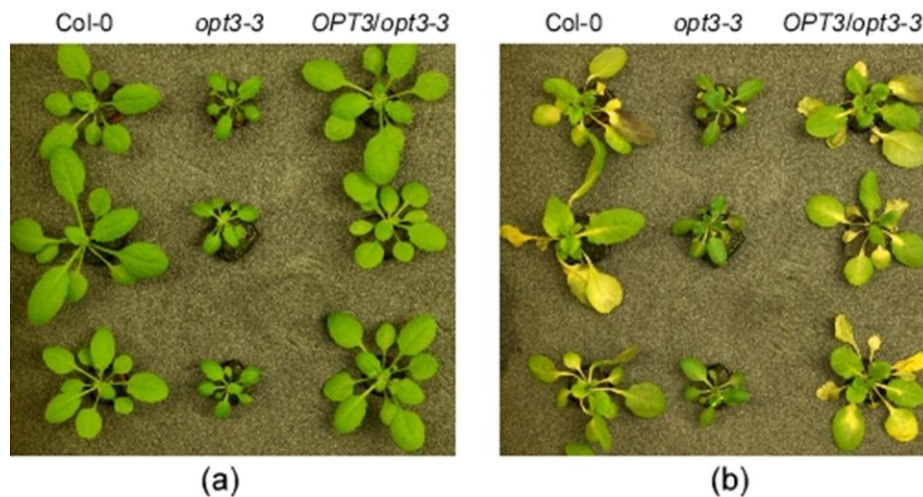


**Figure 5.** Complementation of *opt3-3* mutant with genomic fragment containing *OPT3*. Wild-type plants (Col-0), *OPT3* mutant (*opt3-3*) and T<sub>2</sub>-generation transgenic

*opt3-3* plants expressing *OPT3* genomic DNA (*OPT3/opt3-3*) were grown hydroponically without (a) or with (b) 25  $\mu\text{M}$   $\text{CdCl}_2$ . Note that after exposure to 25  $\mu\text{M}$   $\text{CdCl}_2$  for 6 days in hydroponic media, transgenic plants were as sensitive to Cd as wild-type plants.

We also analyzed the effect of Cd on the expression of *OPT3* and found that the short term-exposure of hydroponically cultured wild-type plants to Cd altered the level of *OPT3* mRNA in roots and shoots (Fig. 6). Together, these data suggest that *OPT3* may function in Cd homeostasis.

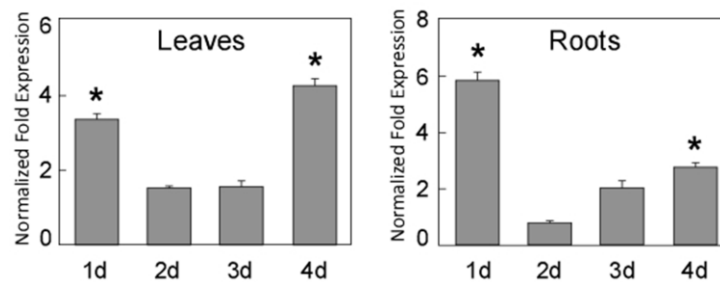


**Figure 6.** Expression of *OPT3* is responsive to Cd. The relative levels of *OPT3* expression in leaves (Leaves) and roots (Roots) of bolting Col-0 plants during a 4 days (1d-4d) exposure to 25  $\mu\text{M}$  of Cd were quantified by qRT-PCR. Shown are mean  $\pm$ SE; n=3; asterisks [\*] indicate statistically significant differences ( $p < 0.001$ ) Cd grown plant vs. corresponding control plant. Normalized fold expression of *OPT3* is calculated by normalizing expressions of *OPT3* in leaves or roots of plants under Cd exposure to the expression in corresponding tissues of plants cultured without Cd.

**OPT3 mediates root-to-leaf partitioning of Cd, PCs and GSH.** Increased sensitivity of roots and decreased sensitivity of leaves of *opt3-3* to Cd in comparison with wild-type plants prompted us to examine root-to-leaf partitioning of Cd and its ligands, GSH and PCs, that are implicated in Cd detoxification (Grill, 1989; Howden et al., 1995; Clemens et al., 1999; Ha et al., 1999; Vatamaniuk, 1999, 2001). We analyzed contents of PCs (PC<sub>2</sub>, PC<sub>3</sub> and PC<sub>4</sub>), GSH, and Cd, as well as Fe, Cu, Zn and Mn in

leaves and roots of *opt3-3* and wild-type plants at early bolting stage, cultured in the absence or presence of Cd in hydroponic media (Fig. 7 and Fig. 8). Accordingly, we also analysed their translocation from roots to leaves by dividing the content in roots by the corresponding content in leaves (Table 1).

Our data showed that: **1)** In plants cultured under standard conditions, without supplementing the medium with Cd, trace amount of Cd (a contaminant in salts used to prepared culture medium) was detected by ICP-MS in both wild-type and *opt3-3* plants. Cd concentration in leaves of *opt3-3* plants (6.7 mg/kg) was 7.5-fold higher than that in wild-type plants (0.9 mg/kg). Cd concentration in roots of *opt3-3* plants (4.4 mg/kg) was 3 fold-higher than that of wild-type plants (1.5 mg/kg). Fe concentration in leaves of *opt3-3* (669.7 mg/kg) was 7.9-fold higher than in wild-type (84.6 mg/kg), but was similar in roots of wild-type and *opt3-3* plants. Also, accumulation of GSH was 2- and 1.4-fold higher in leaves and roots, respectively, in *opt3-3* plants compared to wild-type plants. PCs were not detected in plants cultured in a medium without Cd.

**2)** After short-term (3 days) exposure to 25  $\mu$ M of Cd, leaves of the *opt3-3* mutant plants accumulated 73%, 25%, 64%, 76% and 84% less Cd, GSH, PC<sub>2</sub>, PC<sub>3</sub>, and PC<sub>4</sub> respectively, than leaves of wild-type plants. In contrast, roots of *opt3-3* accumulated 20%, 40%, 30%, 40% and 50% more Cd, GSH, PC<sub>2</sub>, PC<sub>3</sub>, and PC<sub>4</sub>, respectively, than roots of wild type. The fold-change in Cd accumulation in different tissues correlated with fold-change in both GSH and PCs accumulation in the *opt3-3* mutant. Analysis of the root-to-shoot partitioning ratio of different chain-length PCs (where GSH is PC<sub>1</sub>) showed that while there was no difference in root-to-leaf

partitioning of different chain-length PCs in wild-type plants, there was a substantial difference in the *opt3-3* mutant (Table 1). We found that the retention of PCs in roots of *opt3-3* mutant increased with the increase in PCs' chain length (Table 1).

3) In addition to Fe and Cd, *opt3-3* had elevated levels of Cu, Zn and Mn in both roots and leaves, while the root-to-leaf partitioning of Cu, Zn and Mn in *opt3-3* was similar to wild type plants regardless of Cd treatment (Fig. 8 and Table 1).

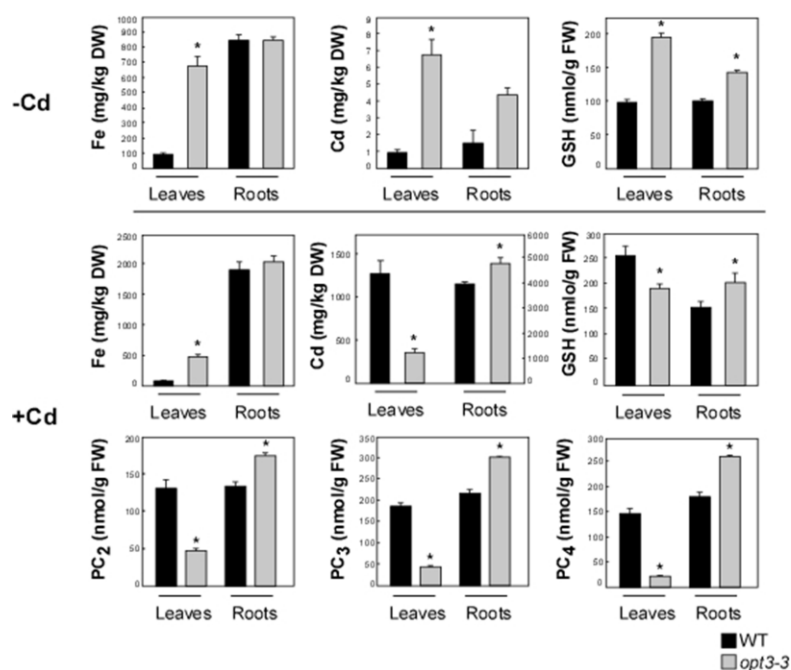


**Figure 7.** Concentration of Cd, Fe, different chain length PCs (PC<sub>2</sub>, PC<sub>3</sub> and PC<sub>4</sub>) and GSH in leaves (Leaves) and roots (Roots) of Col-0 (WT) and *opt3-3(opt3-3)* cultured hydroponically without (-Cd) or with 25  $\mu$ M of Cd for 3 days (+Cd). Shown are mean  $\pm$  SE; n=5; asterisks [\*] indicate statistically significant differences (p<0.001) *opt3-3* vs. Col-0. Plants were grown hydroponically to the early bolting stage before 25  $\mu$ M of CdCl<sub>2</sub> was added to the culture medium.

**Table 1.** Root-to-leaf partitioning of GSH, PCs, Cd, Fe, Cu, Zn, and Mn in Col-0 (Col-0) and *opt3-3* (*opt3-3*) plants under normal growth condition (-Cd) or after 3 days of exposure to 25  $\mu$ M of Cd in hydroponic culture media (+Cd). The root-to-leaf partitioning was calculated by dividing the content in roots by the corresponding content in leaves of Col-0 and *opt3-3*, respectively. Shown are mean  $\pm$ SE; n=5; asterisks [\*] indicate statistically significant differences (p<0.001) *opt3-3* vs.Col-0.

	-Cd		+Cd	
	Col-0 (Root/Leaf)	<i>opt3-3</i> (Root/Leaf)	Col-0 (Root/Leaf)	<i>opt3-3</i> (Root/Leaf)
<b>GSH</b>	1.03 $\pm$ 0.11	0.73 $\pm$ 0.05*	0.61 $\pm$ 0.12	1.07 $\pm$ 0.23*
<b>PC2</b>			1.05 $\pm$ 0.23	3.71 $\pm$ 0.20*
<b>PC3</b>			1.18 $\pm$ 0.17	7.07 $\pm$ 0.84*
<b>PC4</b>			1.24 $\pm$ 0.25	13 $\pm$ 1.60*
<b>Cd</b>	1.48 $\pm$ 0.85	0.66 $\pm$ 0.06*	3.18 $\pm$ 0.59	14.04 $\pm$ 2.48*
<b>Fe</b>	10.36 $\pm$ 2.3	1.29 $\pm$ 0.29*	25.66 $\pm$ 4.28	4.43 $\pm$ 0.90*
<b>Cu</b>	4.91 $\pm$ 1.60	2.74 $\pm$ 0.84	7.82 $\pm$ 0.35	6.84 $\pm$ 0.53
<b>Zn</b>	5.56 $\pm$ 1.67	4.92 $\pm$ 2.06	4.71 $\pm$ 0.17	4.17 $\pm$ 0.54
<b>Mn</b>	2.71 $\pm$ 0.30	2.48 $\pm$ 0.22	2.39 $\pm$ 0.19	2.5 $\pm$ 0.28

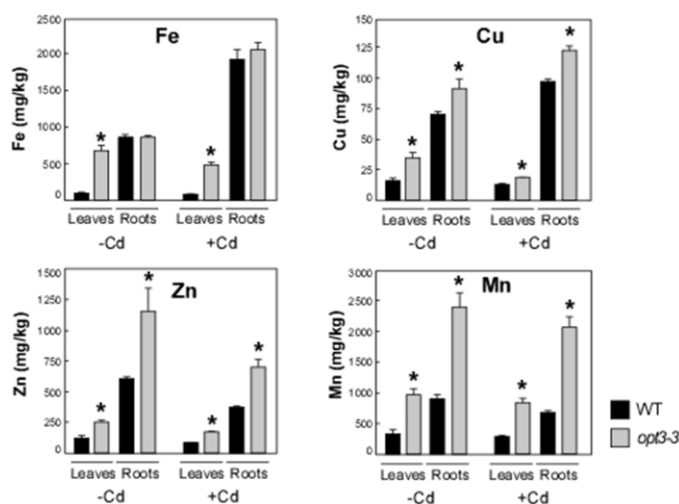


**Figure 8.** Cd, Fe, Cu, Zn and Mn concentrations in leaves and roots of wild-type (Col-0) and *opt3-3* mutant (*opt3-3*) under normal hydroponic condition (-Cd) or after 3days of exposure to 25  $\mu$ M of Cd (+Cd) in hydroponic culture medium. Shown are mean  $\pm$ SE; n=5; asterisks [\*] indicate statistically significant differences (p<0.001) *opt3-3* vs.Col-0.



**OPT3 primarily functions in the shoot and contributes to PC translocation into leaves.** Under standard hydroponic conditions, *OPT3* expression in leaves of mature wild-type plants was 10-fold higher than in roots, suggesting that it might primarily function in shoots (Fig. 9).

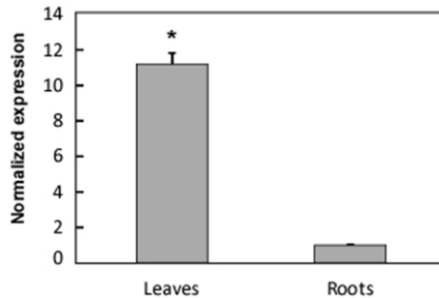


**Figure 9.** Expression of *OPT3* is 10-fold higher in leaves than in roots. Expression of *OPT3* in leaves (Leaves) and roots (Roots) of 28-day-old wild-type plants was quantified by qRT-PCR. Shown are mean  $\pm$ SE; n=3; asterisk [\*] indicates a significant difference ( $p < 0.05$ ) between leaves and roots. Normalized fold expression of *OPT3* is calculated by normalizing expressions of *OPT3* in leaves to its expression level in roots.

To determine whether *OPT3* acts in the root or shoot in Cd resistance, we performed reciprocal grafting experiments using wild-type and *opt3-3* mutant plants. Reciprocal grafts for WT, Col-0/Col-0 (shoot/root), and *opt3-3*, *opt3-3/opt3-3* (shoot/root), served as control. Grafted plants were cultured hydroponically in a medium with or without Cd. We found that in a medium devoid of Cd, grafts of Col-0/*opt3-3* (shoot/root) were morphologically similar to Col-0 plants, while *opt3-3*/Col-0 (shoot/root) grafts were similar to *opt3-3* plants, and had necrotic lesions in cotyledons and relatively older leaves (Fig.10). After exposure to 25  $\mu$ M of Cd for 5 days, leaves of Col-0/*opt3-3* (shoot/root) grafts showed Cd toxicity symptoms similar to that observed in Col-0 plants (Fig. 10a). In contrast, similar to leaves of *opt3-3* mutant, leaves of Cd-exposed *opt3-3*/Col-0 grafts did not show toxicity symptoms (Fig. 10b). These data suggest that *OPT3*'s function in shoots, but not in roots is responsible for

the observed Cd toxicity in leaves.

Analysis of PC content in roots and shoots of reciprocally grafted plants showed that the total PC content in roots of the Cd-cultured *opt3-3*/Col-0 grafts was 50% higher, while there was a 73% reduction of PCs in shoots in comparison with the corresponding tissues of control grafts Col-0/Col-0 (shoot/root). By contrast, the PC concentration in leaves of Col-0/*opt3-3* was no different from Col-0/Col-0 (Fig. 10d). These data suggest that OPT3's function in leaves, not in roots contributes to PC accumulation in leaves of Cd-treated plants.

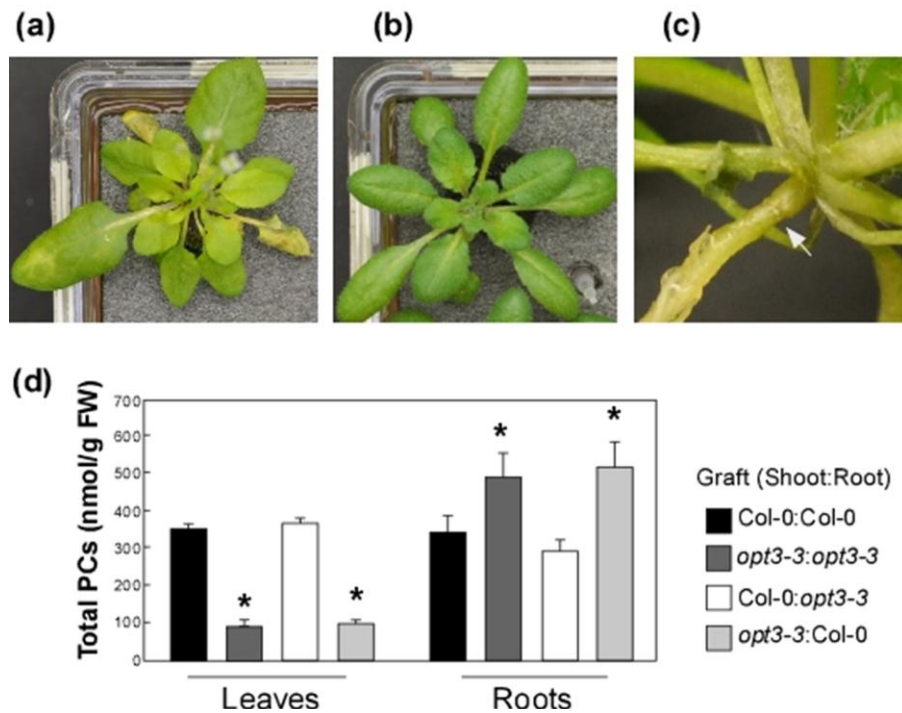


**Figure 10.** Sensitivity of reciprocally grafted wild-type and *opt3-3* mutant to Cd. (a) Thirty-day-old Col-0/*opt3-3* (shoot/root) graft was exposed to 25  $\mu\text{M}$  of Cd for 5 days in hydroponic solution. (b) Thirty-day-old *opt3-3*/Col-0 (shoot/root) graft was exposed to 25  $\mu\text{M}$  of Cd for 5 days in hydroponic solution. (c) Graft junction. (d) Total PCs concentrations in leaves and roots of 30-day-old grafts after exposure to 25  $\mu\text{M}$  of Cd for 2 days. Shown are mean  $\pm$  SE; n=3; asterisks [\*] indicate statistically significant differences ( $p < 0.001$ ) Col-0:*opt3-3* and *opt3-3*/Col-0 vs. Col-0/Col-0.

**OPT3 localizes to the plasma membrane and is expressed in leaf xylem parenchyma.** The Arabidopsis Information Resource predicts that OPT3 is a membrane protein and THHMM (v2.0) predicts that OPT3 has 16 transmembrane helices. Using *A. thaliana* protoplasts transiently expressing OPT3 fused with GFP at the N- or C-terminus, we further showed that OPT3 resides on the plasma-membrane (Fig. 11a). This finding is consistent with results of the proteomic analysis of plasma membrane-localized proteins (Kierszniowska et al., 2009).

To determine the tissue specificity of *OPT3* expression, we generated transgenic plants that carry a  $\beta$ -glucuronidase (GUS) reporter whose expression is driven by the *OPT3* promoter. Histochemical analysis of GUS activity showed that the GUS reporter gene was specifically expressed in the vascular tissues, and predominantly in cotyledons, mature leaves, and sepals (Fig. 11b and d). Consistent with results of the qRT-PCR studies (Fig. 6), GUS activity was induced by Cd. We observed an increased GUS activity in younger leaves, the hypocotyl and roots of Cd-exposed *OPT3* promoter-GUS expressing transgenic plants (Fig. 11c).

Microscopic analyses of the tissue-specificity of *OPT3* expression in transverse sections through the petiole and lamina of Cd-exposed transgenic plants expressing the *OPT3* promoter-GUS construct, showed that activity of the *OPT3* promoter was located in cells associated with the xylem (Fig. 11e and f).

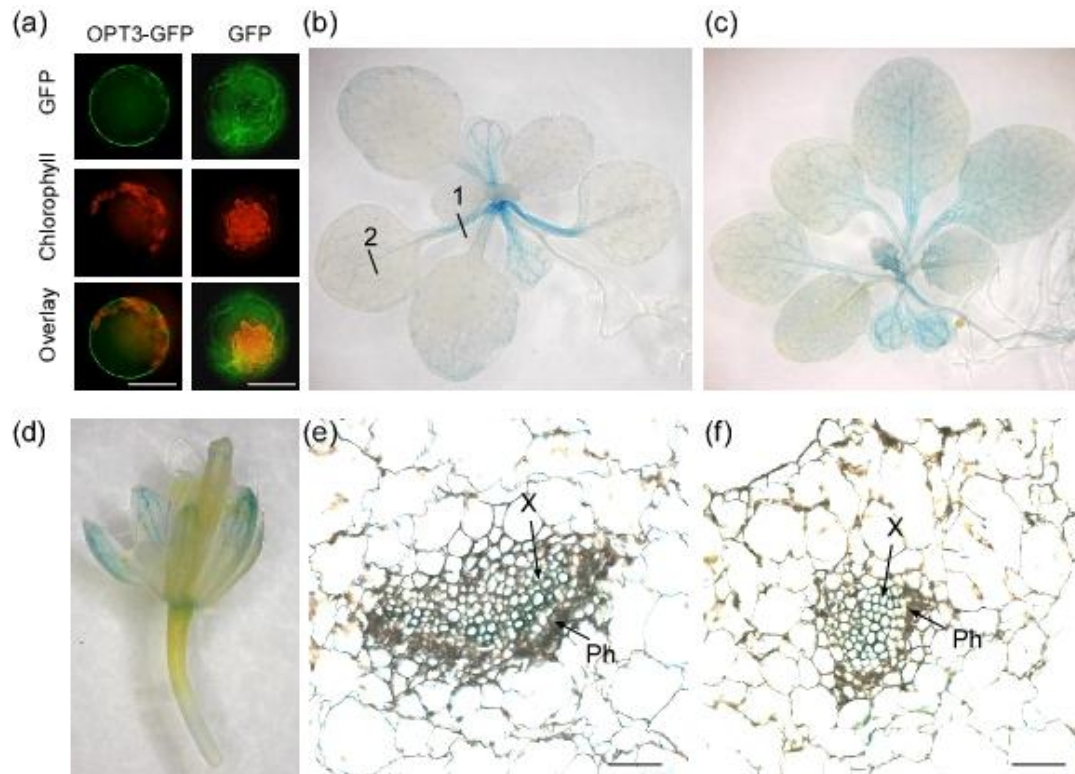


**Figure 11.** Subcellular localization and tissue-specificity of *OPT3* expression. **(a)** *OPT3* resides on the plasma-membrane. When *OPT3* was fused to GFP and transiently expressed in protoplasts, GFP-*OPT3* is localized to the plasma membrane (Bar=20  $\mu$ m). GFP has green fluorescence; chloroplasts have red autofluorescence; green fluorescence microscopy is overlaid with red fluorescence microscopy. **(b-f)** *OPT3p-GUS* expression pattern in transgenic plants showed that *OPT3* is predominantly expressed in vascular tissue, specifically in xylem of petioles and lamina and its expression is induced by Cd exposure. GUS activity is indicated in blue. **(b)** GUS activity was analyzed in twenty-day-old seedlings cultured at standard conditions in hydroponics. **(c)** GUS activity was analyzed in twenty -day-old seedlings exposed to Cd for 3 days. **(d)** GUS activity in flowers. **(e)** GUS activity in a transverse section through the petiole. The position of the section is indicated in **(b)** as position 1 (Bar = 50  $\mu$ m); **(f)** GUS activity in a transverse section through the middle region of leaf (indicated by position 2 in **(b)**). X, xylem; Ph, phloem (Bar = 50  $\mu$ m).

***PCS1* and *OPT3* do not act in a simple linear Cd detoxification pathway.** Our data suggest that *OPT3* contributes to the distribution of PCs in Cd-grown plants. To test whether or not PCs are the substrates of *OPT3*, or in other words, *OPT3* and *PCS1* act in the same genetic pathway for heavy metal detoxification, we generated the *opt3*-

*3cad1-3* double mutant that lacks both OPT3 and PC synthase (alias CAD1) by crossing *opt3-3* with the *cad1-3* mutant. We expected that if *PCS1* acts upstream of *OPT3* in a simple linear Cd detoxification pathway, the *opt3-3cad1-3* double mutant might have similar Cd sensitivity to the *cad1-3*. However, if *PCS1* and *OPT3* act in different detoxification pathways, heavy metal sensitivity of *opt3-3cad1-3* double mutant could be more sensitive to Cd than *opt3-3* or/and *cad1-3* mutant.

Our results show that in the absence of Cd, *opt3-3*, *cad1-3* and *opt3-3cad1-3* double mutant seedlings germinated and grew similarly to Col-0 plants on ½MS plates (Fig. 12a and 12b). However, when germinated and grown on ½ MS supplemented with 10 or 20 µM of CdCl<sub>2</sub> for 10 days, root growth of the *opt3-3cad1-3* double mutant was the most inhibited. We also observed that under exposure to a lower concentration of Cd (10 µM), the *opt3-3* was more sensitive than the *cad1-3*. However, at higher concentration of Cd (more than 20 µM) *cad1-3* was more sensitive than the *opt3-3* mutant. Neither the *cad1-3* nor the *opt3-3cad1-3* double mutant germinated on ½ MS plates supplemented with 50 µM of CdCl<sub>2</sub> (Fig. 12a and 12b).

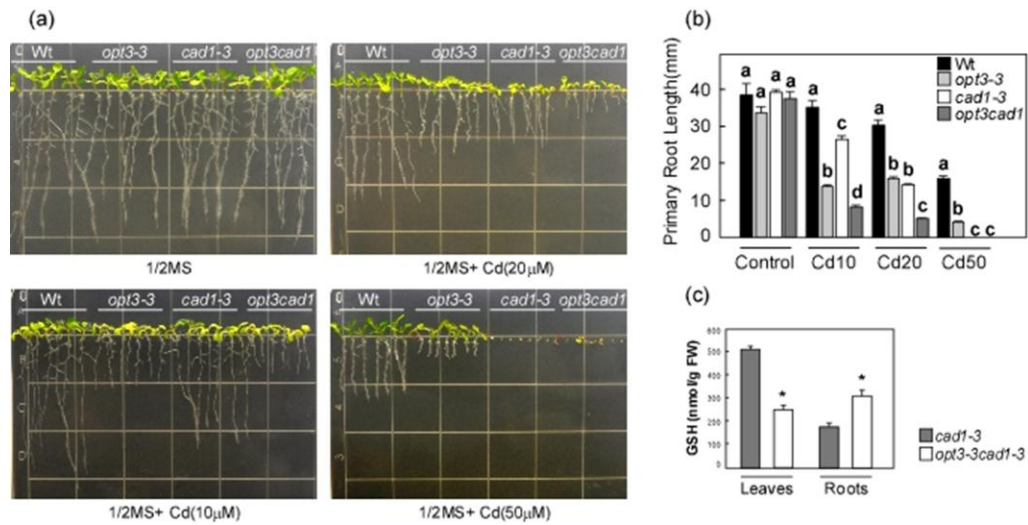


**Figure 12.** Sensitivity of *opt3-cad1-3* double mutant to different concentration of Cd. **(a)** Seeds of Col-0 (Wt), *opt3-3* (*opt3-3*), *cad1-3* (*cad1-3*) and *opt3-3cad1-3* (*opt3cad1-3*) were germinated and grown vertically for 10 days on 1/2 MS without or with indicated concentration of CdCl<sub>2</sub>. **(b)** Lengths of primary roots of corresponding seedlings in **(a)**. Different letters indicate significant differences (p<0.05). **(c)** GSH concentrations in leaves (Leaves) and roots (Roots) of *cad1-3* (*cad1-3*) and *opt3-3cad1-3* (*opt3cad1-3*) double mutant grown with exposure to 25 μM of Cd for 3 days. Shown are mean ±SE; n=5; asterisks [\*] indicate statistically significant differences (p<0.001) *opt3-3cad1-3* vs. *cad1-3*. Plants were grown hydroponically to early bolting stage before application of 25 μM of Cd in the culture solution.

**OPT3 contributes to GSH accumulation in leaves.** Since the *cad1-3* mutant lacks PC synthase activity and thus lacks PCs, the *opt3-3cad1-3* double mutant provides a clean genetic background to further evaluate the role of OPT3 in the root-to-shoot partitioning of GSH, a PCs precursor. We analyzed GSH content in leaves and roots of the *opt3-3cad1-3* double mutant and *cad1-3* mutant plants grown until early bolting before Cd was added to the hydroponic medium. Under Cd exposure, the root-to-leaf partitioning of GSH (concentration in root divided by concentration in leaf) was 1.24 in the *opt3-3cad1-3* double mutant versus 0.35 in the *cad1-3* mutant, compared with

1.07 in *opt3-3* mutant versus 0.61 in Col-0, which suggests that OPT3 is involved in the root-to-leaf partitioning of GSH to a greater degree in the *cad1* background than in the *CAD1* background (Fig. 12c).

**OPT3 transports Cd ion but not GSH in yeast cells.** To further address the substrate specificity of OPT3, we expressed *OPT3* in the *S. cerevisiae* ABC822 strain ( $\Delta opt1$ ), which is GSH uptake deficient mutant (Bourbouloux et al., 2000). If OPT3 is a GSH transporter and mediates influx of GSH, we will expect to see that OPT3 can rescue growth of ABC822 in SC-S media (see the recipe in the Materials and Methods) with GSH as the only S source. Our yeast growth assay showed that neither OPT3 nor N terminus truncated OPT3 (OPT3(-N), which lacks of the first 77 amino acid residues of OPT3) rescued ABC822 in SC-S media with GSH as only S source, indicating that OPT3 does not mediate GSH influx in yeast cells (Fig. 13). We expressed N terminus truncated OPT3, because by doing sequence comparisons, we found that OPT3 is almost identical to BjGT1 except that OPT3 has the extra 77 amino acid residues at the N terminus, which we hypothesized could be involved in regulation of transport activity.

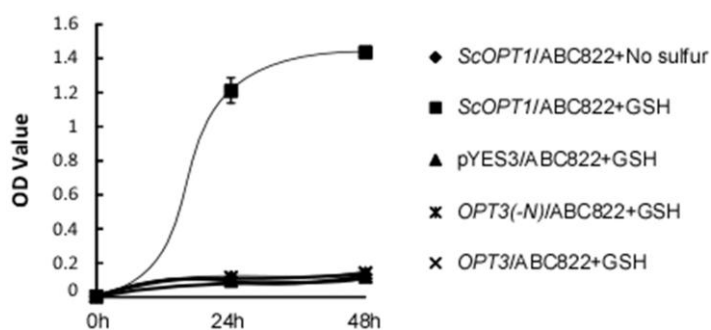


**Figure 13.** Growth assay of ABC822 ( $\Delta opt1$ ) strain transformed with pYES3-*OPT3* (*OPT3*/ABC822), pYES3-*OPT3* (-N) (N terminal truncated *OPT3*, which lacks of the first 77 amino acid residues of *OPT3*) (*OPT3* (-N)/ABC822), pYES3-*ScOPT1* (*ScOPT1*/ABC822) or empty pYES3 construct (pYES3/ABC822). Yeast cells were grown in SD medium to  $OD_{600}=1.0$ , washed three times in cold sterile water, and diluted to  $OD_{600}=0.004$  in SC-S media supplemented without (+No sulfur) or with 200  $\mu$ M of GSH (+GSH). OD values were measured after 1 and 2 day of culture respectively (shaking at 250 rpm at 30  $^{\circ}$ C).

Consistent with growth assays, our *in vitro* GSH uptake assays demonstrated that expression of *OPT3* did not increase the uptake of GSH (Fig. 14).

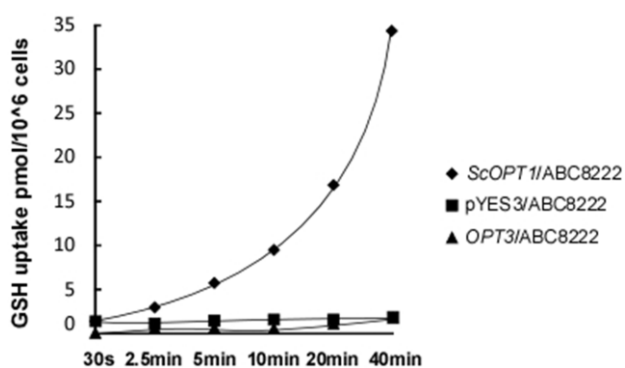


**Figure 14.** Time course of [ $^{32}$ S]GSH uptake by the ABC822 ( $\Delta opt1$ ) strain transformed with the empty pYES3 vector (pYES3/ABC822), the pYES3-*OPT3* (*OPT3*/ABC822) or pYES3-*ScOPT1* (*ScOPT1*/ABC822) construct in a uptake medium containing 100  $\mu$ M [ $^{32}$ S]GSH.



We observed, however, that heterologous expression of *OPT3* in the ABC822 ( $\Delta opt1$ ) increased its sensitivity to Cd exposure suggesting that *OPT3* may directly mediate Cd influx (Fig. 15).

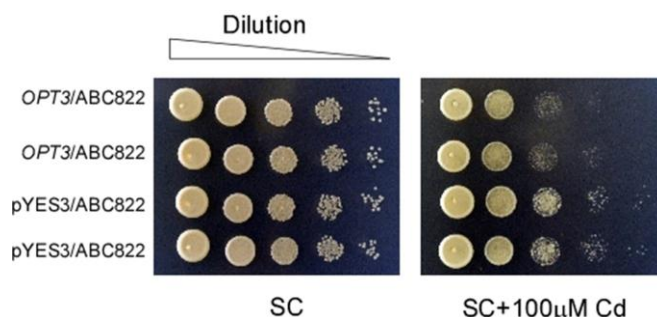


**Figure 15.** Cd sensitivity assay of ABC822 strain ( $\Delta opt1$  mutant) transformed with empty pYES3 (pYES3/ABC822) or pYES3-*OPT3* construct (*OPT3*/ABC822) on SC media supplemented with 100  $\mu$ M of Cd. For the each construct, two independent cell lines were shown.

To test this hypothesis, we performed *in vitro*  $^{109}\text{Cd}$  uptake studies using the ABC8222 strain transformed with the pYES3 empty vector or the pYES3-*OPT3* construct. This assay showed that *OPT3* directly mediates transport of Cd into yeast cells (Fig. 16).

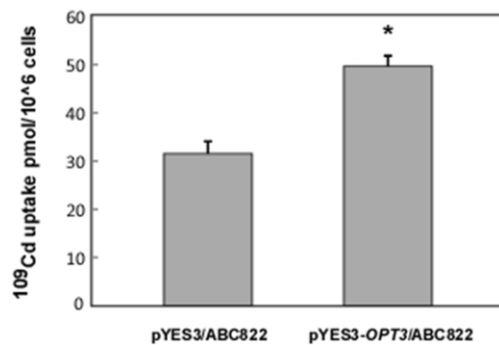


**Figure 16.**  $^{109}\text{Cd}$  uptake by the ABC822 ( $\Delta opt1$ ) strain transformed with the empty pYES3 empty vector or the pYES3-*OPT3* construct in uptake medium contained 25  $\mu$ M of  $^{109}\text{Cd}$  for 5 minutes. Asterisk [\*] indicates a significant difference ( $p < 0.001$ ) pYES3-*OPT3* vs. pYES3 empty vector.

## DISCUSSION

**OPT3 mediates root-to-shoot translocation of Cd by reabsorbing it from the xylem in the shoot.** Our seedling growth assays and mature plant Cd tolerance assays showed that *opt3-3* roots were more sensitive to Cd than those of wild-type plants, while *opt3-3* leaves were more tolerant than those of wild-type plants. The differential sensitivity of roots and leaves of the *opt3-3* mutant to Cd led us to examine the tissue content of Cd and putative ligands: GSH and PC. The concentrations of Cd, Fe, GSH, PC, Cu, Mn, and Zn were determined in roots and leaves of the *opt3-3* mutant and wild-type plants grown without or with Cd for 3 days. Also, their root-to-leaf partitioning was quantified by dividing the concentration in roots by the corresponding concentration in leaves. Consistent with the phenotype observed for the *opt3-3* mutant under Cd exposure, the *opt3-3* mutant accumulated 76% less Cd in leaves but 20% more Cd in roots than did wild-type plants, and Cd distribution was closely correlated with GSH and PCs (Fig. 2, Fig. 4, Fig. 7 and Table 1). Our data above supports the suggestion that OPT3 contributes to Cd, PCs and GSH accumulation in leaves. We also found that while the *opt3-3* accumulated higher concentrations of Cu, Zn and Mn in both roots and leaves than in wild-type plants, root-to-leaf partitioning of Cu, Zn and Mn in *opt3-3* was not different from the wild-type plants regardless of Cd treatment (Fig. 8 and Table 1). This observation suggested that OPT3 may not directly mediate root-leaf partitioning of Cu, Zn and Mn, and other transporter(s) may be directly involved in the increased accumulation of these elements in the *opt3-3* mutant.

We further showed that OPT3 mainly functions in shoots using shoot-root grafts between wild-type and *opt3-3* mutant plants (Fig. 10). Subcellular localization

and tissue specificity of OPT3 showed that OPT3 is located to the plasma-membrane and is specifically expressed in the xylem parenchyma in the petioles and leaves (Fig. 11). Functional studies of OPT3 in yeast heterologous systems showed that expression of *OPT3* in yeast ABC822 ( $\Delta opt1$ ), which is a GSH uptake deficient mutant, increased its sensitivity to Cd (Fig.15). Also, our *in vitro*  $^{109}\text{Cd}$  uptake assay using yeast cells transformed with the pYES3 empty vector or the pYES3-*OPT3* construct showed that OPT3 directly mediates Cd influx in yeast cells (Fig. 16).

Taken together, the evidence above suggests that OPT3 mediates long-distance transport of Cd from root to shoot by re-absorbing the Cd ion from xylem.

***PCSI* and *OPT3* do not act in a simple linear Cd detoxification pathway.** As GSH is the substrate for PCs biosynthesis, in order to differentiate between GSH and PC and to address whether PC is the substrate of OPT3, we introduce another mutant *cad1-3*, a PCs deficient mutant, into our research. The *opt3-3cad1-3* double mutants were generated from a cross between the *opt3-3* and the *cad1-3*. The idea is that if PC is the only substrate or a major substrate of OPT3, or in other words, *OPT3* and *PCSI* are in the same pathway for heavy metal tolerance, we would expect to see that the *opt3-3cad1-3* double mutant had similar Cd sensitivity as the *cad1-3* mutant. Our result showed that the double mutant was more sensitive than either the *opt3-3* or *cad1-3* single mutant. We also found that the *opt3-3* was more sensitive to Cd than the *cad1-3* at lower Cd concentration while more tolerant than the *cad1* at higher Cd concentration. Our results from the analysis of the *opt3-3cad1-3* double mutant suggest that *OPT3* and *PCSI* are not in a simple linear Cd detoxification pathway (Fig.

12). Therefore, we propose that OPT3 may not directly transport PC but instead may transport Cd<sup>2+</sup> into leaves, which in turn promotes PC synthesis and increased accumulation in leaves. Consistent with this suggestion are the following observations: 1) Heterologous expression of *OPT3* in the *S. cerevisiae*  $\Delta opt1$  mutant increased its sensitivity to Cd exposure (Fig. 15). 2) OPT3 can rescue growth defects of *S. cerevisiae* Fe, Cu and Mn uptake deficient mutants (Wintz et al., 2003). In both cases, OPT3 functions independently from PC, because PCs are not included into yeast culture medium, and PC synthase is not encoded by the *S. cerevisiae* genome.

### **OPT3 does not transport GSH in yeast cells.**

Since the *cad1-3* lacks the PCs, the *opt3-3cad1-3* double mutant provided a clean genetic background to investigate the role of OPT3 in root-to-leaf partitioning of GSH. Compared with the *cad1-3* mutant, root-to-leaf partitioning of GSH is significantly changed in the *opt3-3cad1-3* double mutant, suggesting that OPT3 is involved in GSH root-to-leaf partitioning. To further answer a question of whether or not GSH is the substrate of OPT3, we expressed *OPT3* in the *S. cerevisiae* ABC822 strain ( $\Delta opt1$ ) which is a GSH uptake deficient mutant. If OPT3 is a GSH transporter and mediates influx of GSH, we will expect to see that OPT3 can rescue growth of ABC822 in SC-S media with GSH as the only S source. Our yeast growth assay showed that neither OPT3 nor N terminus truncated OPT3 [OPT3 (-N)] rescued ABC822 growth in SC-S media with GSH as only S source, indicating that OPT3 does not mediate GSH influx in yeast cells (Fig. 13). In agreement with our growth assays, our *in vitro* GSH uptake assay demonstrated that *OPT3* expression did not increase the uptake of GSH (Fig.

14). Thus, we concluded that the changed root-to-leaf partitioning of GSH in the *opt3-3cad1-3* double mutant, when compared with the *cad1-3*, may result from an altered OPT3-mediated Cd partitioning.

OPT3 is supposed to be an oligopeptide transporter (Koh et al., 2002) and its closest homologue BjGT1 is a GSH transporter (Bogs et al., 2003). Furthermore PCs have long been suggested to be Cd ligands in long-distance transport between root and shoot (Gong et al., 2003; Chen et al., 2006; Mendoza-Cozatl et al., 2008). However, we did not see uptake of GSH by OPT3 expressed in yeast. Nevertheless, the scenario *in planta* can be more complex and we cannot rule out the possibility that other protein can cooperate with OPT3 in the plant cell to alter its transport capabilities and thus, Cd-GS<sub>2</sub> (and/or Cd-PCs) could also serve as the transport substrate (s) for OPT3 *in vivo*.

In conclusion, our results above suggest that OPT3 mediates root-to-shoot long-distance transport of Cd by re-absorbing Cd ion from xylem, which may indirectly result in increased GSH and PC in leaves. OPT3, a member of OPT family appears to be able to directly mediate the transport of ions, and thus may be involved in ions homeostasis in plants. (Fig. 17)

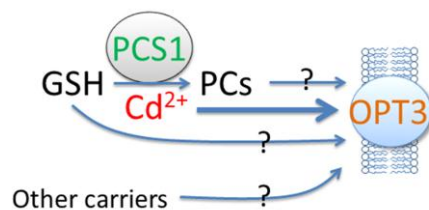


Figure 17. The model of OPT3-mediated transport of Cd. Both our *in vivo* and *in vitro* data supported that OPT3 directly transports Cd ions. *PCS1* and *OPT3* do not act in a simple linear Cd detoxification pathway. Question marks (?) indicate that further evidence is needed.

## MATERIALS AND METHODS

**Isolation of *opt3* mutant alleles, plant transformation and generation of the *opt3-3cad1-3* double mutant.** All plant lines used in the study were in the *A. thaliana* Columbia (Col-0) background. Information about *opt3-2* (SALK\_021168C) and *opt3-3* (SALK\_058794C) T-DNA insertion alleles was obtained from the SIGnAL Web site at <http://signal.salk.edu>, and seeds were obtained from the *Arabidopsis* Biological Resource Center (Alonso *et al.*, 2003). *opt3-2* allele is also described in (Stacey *et al.*, 2002; Stacey *et al.*, 2008). In order to identify homozygous mutants, PCR-based screening was employed using combinations of T-DNA left border and gene specific primers (Table 2). Transformation was performed following a simplified *Arabidopsis* transformation protocol (Clough and Bent, 1998).

In order to attain the *opt3pcs1* double mutant, the *opt3-3* mutant was crossed with homozygous PC synthase-deficient *cad1-3* allele (a generous gift of Dr. Cobbett (University of Melbourne, Australia). This allele is described in (Howden *et al.*, 1995). Seeds of F2 plants were collected and homozygous population for both alleles was identified using dCAPS (Derived Cleaved Amplified Polymorphic Sequence) approach (Neff *et al.*, 1998; Neff *et al.*, 2002) and primer pairs that will introduce a *Bam*H1 restriction site into the wild-type, but not into *cad1-3* allele (Table 2). Homozygous *cad1-3* allele in *opt3-3cad1-3* plants was selected after *Bam*H1 restriction digestion of a 132 bp-long PCR product.

***Arabidopsis* grafting.** Ten-day-old seedlings were used for grafting experiments that were performed as described in (Rus *et al.*, 2006). After recovery for 5 days, robust grafts lacking adventitious roots on the scion were transferred to hydroponics and

cultured for 2.5 weeks before CdCl<sub>2</sub> (25 μM) was added to the hydroponic medium. Grafts were photographed and tissues were collected at indicated time points.

**Vector construction.** *OPT3*-containing a 6.8 kilobase (kb) genomic fragment was amplified and cloned into pPZP-RCS2-hpt (Goderis et al., 2002) for genetic complementation. For isolation of the promoter of *OPT3*, a 3.5kb genomic sequence upstream of *OPT3* start codon was amplified and cloned into pGUS1 (Diener et al., 2000). To fuse GFP (green fluorescent protein) to the N terminal of *OPT3*, full-length CDS of *OPT3* was amplified and then cloned into of pGWB406 (Nakagawa et al., 2007). For expression of *OPT3* in *S. cerevisiae*, full-length CDS or N terminus truncated of *OPT3* (designated as OPT3 (-N) which lacks the first 77 amino acid residues of *OPT3*) was cloned into yeast-*E. coli* shuttle vector pYES3 (Lu et al., 1997). CDS of *ScOPT1* was also cloned into vector pYES3. Conversion of pPZP-RCS2-hpt, pGUS1 and pYES3 into gateway destination vectors followed the protocol of Gateway® Vector Conversion System (Invitrogen).

**Plant growth conditions and Cd treatment.** Seedlings were grown on solid, half-strength MS medium (½ MS) supplemented with 1% sucrose, 0.8% agar and the indicated concentrations of Cd. For hydroponic culture, plants firstly were germinated on ½ MS for 8 days and then transferred to one-quarter-strength *Arabidopsis* hydroponic solution as described in (Arteca and Arteca, 2000). Full strength *Arabidopsis* hydroponic solution contained 5 mM KNO<sub>3</sub>, 2.5 mM KH<sub>2</sub>PO<sub>4</sub>, 2.0 mM MgSO<sub>4</sub>, 2.0 mM Ca(NO<sub>3</sub>)<sub>2</sub>, 70 μM H<sub>3</sub>BO<sub>3</sub>, 40 μM Fe(III)HBED, 0.5 μM CuSO<sub>4</sub>, 14 μM MnCl<sub>2</sub>, 1.0 μM ZnSO<sub>4</sub>, 0.2 μM NaMoO<sub>4</sub>, 10 μM NaCl and 0.01 μM CoCl<sub>2</sub>). The hydroponic solution was changed every 5 days. At the early bolting stage (plants were

about 4-weeks-old), 25  $\mu\text{M}$  of  $\text{CdCl}_2$  was applied. Roots and leaves were then harvested at indicated time.

All plants were grown in a 12-h-light/12-h-dark photoperiod (at a photosynthetic photon flux density of  $250 \mu\text{mol m}^{-2} \text{s}^{-1}$ ) at a 23/19  $^\circ\text{C}$  light/dark temperature regime and 75% relative humidity.

**RNA isolation and quantitative real time PCR (qRT-PCR).** To quantify expression of *OPT3* in roots and shoots with/without Cd treatment, total RNAs were isolated and treated with DNaseI. Then cDNA was prepared using AffinityScript qPCR cDNA Synthesis kit (Stratagene). qRT-PCR was performed using the CFX96 qPCR Detection System (Bio-Rad) and gene-specific primers for *OPT3* and *F-box* (At5g1571) as a reference gene. Statistical analysis of qRT-PCR data was performed with REST2009 (Pfaffl et al., 2002).

**Subcellular localization and tissue specificity of *OPT3* expression.** Subcellular localization of *OPT3* was analyzed in *A. thaliana* protoplasts transiently expressing *OPT3*-GFP fusion protein (GFP was fused onto N terminus of *OPT3*) from the pGWB406 (Nakagawa et al., 2007). Protoplasts isolation and transfection were performed as described (Zhai et al., 2009; Zhai et al., 2009). Histochemical GUS staining and microscopy of transgenic plants expressing *OPT3* promoter-GUS fusions was performed according to the protocol of Jefferson et al (Jefferson et al., 1987). GUS stained petiole and hypocotyl were fixed and embedded into paraffin and for sectioning (10  $\mu\text{m}$ ) as described in Shimizu et al (Shimizu et al., 2009).

**Heterologous expression of *OPT3* in *Saccharomyces cerevisiae*, yeast Cd sensitivity drop assay, yeast growth assays.** pYES3-*OPT3*, or pYES3-*OPT3*(-N) (N



terminal truncation), or pYES3-*ScOPT1* or empty pYES3 vectors were introduced into *S. cerevisiae* strain ABC822 ( $\Delta opt1$ ) (*MATa*; *ura3-52*; *leu2* $\Delta 1$ ; *lys2-801*; *his3* $\Delta 200$ ; *trp1* $\Delta 63$ ; *ade2-101*; *hgt1* $\Delta$ ::*LEU2*) respectively, following the protocol of Small-Scale Yeast Transformation (Invitrogen). Transformed yeast cells were selected on solid AHC medium (6.7 g/L of yeast nitrogen base without amino acid, 10 g/L of casamino acid, and 2% of glucose and 2% agar).

To test if OPT3 would alter Cd sensitivity of yeast mutant cells, ABC822 transformed with pYES3-*OPT3* or empty vector were grown in AHC medium to an  $OD_{600}=1.0$ . Cells were then serially 10-fold diluted and 8  $\mu$ L from each dilution were spotted onto solid synthetic complete (SC) plate (6.7 g/L of yeast nitrogen base without amino acid, 2% of glucose, 2% agar, 0.77 g/L CSM-Ura (MP Biomedicals)) supplemented with the indicated concentration of Cd, and grown at 30 °C for 2-3 days.

To test whether OPT3 would rescue ABC822 in the media with GSH as only S source, ABC822 transformed with pYES3-*OPT3*, pYES3-*OPT3(-N)*, pYES3-*ScOPT1* or empty vector were grown in AHC medium to an  $OD_{600}=1.0$ . Cells were then washed in ice-cold water 3 times and inoculated (1:200) into SC-S media supplemented without or with 200  $\mu$ M of GSH. SC-S was prepared according to the YNB recipe (Bacto Yeast Nitrogen Base without amino acids and ammonium sulfate, DIFCO Laboratories, Detroit), with the modification that all sulfur containing reagents in macroelements and microelements were substituted with equal amounts of the corresponding chloride salt (i.e.  $CuCl_2$ ,  $MgCl_2$ ,  $ZnCl_2$ ,  $MnCl_2$ , and  $NH_4Cl$ ) and was supplemented with required amino acids: His, Trp, Ade and Lys.

**Analysis of PCs and GSH content.** PCs and GSH content was analyzed in roots and

leaves of Col-0 and *opt3-3* plants cultured hydroponically with or without Cd. Fresh plant tissues were homogenized in ice-cold 5% of 5-sulfosalicylic acid and centrifuged at 13000 rpm for 10min before aliquots of the supernatant (50  $\mu$ L) were injected into an Econosphere C18, 150 $\times$ 4.6-mm RP-HPLC column (Alltech). The column was developed with a linear gradient of water, 0.05% (v/v) phosphoric acid, and 17% (v/v) acetonitrile, 0.05% (v/v) phosphoric acid at a flow rate of 1 mL/min. For the quantification of PCs and GSH, thiols were estimated spectrophotometrically at 412 nm by reacting aliquots (450  $\mu$ L) of the column fractions with 0.8 mM 5,5'-dithiobis(2-nitrobenzoic acid) (450  $\mu$ L) dissolved in 250 mM phosphate buffer (pH 7.6). Calibration was with GSH. Fractions containing GSH and PC were identified based on their co-migration with commercially available GSH standards (Sigma) or *in vitro*-synthesized PCs (Vatamaniuk *et al.*, 2000).

**Elemental Analysis.** Elemental composition was analyzed in *A. thaliana* and *S. cerevisiae*. For studies in *A. thaliana*, plants were cultured hydroponically as described above. When plants reached early bolting stage, hydroponic medium was supplemented with 25  $\mu$ M CdCl<sub>2</sub> and plant were cultured for additional 3-4 days (as indicated). Roots and shoots were harvested and roots were desorbed by washing with 10 mM EDTA followed by washing in a solution with 0.3 mM bathophenanthroline disulphonate and 5.7 mM sodium dithionite and then rinsed with deionized water (Cailliatte *et al.*, 2010). Shoots were rinsed with deionized water. Root and shoot tissues were dried for 2 days at 80°C. Elemental analysis was performed using inductively coupled plasma mass spectrometry (ICP-MS) as described (Lahner *et al.*, 2003). For ICP-MS-based Cd analysis in *S. cerevisiae*, growth of yeast cells and

analysis was carried out as previously described (Danku *et al.*, 2009).

***In vitro* cadmium and GSH uptake.** Uptake studies were performed as previously described (Pence *et al.*, 2000; Zhang *et al.*, 2004). Briefly, ABC822 (*Δopt1*) strain transformed with pYES3-*ScOPT1*, YES3-*OPT3* or the empty pYES3 construct was grown respectively in YNB-URA to  $OD_{600} = 0.8$ . Cultures were harvested and washed first with the same volume of water, followed by a washing buffer (20 mM MES/KOH, 0.5 mM  $CaCl_2$  and 0.25 mM  $MgCl_2$  at pH 5.0) before re-suspension in transport buffer (washing buffer with 2% (w/v) glucose). All buffers were ice-cold and cells were kept on ice until the uptake experiment. After warming to room temperature, cells were mixed with equal volumes of radiolabeled  $^{109}Cd$  solution and [ $^{32}S$ ] GSH. Final concentration of  $^{109}Cd$  was 25  $\mu M$  and [ $^{32}S$ ] GSH was 100  $\mu M$ , respectively. At selected time points, 100  $\mu l$  aliquots were centrifuged through a silicone oil/dionyl phthalate mixture onto 10ul of 40% perchloric acid as described by Pence *et al.*  $^{109}Cd$  content in yeast pellets were determined by  $\gamma$  detection and converted to Cd or GSH influx values.

**Table 2.** Primers used in this research.

<b>Primer Names</b>	<b>Sequences (5'-3')</b>
LBb1.3	atfttgccgatttcggaac
Fw( <i>opt3-2</i> genotyping)	caaaatccattcggacatgctc
Rv( <i>opt3-2</i> genotyping)	gaggctaaaactccaccaag
Fw( <i>opt3-3</i> genotyping)	cggacaaccaatagaaagtgc
Rv( <i>opt3-3</i> genotyping)	gagaagtgggtgggaagagtc
Fw( <i>cad1-3</i> genotyping)	aattgcagactgggactggt
Rv( <i>cad1-3</i> genotyping)	ctcccaaagaagttaagaggat
Fw( <i>OPT3</i> genomic locus)	<b>tcgtcggggacaactttgtacaaaaaagttgg</b> tcagaatctccaatcctactctcc
Rv( <i>OPT3</i> genomic locus)	<b>ggcgccgcacaactttgtacaagaaagttgggt</b> tgatgcaattccaatgggtg
Fw( <i>OPT3</i> promoter)	<b>tcgtcggggacaactttgtacaaaaaagttgg</b> gtccagtaggccatttcacat
Rv( <i>OPT3</i> promoter)	<b>ggcgccgcacaactttgtacaagaaagttgggt</b> ctggcagaaagtgaatgctgtt
Fw( <i>OPT3</i> CDS)	<b>tcgtcggggacaactttgtacaaaaaagttgg</b> gaaaatggacgcggagaag
Fw( <i>OPT3</i> (-N) CDS)	<b>ggggacaagttgtacaaaaaagcaggcttc</b> accatgcagatcgctgtttgccca
Rv( <i>OPT3</i> CDS*)	<b>ggcgccgcacaactttgtacaagaaagttgggt</b> ttagaaaacgggacagccttt
Rv( <i>OPT3</i> CDS)	<b>ggcgccgcacaactttgtacaagaaagttgggt</b> gaaaacgggacagcctttgg
Fw( <i>OPT3</i> real-time)	ctcttcacgtcttgaccactc
Rv( <i>OPT3</i> real-time)	acttgtttctctctcgtgc
Fw(F-box real-time)	tttcggctgagaggttcgagt
Rv(F-box real-time)	gattccaagacgtaagcagatcaa

CDS\*, CDS with stop codon. *att* sites are marked in bold.

## REFERENCE

Alonso JM, Stepanova AN, Leisse TJ, Kim CJ, Chen H, Shinn P, Stevenson DK, Zimmerman J, Barajas P, Cheuk R, Gadrinab C, Heller C, Jeske A, Koesema E, Meyers CC, Parker H, Prednis L, Ansari Y, Choy N, Deen H, Geralt M, Hazari N, Hom E, Karnes M, Mulholland C, Ndubaku R, Schmidt I, Guzman P, Aguilar-Henonin L, Schmid M, Weigel D, Carter DE, Marchand T, Risseuw E, Brogden D, Zeko A, Crosby WL, Berry CC, Ecker JR (2003) Genome-Wide Insertional Mutagenesis of Arabidopsis

thaliana. *Science* **301**: 653-657

**Arteca RN, Arteca JM** (2000) A novel method for growing *Arabidopsis thaliana* plants hydroponically. *Physiologia Plantarum* **108**: 188-193

**Bogs J, Bourbonloux A, Cagnac O, Wachter A, Rausch T, Delrot S** (2003) Functional characterization and expression analysis of a glutathione transporter, BjGT1, from *Brassica juncea*: evidence for regulation by heavy metal exposure. *Plant Cell and Environment* **26**: 1703-1711

**Bourbouloux A, Shahi P, Chakladar A, Delrot S, Bachhawat AH** (2000) Hgt1p, a high affinity glutathione transporter from the yeast *Saccharomyces cerevisiae*. *Journal of Biological Chemistry* **275**: 13259-13265

**Cagnac O, Bourbonloux A, Chakrabarty D, Zhang MY, Delrot S** (2004) AtOPT6 transports glutathione derivatives and is induced by primisulfuron. *Plant Physiology* **135**: 1378-1387

**Cailliatte R, Schikora A, Briat J-F, Mari S, Curie C** (2010) High-Affinity Manganese Uptake by the Metal Transporter NRAMP1 Is Essential for *Arabidopsis* Growth in Low Manganese Conditions. *Plant Cell* **22**: 904-917

**Chen A, Komives EA, Schroeder JI** (2006) An improved grafting technique for mature *Arabidopsis* plants demonstrates long-distance shoot-to-root transport of phytochelatin in *Arabidopsis*. *Plant physiology* **141**: 108-120

**Clemens S** (2001) Molecular mechanisms of plant metal tolerance and homeostasis. *Planta* **212**: 475-486

**Clemens S, Antosiewicz DM, Ward JM, Schachtman DP, Schroeder JI** (1998) The plant cDNA LCT1 mediates the uptake of calcium and cadmium in yeast. *Proc Natl Acad Sci U S A* **95**: 12043-12048

**Clemens S, Kim EJ, Neumann D, Schroeder JI** (1999) Tolerance to toxic metals by a gene family of phytochelatin synthases from plants and yeast. *Embo J* **18**: 3325-3333

- Clough SJ, Bent AF** (1998) Floral dip: a simplified method for *Agrobacterium*-mediated transformation of *Arabidopsis thaliana*. *Plant Journal* **16**: 735-743
- Danku JMC, Gumaelius L, Baxter I, Salt DE** (2009) A high-throughput method for *Saccharomyces cerevisiae* (yeast) ionomics. *Journal of Analytical Atomic Spectrometry* **24**: 103-107
- Diener AC, Li H, Zhou W, Whoriskey WJ, Nes WD, Fink GR** (2000) Sterol methyltransferase 1 controls the level of cholesterol in plants. *The Plant Cell Online* **12**: 853-870
- Goderis IJWM, De Bolle MFC, François IEJA, Wouters PFJ, Broekaert WF, Cammue BPA** (2002) A set of modular plant transformation vectors allowing flexible insertion of up to six expression units. *Plant Molecular Biology* **50**: 17-27
- Gong JM, Lee DA, Schroeder JI** (2003) Long-distance root-to-shoot transport of phytochelatin and cadmium in *Arabidopsis*. *Proceedings of the National Academy of Sciences of the United States of America* **100**: 10118-10123
- Grill E, Löffler, S., Winnacker, E. L., Zenk, M. H.** (1989) Phytochelatin, the heavy-metal-binding peptides of plants, are synthesized from glutathione by a specific gamma-glutamylcysteine dipeptidyl transpeptidase (phytochelatin synthase). *Proc Natl Acad Sci U S A* **86**: 6838-6842
- Ha SB, Smith AP, Howden R, Dietrich WM, Bugg S, O'Connell MJ, Goldsbrough PB, Cobbett CS** (1999) Phytochelatin synthase genes from *Arabidopsis* and the yeast *Schizosaccharomyces pombe*. *Plant Cell* **11**: 1153-1163
- Howden R, Goldsbrough PB, Andersen CR, Cobbett CS** (1995) Cadmium-sensitive, *Cad1* Mutants of *Arabidopsis-Thaliana* Are Phytochelatin Deficient. *Plant Physiology* **107**: 1059-1066
- Jefferson RA, Kavanagh TA, Bevan MW** (1987) GUS fusions: beta-glucuronidase as a sensitive and versatile gene fusion marker in higher plants. *The EMBO journal* **6**: 3901-3907

- Kierszniowska S, Seiwert B, Schulze WX** (2009) Definition of Arabidopsis sterol-rich membrane microdomains by differential treatment with methyl- $\beta$ -cyclodextrin and quantitative proteomics. *Molecular & Cellular Proteomics* **8**: 612-623
- Koh S, Wiles AM, Sharp JS, Naider FR, Becker JM, Stacey G** (2002) An oligopeptide transporter gene family in Arabidopsis. *Plant Physiology* **128**: 21-29
- Lahner B, Gong J, Mahmoudian M, Smith EL, Abid KB, Rogers EE, Guerinot ML, Harper JF, Ward JM, McIntyre L, Schroeder JI, Salt DE** (2003) Genomic scale profiling of nutrient and trace elements in Arabidopsis thaliana. *Nat Biotechnol* **21**: 1215-1221
- Lu YP, Li ZS, Rea PA** (1997) AtMRP1 gene of Arabidopsis encodes a glutathione S-conjugate pump: isolation and functional definition of a plant ATP-binding cassette transporter gene. *Proceedings of the National Academy of Sciences of the United States of America* **94**: 8243-8248
- Mendoza-Cozatl DG, Butko E, Springer F, Torpey JW, Komives EA, Kehr J, Schroeder JI** (2008) Identification of high levels of phytochelatins, glutathione and cadmium in the phloem sap of Brassica napus. A role for thiol-peptides in the long-distance transport of cadmium and the effect of cadmium on iron translocation. *Plant Journal* **54**: 249-259
- Mendoza-Cozatl DG, Zhai Z, Jobe TO, Akmakjian GZ, Song WY, Limbo O, Russell MR, Kozlovskyy VI, Martinoia E, Vatamaniuk OK** (2010) Schizosaccharomyces pombe Abc2 transporter mediates phytochelatin accumulation in vacuoles and confers cadmium tolerance. *Journal of Biological Chemistry* **285**: 40416-40426
- Nakagawa T, Suzuki T, Murata S, Nakamura S, Hino T, Maeo K, Tabata R, Kawai T, Tanaka K, Niwa Y, Watanabe Y, Nakamura K, Kimura T, Ishiguro S** (2007) Improved gateway binary vectors: High-performance vectors for creation of fusion constructs in Transgenic analysis of plants. *Bioscience Biotechnology and Biochemistry* **71**: 2095-2100
- Neff MM, Neff JD, Chory J, Pepper AE** (1998) dCAPS, a simple technique for the

genetic analysis of single nucleotide polymorphisms: experimental applications in *Arabidopsis thaliana* genetics. *The Plant Journal* **14**: 387-392

**Neff MM, Turk E, Kalishman M** (2002) Web-based primer design for single nucleotide polymorphism analysis. *Trends in Genetics* **18**: 613-615

**Ortiz DF, Kreppel L, Speiser DM, Scheel G, McDonald G, Ow DW** (1992) Heavy metal tolerance in the fission yeast requires an ATP-binding cassette-type vacuolar membrane transporter. *EMBO J.* **11**: 3491-3499

**Osawa H, Stacey G, Gassmann W** (2006) ScOPT1 and AtOPT4 function as proton-coupled oligopeptide transporters with broad but distinct substrate specificities. *Biochemical Journal* **393**: 267-275

**Pence NS, Larsen PB, Ebbs SD, Letham DLD, Lasat MM, Garvin DF, Eide D, Kochian LV** (2000) The molecular physiology of heavy metal transport in the Zn/Cd hyperaccumulator *Thlaspi caerulescens*. *Proceedings of the National Academy of Sciences of the United States of America* **97**: 4956-4960

**Pfaffl MW, Horgan GW, Dempfle L** (2002) Relative expression software tool (REST (c)) for group-wise comparison and statistical analysis of relative expression results in real-time PCR. *Nucleic Acids Research* **30**: e36

**Romanyuk ND, Rigden DJ, Vatamaniuk OK, Lang A, Cahoon RE, Jez JM, Rea PA** (2006) Mutagenic definition of a papain-like catalytic triad, sufficiency of the N-terminal domain for single-site core catalytic enzyme acylation, and C-terminal domain for augmentative metal activation of a eukaryotic phytochelatin synthase. *Plant Physiol* **141**: 858-869

**Rus A, Baxter I, Muthukumar B, Gustin J, Lahner B, Yakubova E, Salt DE** (2006) Natural variants of AtHKT1 enhance Na<sup>+</sup> accumulation in two wild Populations of *Arabidopsis*. *Plos Genetics* **2**: 1964-1973

**Shigaki T, Hirschi K** (2000) Characterization of CAX-like genes in plants: implications for functional diversity. *Gene* **257**: 291-298



- Shimizu R, Ji JB, Kelsey E, Ohtsu K, Schnable PS, Scanlon MJ** (2009) Tissue Specificity and Evolution of Meristematic WOX3 Function. *Plant Physiology* **149**: 841-850
- Song W, Park J, Mendoza-Cózatl D, Suter-Grotemeyer M, Shim D, Hörtensteiner S, Geisler M, Weder B, Rea P, Rentsch D** (2010) Arsenic tolerance in Arabidopsis is mediated by two ABCC-type phytochelatin transporters. *Proceedings of the National Academy of Sciences* **107**: 21187-21192
- Song WY, Martinoia E, Lee J, Kim D, Kim DY, Vogt E, Shim D, Choi KS, Hwang I, Lee Y** (2004) A novel family of cys-rich membrane proteins mediates cadmium resistance in Arabidopsis. *Plant Physiology* **135**: 1027-1039
- Speiser DM, Ortiz DF, Kreppel L, Scheel G, McDonald G, Ow DW** (1992) Purine biosynthetic genes are required for cadmium tolerance in *Schizosaccharomyces pombe*. *Mol Cell Biol* **12**: 5301-5310
- Stacey MG, Koh S, Becker J, Stacey G** (2002) AtOPT3, a Member of the Oligopeptide Transporter Family, Is Essential for Embryo Development in Arabidopsis. *Plant Cell* **14**: 2799-2811
- Stacey MG, Patel A, McClain WE, Mathieu M, Remley M, Rogers EE, Gassmann W, Blevins DG, Stacey G** (2008) The Arabidopsis AtOPT3 protein functions in metal homeostasis and movement of iron to developing seeds. *Plant Physiol* **146**: 589-601
- Stacey MG, Patel A, McClain WE, Mathieu M, Remley M, Rogers EE, Gassmann W, Blevins DG, Stacey G** (2008) The Arabidopsis AtOPT3 protein functions in metal homeostasis and movement of iron to developing seeds. *Plant Physiology* **146**: 589-601
- Stadtman ER** (1990) Metal ion-catalyzed oxidation of proteins: biochemical mechanism and biological consequences. *Free Radic Biol Med* **9**: 315-325
- Thomine S, Wang R, Ward JM, Crawford NM, Schroeder JI** (2000) Cadmium

and iron transport by members of a plant metal transporter family in Arabidopsis with homology to Nramp genes. Proceedings of the National Academy of Sciences of the United States of America **97**: 4991-4996

**Vande Weghe JG, Ow DW** (2001) Accumulation of metal-binding peptides in fission yeast requires hmt2+. Mol Microbiol **42**: 29-36

**Vatamaniuk OK, Bucher, E. A., Ward, J. T., Rea, P. A.** (2001) A new pathway for heavy metal detoxification in animals. Phytochelatin synthase is required for cadmium tolerance in *Caenorhabditis elegans*. J Biol Chem **276**: 20817-20820

**Vatamaniuk OK, Mari S, Lang A, Chalasani S, Demkiv LO, Rea PA** (2004) Phytochelatin synthase, a dipeptidyltransferase that undergoes multisite acylation with gamma-glutamylcysteine during catalysis: stoichiometric and site-directed mutagenic analysis of arabidopsis thaliana PCS1-catalyzed phytochelatin synthesis. J Biol Chem **279**: 22449-22460

**Vatamaniuk OK, Mari S, Lu YP, Rea PA** (2000) Mechanism of heavy metal ion activation of phytochelatin (PC) synthase: blocked thiols are sufficient for PC synthase-catalyzed transpeptidation of glutathione and related thiol peptides. J Biol Chem **275**: 31451-31459

**Vatamaniuk OK, Mari, S., Lu, Y. P., Rea, P. A.** (1999) AtPCS1, a phytochelatin synthase from Arabidopsis: isolation and in vitro reconstitution. Proc Natl Acad Sci U S A **96**: 7110-7115

**Vert G, Grotz N, Dedaldechamp F, Gaymard F, Guerinot ML, Briat JF, Curie C** (2002) IRT1, an Arabidopsis transporter essential for iron uptake from the soil and for plant growth. The Plant Cell Online **14**: 1223-1233

**Waalkes MP** (2000) Cadmium carcinogenesis in review. J Inorg Biochem **79**: 241-244

**Waisberg M, Joseph, P., Hale, B., Beyersmann, D.** (2003) Molecular and cellular mechanisms of cadmium carcinogenesis. Toxicology **192**: 95-117

- Wintz H, Fox T, Wu YY, Feng V, Chen WQ, Chang HS, Zhu T, Vulpe C (2003)** Expression profiles of *Arabidopsis thaliana* in mineral deficiencies reveal novel transporters involved in metal homeostasis. *Journal of Biological Chemistry* **278**: 47644-47653
- Wong CKE, Cobbett CS (2009)** HMA P-type ATPases are the major mechanism for root-to-shoot Cd translocation in *Arabidopsis thaliana*. *New Phytologist* **181**: 71-78
- Zhai Z, Jung HI, Vatamaniuk OK (2009)** Isolation of protoplasts from tissues of 14-day-old seedlings of *Arabidopsis thaliana*. *J Vis Exp*: pii: 1149. doi: 1110.3791/1149
- Zhai Z, Sooksa-nguan T, Vatamaniuk OK (2009)** Establishing RNA interference as a reverse-genetic approach for gene functional analysis in protoplasts. *Plant Physiology* **149**: 642-652
- Zhang MY, Bourbonloux A, Cagnac O, Srikanth CV, Rentsch D, Bachhawat AK, Delrot S (2004)** A novel family of transporters mediating the transport of glutathione derivatives in plants. *Plant Physiology* **134**: 482-491

## CHAPTER 2

*Schizosaccharomyces pombe* Abc2 transporter mediates phytochelatin accumulation in vacuoles and confers cadmium tolerance

Mendoza-Cózatl DG, Zhai Z, Jobe TO, Akmakjian GZ, Song WY, Limbo O, Russell MR, Kozlovskyy VI, Martinoia E, Vatamaniuk OK, Russell P, Schroeder JI (2010).

Published in *J Biol Chem.*, December 2010, Vol. 285, No. 52, pp. 40416-40426

### ABSTRACT

This part of my dissertation has been done in collaboration with three other groups (Drs. Julian Schroeder [UCSD, CA, USA], Paul Russell [The Scripps Research Institute, CA, US] and Dr. Enrico Martinoia [University Zurich, Switzerland]). My contribution was in the isolation of intact vacuoles from Cd-cultured *S. pombe* mutant lines and analysis of PCs and low and high-molecular weight Cd-PC complexes using RP-HPLC and gel-filtration chromatography. Our efforts led to the identification of Abc2, a long-sought vacuolar phytochelatin transporter in *Schizosaccharomyces pombe*.

### INTRODUCTION

PCs are small, metal-binding peptides with the general structure  $(\gamma\text{-Glu-Cys})_n\text{-Gly}$  ( $n=2-11$ ) (Kondo et al., 1984; Grill et al., 1985; Jackson et al., 1987). They have been found in virtually all plants, algae, certain fungi and the nematode *C. elegans* (Grill et al., 1985; Mutoh and Hayashi, 1988; Hayashi et al., 1991; Clemens, 2001; Vatamaniuk et al., 2001). PCs are synthesized from glutathione (GSH) and related

thiols by PC synthases (PCS),  $\gamma$ -glutamylcysteine dipeptidyl transpeptidases (EC 2.3.2.15), that in the presence of heavy metals transfer the  $\gamma$ -glutamylcysteinyl moiety from one molecule of GSH or previously synthesized PCs, onto the N-terminus of GSH or PCs to generate polymers containing 2-11  $\gamma$ -Glu-Cys repeats, followed by C-terminus Gly (Grill, 1989; Vatamaniuk et al., 2000; Vatamaniuk et al., 2004). Once produced, PCs efficiently chelate Cd and other heavy metals and form low-molecular-weight cytosolic PC-Cd complexes, which are transported into the vacuole where high-molecular-weight complexes are formed and stabilized by incorporation of inorganic  $S^{2-}$  (Ortiz et al., 1992; Speiser et al., 1992; Vande Weghe and Ow, 2001).

Early studies in isolated vacuoles indicated that PC transport was mediated by ABC-type transporters (Ortiz et al., 1995; Salt and Rauser, 1995). In *S. pombe*, HMT1, a half-molecule ABC transporter (comprising only one NBF and one TMD) had been long believed to be the PC-Cd transporter on the vacuolar membrane because: first, it is vacuolar membrane localized; second, *S. pombe hmt1* mutant cells are hypersensitive to Cd; third, vacuolar membrane enriched vesicles isolated from *S. pombe hmt1* mutant cells overexpressing SpHMT1 conferred Cd-PC transport *in vitro* (Ortiz, 1995). Although the *A. thaliana* genome encodes 129 ABC proteins, it lacks the HMT1 orthologue (Sanchez-Fernandez et al.). Interestingly, orthologues of HMT1 are present in animals including *Drosophila* and humans, which do not possess PC synthase machinery. That raised the question that either HMT's functions have diverged in different species or that they function in metal detoxification by another mechanism. Our genetic studies of CeHMT1, an SpHMT1 orthologues in *C. elegans*, and biochemical studies of HMT1 of *Drosophila* and *S. pombe* showed that HMTs

function in Cd detoxification is conserved in different species, but they are not *bona fide* Cd-PC transporters and while they may mediate Cd-PC transport, they function in heavy metal tolerance by another mechanism (Vatamaniuk et al 2005, Sooksa-nguan et al, 2009). Data from our lab were further complemented by the finding of our colleagues that showed that SpHMT1 confers Cd tolerance independently of PC synthase (Preveral, 2009). Therefore, the identity of vacuolar membrane Cd-PC transporter(s) in plants, *S. pombe* and *C. elegans* is unknown.

Having only 5 ABC transporters, ABC1-4 and Hmt1, located to the vacuolar membrane, makes *S. pombe* an ideal system for screening for PC transporters if they belong to the ABC transporter family. The series of *S. pombe* mutants for ABC1-4 and Hmt1 produced by the Russell lab were used in this study to screen for PC transporters. Our rationale was that vacuoles isolated from Cd-treated mutant cells lacking a vacuolar heavy metal PC transporter will also lack PCs and heavy metal PC complexes. By doing this, we found Abc2, a full-size ABC transporter of the MRP/ABCC subfamily, mediates accumulation of PCs in *S. pombe* vacuoles. This was shown by Cd sensitivity assays using ABC transporter deletion mutants, complementation experiments and analyses of the PC content in purified vacuoles from Cd-cultured mutant strains. The identification of Abc2 as a PC transporter opens the possibility to identify the long-sought PC transporters in plants and other organisms.

## RESULTS AND DISCUSSION

This section presents only results from my own experiments that were included into the published manuscript.

### **Abc2 mediates PC accumulation in vacuoles.**

To identify which of five, vacuolar membrane-localized ABC transporters of *S. pombe* contribute to Cd-PC transport, intact vacuoles were isolated from the Cd-cultured mutants lacking either individual or all five vacuolar ABC transporters and vacuolar PC content was determined by reverse-phase (RP)-HPLC. It was found that vacuoles isolated from wild-type cells accumulated high levels of PCs (Fig. 1). As we found previously (Sooksa-Nguan et al., 2009), the vacuoles from *hmt1* mutant strain exhibited a reduction in PC<sub>2</sub> content but the PC<sub>3</sub> content remained unaffected (Fig. 1).

Likewise, vacuoles from the *abc2* mutant showed a significant reduction in PC<sub>2</sub> content. In contrast, PCs were not detected in vacuoles from either the *abc1-4hmt1* quintuple or *abc2hmt1* double mutants (Fig. 1). Expression of *Abc2* restored accumulation of both PC<sub>2</sub> and PC<sub>3</sub> in *abc1-4hmt1* vacuoles, demonstrating that *Abc2* is sufficient to mediate PC accumulation in *S. pombe* vacuoles *in vivo* (Fig. 1). Expression of *HMT1* also restored the accumulation of PCs in vacuoles (Fig. 1) and, as previously reported, Cd tolerance (Ortiz et al., 1992). These results suggest that both *HMT1* and *Abc2* mediate vacuolar accumulation of PCs. One central implication of this finding is that, in contrast to *HMT1*, plants have *Abc2* homologues (MRP/ABCC subfamily of ABC-type transporters), providing a new avenue to address the long-standing problem of how PCs are sequestered into plant vacuoles.

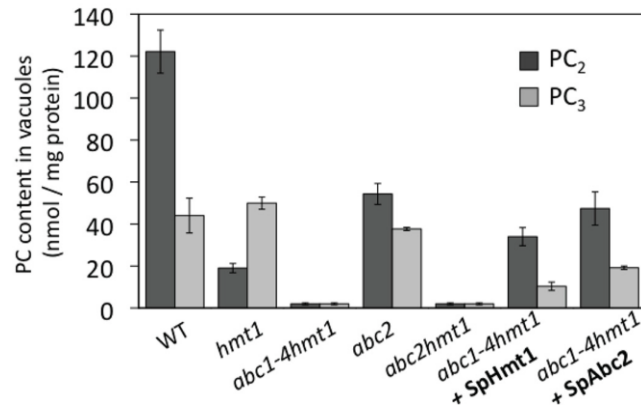


**Figure 1.** PC accumulation in vacuoles was decreased in the *hmt1* mutant and abolished in the *abc1-4 hmt1* quintuple and the *abc2 hmt1* double mutant. Expression of *Abc2* in the *abc1-4 hmt1* quintuple mutant restored the accumulation of PCs in vacuoles. *Hmt1* also restored vacuolar accumulation of PCs. Note: Figure 1 is Figure 3F in the published manuscript.

#### **Abc2 contributes to accumulation of HMWCs in vacuoles.**

Cadmium, PCs, and sulfide form high molecular weight complexes (HMWCs) surrounding cadmium-sulfur cores (CdS) and these complexes are considered the final step in Cd sequestration inside vacuoles (Speiser et al., 1992; Wu et al., 1995).

HMWCs were analyzed in vacuole preparations obtained from the *abc* mutants. We found that *S. pombe* wild-type vacuoles accumulated HMWCs (Fig. 2A) in the same fractions as *in vitro* synthesized HMWCs (Fig. 2B). The *hmt1* mutant exhibited a decreased content of these complexes (Fig. 2A), while the *abc2hmt1* double mutant had a negligible content of HMWC in vacuoles (Fig.2A).



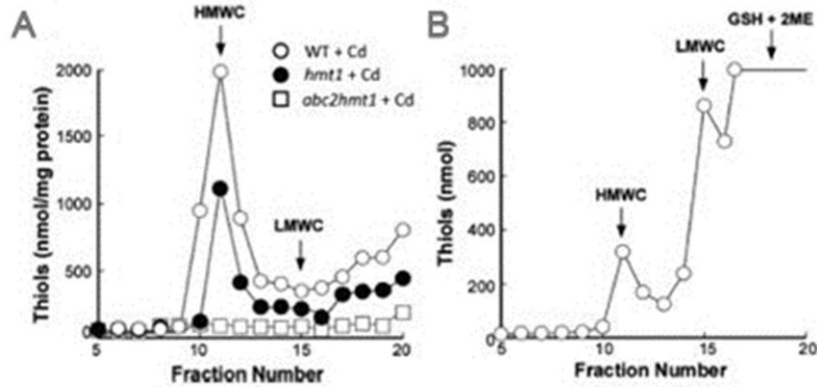


**Figure 2.** HMWCs in purified vacuoles from *S. pombe* wild type (A, open circles) have an identical elution pattern compared with a HMWC standard synthesized *in vitro* (B). Vacuoles isolated from the *hmt1* mutant showed reduced content of HMWCs (A, filled circles) whereas no HMWCs were detected in purified vacuoles isolated from the *abc2 hmt1* double mutant (A, open squares). Figure 2A and B are Figure 4G and H respectively in the published manuscript.

In conclusion, we have determined that Abc2, a full-size ABC transporter of the MRP/ABCC family, mediates accumulation of PCs and HMW Cd-PC complexes in vacuoles. The identification of Abc2 as a PC transporter opens the possibility to identify the long-sought PC transporters in plants and other organisms. These transporters, in combination with other genes, hold the potential to enhance the heavy metal tolerance and accumulation capacity of organisms for their use in bioremediation of soils and waters contaminated with heavy metals, or for circumventing heavy metal accumulation in edible parts of crop plants.

## MATERIALS AND METHODS

Below, I provided only methods from my own experiments that were included into the manuscript.

## Yeast strains

*Schizosaccharomyces pombe* strains used in this work are described in Table 1.

**Table 1** *Schizosaccharomyces pombe* strains used in this study.

Strain	Genotype	Source
Wild type	h- ura4-D18 leu1-32	
<i>pcs</i>	h- ura4-D18 leu1-32 pcs::kanMX4	This study
<i>hmt1</i>	h- ura4-D18 leu1-32 hmt1::natMX6	This study
<i>pcshmt1</i>	h- ura4-D18 leu1-32 hmt1::natMX6 pcs::kanMX4	This study
<i>abc2</i>	h- ura4-D18 leu1-32 ade6 abc2::kanMX4	This study
<i>abc2hmt1</i>	h- ura4-D18 leu1-32 ade6 abc2::kanMX4 hmt1::natMX6	This study
<i>abc3hmt1</i>	h- ura4-D18 leu1-32 ade6 abc3::kanMX4 hmt1::natMX6	This study
<i>abc4hmt1</i>	h- ura4-D18 leu1-32 abc4::kanMX4 hmt1::natMX6	This study
<i>abc2abc3hmt1</i>	h- ura4-D18 leu1-32 ade6 abc2::kanMX4 abc3::kanMX4 hmt1::natMX6	This study
<i>abc2abc4hmt1</i>	h- ura4-D18 leu1-32 abc2::kanMX4 abc4::kanMX4 hmt1::natMX6	This study
<i>abc1abc2abc3abc4</i>	h- ura4-C190T leu1-32 ade7::ura4 abc1::ura4 abc2::ura4 abc3::ura4 abc4::ura4	(Iwaki et al., 2006)
<i>abc1abc2abc3abc4hmt1</i>	h- ura4-C190T leu1-32 ade7::ura4 abc1::ura4 abc2::ura4 abc3::ura4 abc4::ura4 hmt1::natMX6	This study

## Vacuole isolation and vacuolar PC and HMWC measurements

For the isolation of intact vacuoles for subsequent PC and HMWC analyses, *S. pombe* cells were cultured in EMM medium supplemented or not with Cd as described (Sooksa-Nguan et al., 2009). Briefly, 200-ml volumes of stationary phase cultures

were diluted into 1.5 liters of EMM and grown for 4–6 h at 30 °C after which time CdCl<sub>2</sub> was added to a final concentration of 500 µM to activate PC production. Cells were cultured in the presence of CdCl<sub>2</sub> for an additional 18 h, collected by centrifugation, converted to spheroplasts, disrupted and subjected to fractionation by differential centrifugation as described (Sooksa-Nguan et al., 2009). PC content was analyzed in intact vacuoles by HPLC, followed by thiol quantification with Ellman's reagent as described (Vatamaniuk et al., 2000).

HMWC in intact vacuoles were analyzed by gel-filtration FPLC using an AKTA purifier FPLC system (GE Healthcare, NJ, USA). Aliquots of vacuoles (100 µg protein) were injected onto a Superdex peptide 10/300GL column (GE Healthcare) equilibrated with 50 mM Tris-HCl, pH 7.8. The column was developed with the same buffer at a flow rate of 0.5 ml/min; fractions (1 ml) were collected, reacted with Ellman's reagent and analyzed spectrophotometrically at 412 nm as described (Vatamaniuk et al., 2000). The elution profiles of protein markers including cytochrome C (Mr 12,500), aprotinin (Mr 6,512) and vitamin B12 (Mr 1,355) (GE Healthcare, NJ, USA) were analyzed using the same conditions, and detected in collected fractions using the UV detector of the FPLC system.

LMWC standard (a mixture of different chain length PCs) was synthesized *in vitro* using purified AtPCS1-FLAG (Vatamaniuk et al., 2000). HMWC standards were produced from LMWC by addition of CdCl<sub>2</sub> (500 µM final) and Na<sub>2</sub>S to (10-fold molar excess to PCs in LMWC). *In vitro*-synthesized LMWC and HMWC were separated by FPLC as described above.

## REFERENCES

- Clemens S, Schroeder, J. I., Degenkolb, T.** (2001) *Caenorhabditis elegans* expresses a functional phytochelatin synthase. *Eur J Biochem* **268**: 3640-3643
- Grill E, Loffler, S., Winnacker, E. L., Zenk, M. H.** (1989) Phytochelatin, the heavy-metal-binding peptides of plants, are synthesized from glutathione by a specific gamma-glutamylcysteine dipeptidyl transpeptidase (phytochelatin synthase). *Proc Natl Acad Sci U S A* **86**: 6838-6842
- Grill E, Winnacker EL, Zenk MH** (1985) Phytochelatin - the Principal Heavy-Metal Complexing Peptides of Higher-Plants. *Science* **230**: 674-676
- Grill E, Winnacker EL, Zenk MH** (1985) Phytochelatin: The Principal Heavy-Metal Complexing Peptides of Higher Plants. *Science* **230**: 674-676
- Hayashi Y, Isobe M, Mutoh N, Nakagawa CW, Kawabata M** (1991) Cadystins: small metal-binding peptides. *Methods Enzymol* **205**: 348-358
- Iwaki T, Giga-Hama Y, Takegawa K** (2006) A survey of all 11 ABC transporters in fission yeast: two novel ABC transporters are required for red pigment accumulation in a *Schizosaccharomyces pombe* adenine biosynthetic mutant. *Microbiology* **152**: 2309-2321
- Jackson PJ, Unkefer CJ, Doolen JA, Watt K, Robinson NJ** (1987) Poly(Gamma-Glutamylcysteinyl)Glycine - Its Role in Cadmium Resistance in Plant-Cells. *Proceedings of the National Academy of Sciences of the United States of America* **84**: 6619-6623
- Kondo N, Imai K, Isobe M, Goto T, Murasugi A, Wadanakagawa C, Hayashi Y** (1984) Cadystin-a and Cadystin-B, Major Unit Peptides Comprising Cadmium Binding Peptides Induced in a Fission Yeast ----- Separation, Revision of Structures and Synthesis. *Tetrahedron Letters* **25**: 3869-3872
- Mutoh N, Hayashi Y** (1988) Isolation of mutants of *Schizosaccharomyces pombe* unable to synthesize cadystin, small cadmium-binding peptides. *Biochem.*

Biophys. Res. Commun. **151**: 32-39

**Ortiz DF, Kreppel L, Speiser DM, Scheel G, McDonald G, Ow DW** (1992) Heavy metal tolerance in the fission yeast requires an ATP-binding cassette-type vacuolar membrane transporter. *EMBO J.* **11**: 3491-3499

**Ortiz DF, Ruscitti T, McCue KF, Ow DW** (1995) Transport of metal-binding peptides by Hmt1, a fission yeast ABC-type vacuolar membrane protein. *J. Biol. Chem.* **270**: 4721-4728

**Ortiz DF, Ruscitti, T., McCue, K.F., Ow, D. W.** (1995) Transport of Metal-binding Peptides by HMT1, A Fission Yeast ABC-type Vacuolar Membrane Protein. *J. Biol. Chem.* **270**: 4721-4728

**Salt DE, Rauser WE** (1995) MgATP-dependent transport of phytochelatin across the tonoplast of oat roots. *Plant Phys.* **107**: 1293-1301

**Sooksa-Nguan T, Yakubov B, Kozlovskyy VI, Barkume CM, Howe KJ, Thannhauser TW, Rutzke MA, Hart JJ, Kochian LV, Rea PA, Vatamaniuk OK** (2009) Drosophila ABC transporter, DmHMT-1, confers tolerance to cadmium. DmHMT-1 and its yeast homolog, SpHMT-1, are not essential for vacuolar phytochelatin sequestration. *J Biol Chem* **284**: 354-362

**Speiser DM, Ortiz DF, Kreppel L, Scheel G, McDonald G, Ow DW** (1992) Purine biosynthetic genes are required for cadmium tolerance in *Schizosaccharomyces pombe*. *Mol Cell Biol* **12**: 5301-5310

**Vande Weghe JG, Ow DW** (2001) Accumulation of metal-binding peptides in fission yeast requires hmt2+. *Mol Microbiol* **42**: 29-36

**Vatamaniuk OK, Bucher EA, Ward JT, Rea PA** (2001) A new pathway for heavy metal detoxification in animals. Phytochelatin synthase is required for cadmium tolerance in *Caenorhabditis elegans*. *J Biol Chem* **276**: 20817-20820

**Vatamaniuk OK, Mari S, Lang A, Chalasani S, Demkiv LO, Rea PA** (2004) Phytochelatin synthase, a dipeptidyltransferase that undergoes multisite

acylation with gamma-glutamylcysteine during catalysis: stoichiometric and site-directed mutagenic analysis of arabidopsis thaliana PCS1-catalyzed phytochelatin synthesis. *J Biol Chem* **279**: 22449-22460

**Vatamaniuk OK, Mari S, Lu YP, Rea PA** (2000) Mechanism of heavy metal ion activation of phytochelatin (PC) synthase: blocked thiols are sufficient for PC synthase-catalyzed transpeptidation of glutathione and related thiol peptides. *J Biol Chem* **275**: 31451-31459

**Vatamaniuk OK, Mari S, Lu YP, Rea PA** (2000) Mechanism of heavy metal ion activation of phytochelatin (PC) synthase: blocked thiols are sufficient for PC synthase-catalyzed transpeptidation of glutathione and related thiol peptides. *J Biol Chem* **275**: 31451-31459

**Wu JS, Sung HY, Juang RH** (1995) Transformation of cadmium-binding complexes during cadmium sequestration in fission yeast. *Biochem Mol Biol Int* **36**: 1169-1175

For further details, see: Mendoza-Cózatl DG, **Zhai Z**, Jobe TO, Akmakjian GZ, Song WY, Limbo O, Russell MR, Kozlovskyy VI, Martinoia E, Vatamaniuk OK, Russell P, Schroeder JI (2010). Tonoplast-localized Abc2 transporter mediates phytochelatin accumulation in vacuoles and confers cadmium tolerance. *J Biol Chem.*, 285(52):40416-26. Epub 2010 Oct 11.

## CHAPTER 3

### Establishing RNA Interference as a Reverse-Genetic Approach for Gene Functional Analysis in Protoplasts

Zhiyang Zhai, Thanwalee Sooksa-nguan, and Olena K. Vatamaniuk

Published in *Plant Physiology*, February 2009, Vol. 149, pp. 642–652

#### ABSTRACT

Double-stranded (ds) RNA interference (RNAi) is widely used for functional analysis of plant genes and is achieved via generating stable transformants expressing dsRNA in planta. This study demonstrated that RNAi can also be utilized to examine gene functions in protoplasts. Because protoplasts are nongrowing cells, effective RNAi-triggered gene silencing depends not only on a depletion of gene transcripts but also on turnover rates of corresponding polypeptides. Herein, we tested if transient RNAi in protoplasts would result in the depletion of a targeted polypeptide and, because protoplasts have a limited life span, if functional assays of RNAi knockout genes would be feasible in protoplasts. We showed that protoplasts transfection with an in vitro-synthesized dsRNA against *Arabidopsis thaliana*  $\beta$ -glutamylcysteine synthase (*ECS1*), a key enzyme in the synthesis of glutathione, resulted in a 95% depletion of *ECS1* transcript, a 72% decrease of ECS1 polypeptide, and a 60% drop in glutathione content. These results were comparable with those obtained upon analysis of *Arabidopsis* seedlings bearing the *cad2-1* mutant allele of *ECS1*. We also improved the procedure for RNAi inactivation of several genes simultaneously. Finally, because

we isolated protoplasts from tissues of 14-d-old seedlings instead of 1-month-old mature plants, the described procedure is rapid (as it only takes 20 d from seed planting to functional studies), suitable for analyzing multiple genes in parallel, and independent of cloning dsRNAs into plant expression vectors. Therefore, RNAi in protoplasts complements existing genetic tools, as it allows rapid, cost- and space-efficient initial screening and selection of genes for subsequent in planta studies.

## INTRODUCTION

The completion of the Arabidopsis Genome Sequencing Project opened a new era in plant biology research, the challenges of which are to determine the functions of all annotated Arabidopsis (*Arabidopsis thaliana*) genes and to extend these studies to other plant species (AGI, 2000). Indeed, although the functions of 69% of the genes were classified according to sequence similarity to proteins of known function in all organisms, only 16,000 of the 29,000 predicted genes have been characterized experimentally, and these studies have been done primarily in Arabidopsis (AGI, 2000; Wortman et al., 2003). A critical step in functional analysis of plant genes is the availability of genetic tools that are applicable to different plant species, are rapid, affordable, and thus can be used as the initial step in the genome-wide screens and selection of genes with traits of interest for subsequent in-depth assessment in planta.

Double-stranded (ds) RNA interference (RNAi) is an RNA-based reverse-genetic approach currently in use for studies of gene function. RNAi silencing is triggered by the introduction of dsRNA into cells where it is detected as aberrant and is processed by the type III RNase Dicers to small, 20- to 26-nucleotide-long, short



interfering RNAs (siRNAs; Bernstein et al., 2001; Brodersen and Voinnet, 2006). One of the two siRNA strands is then incorporated into the RNA-induced-silencing complex, which uses siRNAs to recognize complementary motifs in target nucleic acids. The result is the sequence-specific inhibition of gene expression either at the transcription, mRNA stability, or translational levels (Baulcombe, 2004; Brodersen and Voinnet, 2006; Brodersen et al., 2008). The sequence specificity of RNAi-based gene inactivation allows silencing of individual genes as well as several genes simultaneously. Therefore, RNAi can be used to silence multiple members of a multigene family and homologous gene copies in polyploids by targeting sequences that are unique or shared by these related genes (Waterhouse and Helliwell, 2003; Baulcombe, 2004).

RNAi has proven to be very efficient in interfering with gene expression in various organisms, including vertebrate and invertebrate animals, and has been used for gene function studies in plant systems such as *Physcomitrella patens*, *Petunia hybrida*, *Arabidopsis*, *Papaver somniferum*, rice (*Oryza sativa*), wheat (*Triticum aestivum*), and others (Stam et al., 1997; Fire et al., 1998; Kennerdell and Carthew, 1998; Smith et al., 2000; Waterhouse et al., 2001; Waterhouse and Helliwell, 2003; Allen et al., 2004; Baulcombe 2004; Bezanilla et al., 2005; Miki et al., 2005; Travella et al., 2006; Vidali et al., 2007). In these plant species, RNAi is achieved by transforming plants with constructs that express self-complementary (hairpin) RNA-containing sequences that are homologous to targeted genes, or with constructs expressing artificial microRNAs (Waterhouse and Helliwell, 2003; Helliwell et al., 2005; Schwab et al., 2006).

The generation of the genome-wide collection of artificial microRNA-expressing plasmids and availability of transposon/T-DNA mutant alleles of *Arabidopsis* provided the plant research community with an outstanding resource for functional genomics (Alonso et al., 2003). Using these tools, however, requires growth and propagation of transgenic plants and thus imposes extensive time, labor, and space requirements for maintaining multiple plant lines. Therefore, the availability of a rapid and cost-efficient reverse-genetic approach for the initial genome-wide analysis and selection of a subset of genes of interest for subsequent in planta studies would greatly assist and expedite functional genetic studies.

In this regard, in animals, the development of efficient dsRNA delivery approaches has enabled studies of gene function in cell tissue cultures (Fire et al., 1998; Worby et al., 2001; Wilson and Richardson, 2003). Because of the simplicity of RNAi in animal cell cultures, minimal time and space are required for gene inactivation and subsequent phenotype analysis. In fact, this approach has been recently adapted to a genome-wide high-throughput format, is used as an initial screening step for genes of interest, and has resulted in the identification of novel genes with roles in cell growth and development, life span regulation, muscle differentiation, signal transduction pathways, and other processes (Clemens et al., 2000; Kamath et al., 2003; Boutros et al., 2004; Hamilton et al., 2005; Bai et al., 2008).

Aiming to develop RNAi for rapid functional genetic screens by circumventing the time- and space-intensive production of transgenic RNAi plants, we sought to test if, as in animal cells, RNAi could be used to study gene functions in isolated cells, i.e. protoplasts. We chose protoplasts for the following reasons: (1) protoplasts are easily

prepared; (2) protoplasts are used to study a wide range of cellular functions, such as cellular transport mechanisms and the subcellular localization of proteins (Chen and Halkier, 2000); (3) protoplasts can be isolated from different parts of plants (roots, stems, leaves), thus enabling studies of tissue-specific processes (e.g. nutrient uptake in root cells and storage in leaf cells); and (4) importantly, protoplasts can be readily transfected with nucleic acids (dsRNA or DNA; An et al., 2003, 2005; Yoo et al., 2007). Lastly, it has been shown that transfection of dsRNA into *Arabidopsis* protoplasts reduces the transcript level of the targeted exogenous and endogenous genes (An et al., 2003, 2005). Whether reduction of the endogenous gene-transcript leads to a depletion of the corresponding polypeptide and interferes with its function has not been determined (An et al., 2003, 2005). However, this is important to establish, because protoplasts are nongrowing cells, and the interference with gene function by transient RNAi depends not only on the depletion of transcripts but also on turnover rates of corresponding polypeptides and, thus, on the RNAi depletion of targeted polypeptides. In addition, protoplasts have limited viability; therefore, it is important to determine whether the time frame of the viability of RNAi protoplasts in the artificial media is sufficient for functional analysis. These questions need to be addressed prior to developing a high-throughput RNAi protocol in protoplasts useful for functional genetics.

Herein, we showed that effective RNAi-mediated gene silencing that was achieved in *Arabidopsis* protoplasts was applicable for analysis of gene function. We showed that the transfection of an in vitro-synthesized dsRNA against *Arabidopsis*  $\beta$ -glutamylcysteine synthase (*ECSI*), a key enzyme in the synthesis of glutathione (GSH)

into protoplasts resulted in the depletion of *ECSI* transcript, the decline of ECS1 polypeptide, and the decline of the protoplast content of the end product of ECS1 enzymatic activity, GSH. Importantly, the fold-decrease of GSH content in RNAi protoplasts was comparable with that of the *cad2-1* mutant allele of *ECSI* (Cobbett et al., 1998). We also significantly improved the procedure for the efficient silencing of genes individually and homologous members of gene families simultaneously. The procedure reported in this study is rapid; only 20 d are required for the analysis of gene function. This time period includes growth of *Arabidopsis*, in vitro dsRNA synthesis, protoplast isolation, transfection, and analysis. Therefore, RNAi in protoplasts described here illustrated a rapid, affordable, and potent reverse-genetic approach that is complementary to existing genetic tools, as it allows expediting functional analysis of plant genes and, as detailed in "Conclusion and Future Perspectives," is particularly applicable for biochemical studies for deciphering components of metabolic pathways, establishing of metabolic networks, and, perhaps, can be adapted to high-throughput metabolomics.

## RESULTS

### **Isolation of Intact Protoplasts from 14-d-Old *Arabidopsis* Seedlings and Achieving High Protoplast Transfection Efficiency**

The success of RNAi silencing of genes in protoplasts is contingent on sufficient yield and viability of isolated protoplasts and their transfection efficiency. Isolation of protoplasts was first reported more than 40 years ago (Cocking, 1960) and has since been adapted to study a variety of cellular processes, such as subcellular localization of

proteins and the isolation of intact organelles (Yoo et al., 2007). Most protoplast isolation protocols use leaf tissues of mature *Arabidopsis* (e.g. 35 d old). We modified existing protocols to decrease the time and growth chamber space that are required for isolating protoplasts from mature plants by employing 14-d-old *Arabidopsis* seedlings (Fig.1A).

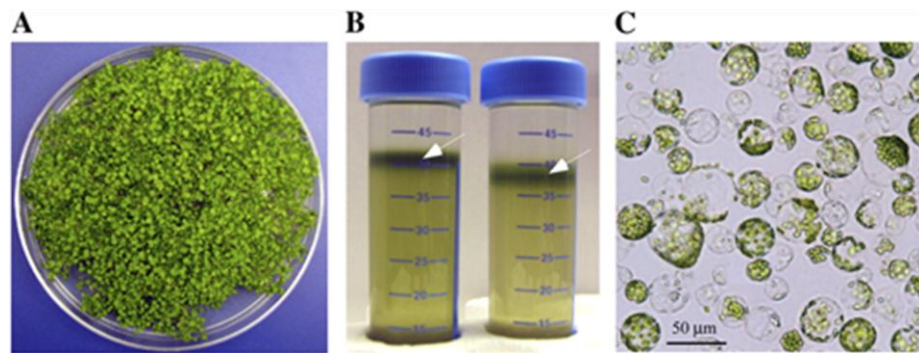


**Figure 1.** Isolation of protoplasts from *Arabidopsis* seedlings. **A**, Tissues from 14-d-old seedlings of *Arabidopsis* were collected and converted to protoplasts by a modified procedure of Chen and Halkier (2000). **B**, Protoplasts were purified by Sucrose density gradient centrifugation and collected at the interface of enzyme solution and W5 buffer (white arrows). **C**, Bright-field microscopy of protoplasts. Microphotographs were collected using a cooled CCD camera interfaced with the Zeiss Axioscope 2 plus microscope.

*Arabidopsis* seedlings were collected from a petri plate, sliced with a razor blade, and converted to protoplasts in a buffer containing Macerozyme R-10 and Cellulase (see "Materials and Methods"). The released protoplasts were purified by Sucrose density gradient centrifugation and collected at the interface of the enzyme and W5 solutions (Fig. 1B). Using this procedure, 1 g of 14-d-old seedlings yielded  $5 \times 10^6$  to  $10^7$  protoplasts (Fig. 1C). The yield of protoplasts from seedlings is comparable with preparations from leaves of mature *Arabidopsis*, but instead of 35 to 36 d, isolation of protoplasts was completed in 15 d. This improvement is significant, because it allowed

us to decrease the time required for RNAi-based analyses in protoplasts.

We then established an efficient transfection procedure for the protoplasts. We employed a simple visual assay to assess the transfection efficiency using fluorescence microscopy. We transfected protoplasts with the pSAT plasmid, expressing the nuclear-targeted red-shifted GFP (EGFP) driven by two cauliflower mosaic virus 35S promoters, oriented in tandem (Tzfira et al., 2005). Protoplasts were transfected using a poly (ethylene glycol) (PEG)-calcium-mediated transfection procedure as previously described (Yoo et al., 2007), except that we used 10 times more protoplasts than detailed in (Yoo et al., 2007). Fluorescent microscopy revealed that more than 90% of transfected protoplasts expressed the nuclear-targeted EGFP, suggesting that we achieved high transfection rates (Fig. 2, A–D).

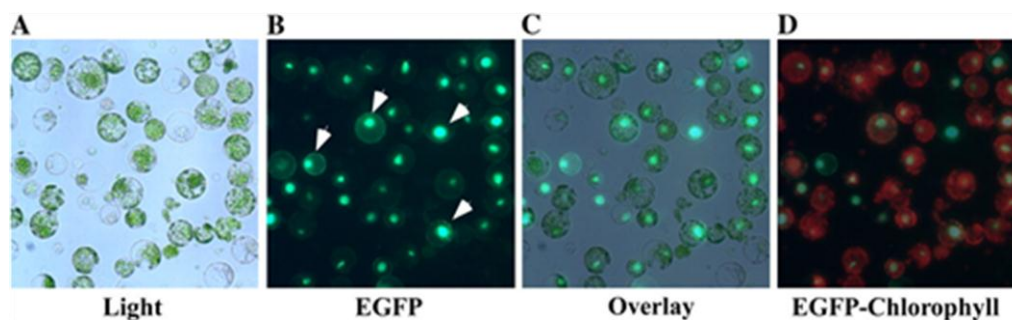


**Figure 2.** The visualization of the efficiency of the transfection of protoplasts with the pSAT vector expressing nuclear-localized EGFP. Bright-field (**A**, Light) and fluorescent microphotographs (**B**, EGFP) were collected on the Zeiss Axioscope 2 plus microscope equipped with appropriate filter sets. White arrows indicate examples of nuclear-localized, EGFP-mediated fluorescence in the pSAT plasmid-transfected protoplasts. **C**, Superimposed bright-field and fluorescent images on **A** and **B** (Overlay) were created to demonstrate the transfection efficiency. **D**, Overlaid images of autofluorescence from chloroplasts and fluorescence from EGFP (EGFP-Chlorophyll) was created to demonstrate that green fluorescence derives solely from EGFP of the pSAT vector.

### **RNAi-Mediated Silencing of the Expression of the Exogenous Gene, *EGFP*, in**

## Protoplasts

We then tested if RNAi effects indeed could be observed in protoplasts and if transfecting in vitro-synthesized dsRNA, rather than a construct expressing dsRNAs in vivo, could induce RNAi effects in protoplasts (An et al., 2005).

We synthesized dsRNA against a 500-bp-long fragment corresponding to a coding sequence of EGFP (dsRNA<sub>EGFP</sub>) and cotransfected it with pSAT-EGFP into protoplasts. To evaluate the transfection efficiency, we transfected a subset of protoplasts with the pSAT-EGFP vector alone. We also transfected a subset of protoplasts with water (mock transfection) and used these protoplasts for monitoring the autofluorescence of chlorophyll. Fluorescent microscopy analysis established that mock-transfected protoplasts exhibited little or no fluorescence in the GFP-specific filter set (Fig. 3A). Weak fluorescence in mock-transfected protoplasts was attributed to chlorophyll autofluorescence. In contrast, as determined by the nuclear-localized, EGFP-mediated fluorescence, 90% of cells transfected with the pSAT-EGFP plasmid appeared to express the plasmid (Fig. 3B). The protoplasts transfection protocol, therefore, delivered nucleic acids efficiently.

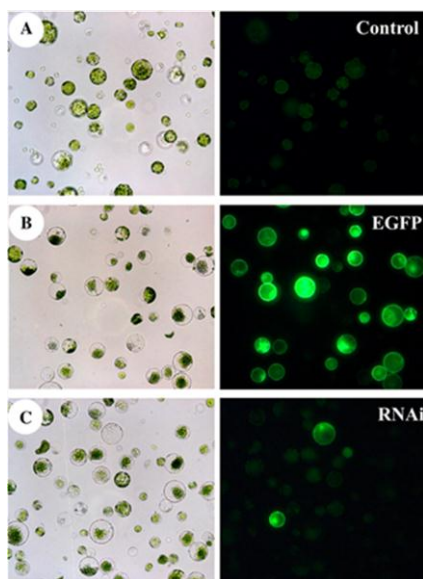


**Figure 3.** Silencing of the exogenous gene, *EGFP*, in protoplasts by RNAi. **A**, Bright-field (left) and fluorescence (right) micrographs of mock-transfected protoplasts (Control). **B**, Light (left) and fluorescence (right) micrographs of protoplasts transfected with the pSAT plasmid expressing nuclear-targeted EGFP (EGFP). **C**, Microphotographs of protoplasts cotransfected with the pSAT plasmid and in vitro-synthesized dsRNA against EGFP (RNAi). Fluorescence micrographs were taken after 24 h of transfection. Images were captured using the same exposure time.

We next tested if the introduction of dsRNA<sub>EGFP</sub> in conjunction with the pSAT-EGFP would affect the expression of EGFP. We determined that cotransfection with dsRNA<sub>EGFP</sub> substantially decreased the number of protoplasts that exhibited the EGFP-mediated fluorescence (Fig. 3C). Based on these data and previous observations (Anet al., 2003), we concluded that indeed, transfection of an in vitro synthesized dsRNA into protoplasts triggers transient RNAi effects.

### **RNAi-Mediated Silencing of the Expression of the Endogenous *Arabidopsis* Gene, *PCSI*, Depends on the Dose of Transfected dsRNA**

We next sought to assay the efficiency of RNAi effects on an endogenous *Arabidopsis* gene and to optimize the potency of RNAi effects relative to the amount of transfected dsRNA. We performed RNAi against *PCSI* (for phytochelatin synthase 1), because the expression of its mRNA in *Arabidopsis* is well characterized (Vatamaniuk et al., 1999, 2000). The reverse transcription (RT)-PCR analysis of mock- and dsRNA<sub>PCSI</sub>-transfected protoplasts established that transfection with 1  $\mu\text{g}$  of dsRNA<sub>PCSI</sub> decreased the abundance of *PCSI* transcript by 60% in comparison with the mock-transfected protoplasts (Fig. 4, A and B). The potency of RNAi effects, however, increased with a higher dose of transfected dsRNA<sub>PCSI</sub> (Fig. 4, A and B). The abundance of *PCSI* transcript in RNAi protoplasts decreased by 70% and 90% when 5  $\mu\text{g}$  and 10  $\mu\text{g}$  of dsRNA<sub>PCSI</sub>, respectively, were used for transfection (Fig. 4B). Because transfection of 10  $\mu\text{g}$  of dsRNA<sub>PCSI</sub> caused the most potent gene-silencing effect, we used 10  $\mu\text{g}$  of dsRNAs for transfection in subsequent studies.

### **RNAi Effects in Protoplasts Last at Least 96 h**

We next determined what the onset of RNAi effects was, how long the RNAi effects



would last, and how long protoplasts would stay alive in our assays. We incubated mock- and dsRNA<sub>PCSI</sub>-transfected protoplasts in W5 media and analyzed the abundance of *PCSI* transcript by RT-PCR at specific time points. We determined that the abundance of *PCSI* transcript in mock-transfected protoplasts remained constant (Fig. 4C). In contrast, RNAi effects in dsRNA<sub>PCSI</sub>-transfected protoplasts were observed within 24 h of transfection, and silencing effects persisted for at least 96 h (Fig. 4C). The approximately 90% decrease in *PCSI* transcript abundance was observed after 72 h of transfection. After 96 h, however, due to the transient nature of dsRNA-induced RNAi in protoplasts, the abundance of *PCSI* became more prominent but was still 75% lower in comparison with mock-transfected protoplasts (Fig. 4C).

These studies demonstrated that RNAi effects in protoplasts were triggered as early as 24 h post-transfection and lasted at least 96 h, thus allowing sufficient time for subsequent functional assays. From then on, we analyzed RNAi effects in protoplasts after 48 h of transfection, unless indicated otherwise.

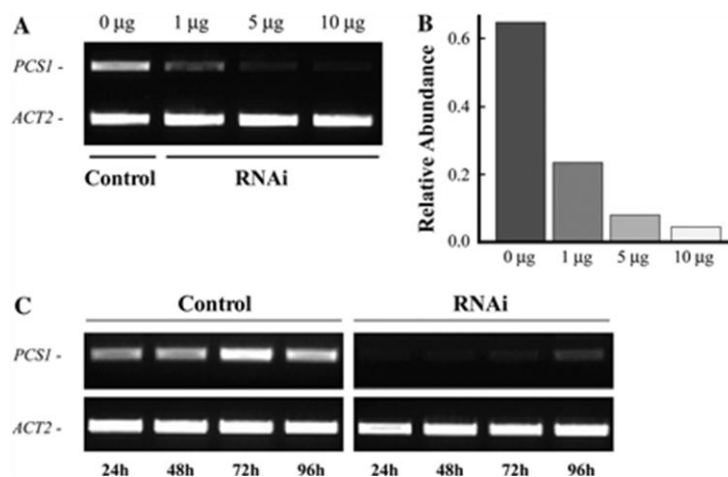


**Figure 4.** Dose and time dependence of transient RNAi silencing of *PCSI* in protoplasts. **A**, Protoplasts were transfected with 1, 5, or 10 µg of dsRNA against *PCSI* (RNAi) or with water (Control) and incubated for 24 h in the dark. Silencing of *PCSI* in dsRNA- and mock-transfected protoplasts was analyzed by RT-PCR. The representative RT-PCR results of three independent transfection events are

shown. **B**, Relative abundance of *PCSI* transcript on the gel in A. Relative abundance was normalized to the level of the transcript of *ACT2* using *GelQuant* software. **C**, RT-PCR analysis of the time dependence of RNAi silencing of *PCSI* in protoplasts. Protoplasts were transfected with 10  $\mu\text{g}$  of dsRNA against *PCSI* (RNAi) or with water (Control). Control and RNAi protoplast samples were collected at indicated time points and analyzed by RT-PCR for the abundance of *PCSI* transcript. *ACT2* was amplified as a control for amount of a template.

### **Gene-Specific or Multiple Gene Interference of Expression of *Arabidopsis* Genes in Protoplasts by RNAi**

Here, we sought to establish if transfecting dsRNA that targets sequences specific or shared among members of multigene family would affect expression of individual genes or several genes at the same time. To select a multigene family for these studies, we used the following criteria: (1) the multigene family must contain a relatively small number of members; (2) several genes of the multigene family must share a high degree of sequence similarity but also must be divergent from other family members; and (3) the expression levels of members of the gene subfamily must be well established. Using these criteria, we selected the hexokinase gene family in *Arabidopsis*, consisting of six members: *HXK1*, *HXK2*, and *HXK3* (for *Arabidopsis* hexokinases 1, 2, and 3), and *HKL1*, *HKL2*, and *HKL3* (*Arabidopsis* hexokinase-like proteins 1, 2, and 3; Karve et al., 2008). Among these, *HXK2* shares 85% amino acid sequence identity with *HXK1*, whereas other family members are more divergent (Karve et al., 2008). These features of the *HXK* family members allowed us to assay the gene-specific and simultaneous interference with the expressions of *HXK1* and *HXK2* in protoplasts by targeting sequences that are unique or shared by these genes.

To silence *HXK1* and *HXK2* simultaneously, as a template for in vitro dsRNA synthesis we selected a part of the coding sequence of *HXK1*, which shares 83% identity with *HXK2* but is distinct from other family members (Fig. 5A). RT-PCR

analysis of transcript abundance of hexokinase gene family members from mock- and dsRNA<sub>HXK1</sub>-transfected protoplasts established that RNAi against sequences that are shared between *HXK1* and *HXK2* depleted the abundance of transcripts of both genes but did not affect expression of other family members (Fig. 5B). When abundance of *HXK1* and *HXK2* transcripts after RT-PCR analysis was normalized to the level of the actin gene, *ACT2*, a 54% and a 46% depletion, respectively, of corresponding transcripts was observed, while abundance of others remained at the level of the mock-transfected protoplasts (not shown) Because protoplasts were isolated primarily from *Arabidopsis* leaves, whereas *HKL3* is expressed exclusively in *Arabidopsis* flowers (Karve et al., 2008), this gene was not amplified by RT-PCR and was not analyzed here. Our data indicated that we can silence genes simultaneously in protoplasts by targeting sequences that are shared among family members.

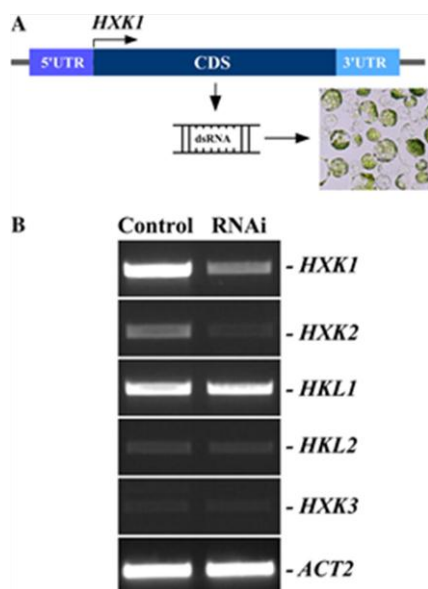


**Figure 5.** Simultaneous interference with the expression of *HXK1* and *HXK2* in protoplasts by RNAi. **A**, dsRNA corresponding to the coding sequence of *HXK1* was synthesized in vitro and delivered into protoplasts. Given the high sequence identity and similarity between *HXK1* and *HXK2* genes, dsRNA against *HXK1* is also predicted to target *HXK2*. **B**, RT-PCR analysis of members of hexokinase gene family. Mock-transfected protoplasts (Control) and dsRNA-transfected protoplasts (RNAi) were collected for RT-PCR analysis after 24 h of transfection. *ACT2* was amplified as a control for amount of a template. 5'-UTR and 3'-UTR are 5'- and 3'-end untranslated regions of *HXK1*, while CDS denotes the coding sequence of *HXK1*.

To test if RNAi against unique sequences of *HXK1* and *HXK2* would interfere with the expression of these genes in protoplasts individually, we selected their 3'-

untranslated regions (UTRs) as templates for in vitro dsRNA synthesis (Fig. 6A). RT-PCR analysis of the abundance of *HXK1* and *HXK2* transcript in mock-, dsRNA<sub>UTRHXK1</sub>-, or dsRNA<sub>UTRHXK2</sub>-transfected protoplasts established that the gene-specific RNAi-mediated silencing can be achieved in protoplasts by targeting the gene-unique, 3'-UTR sequences (Fig. 6B). Transfection of protoplasts with dsRNA<sub>UTRHXK1</sub> depleted the abundance of *HXK1* but not of *HXK2*, whereas transfection of protoplasts with dsRNA<sub>UTRHXK2</sub> depleted the abundance of *HXK2* but not of *HXK1* (Fig. 6B).

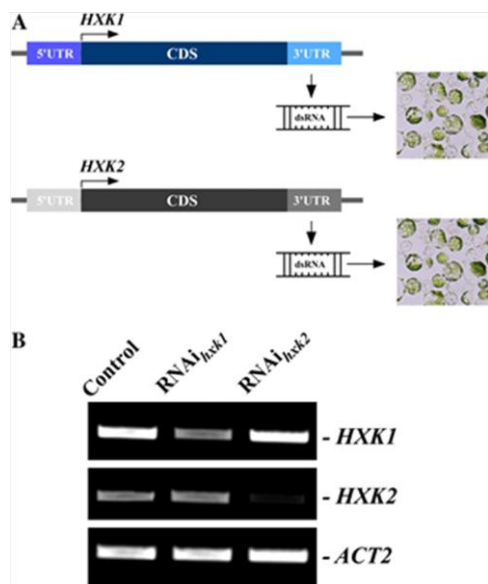


**Figure 6.** Gene-specific interference with the expression of *HXK1* and *HXK2*. **A**, dsRNAs corresponding to the 3'-UTR regions of *HXK1* and *HXK2* genes were synthesized in vitro and transfected into protoplasts to interfere with the expression of *HXK1* or *HXK2*. **B**, RT-PCR analysis of *HXK1* and *HXK2* after RNAi against 3'-UTR regions of *HXK1* or *HXK2* genes. Mock-transfected protoplasts (Control) and dsRNA-transfected protoplasts (RNAi<sub>hxk1</sub> and RNAi<sub>hxk2</sub>) were collected for RT-PCR analysis after 24 h of transfection. *ACT2* was amplified as a control for amount of a template.

### Generation of a Single, PCR-Linked Template for dsRNA Synthesis Targeting of Two Genes Simultaneously

In some cases, for analysis of interactions of different pathways, it is necessary to silence several genes from these pathways simultaneously. This can be achieved by cotransfection of protoplasts with dsRNAs against 3'-UTR for the selected genes. However, cotransfection will result in mutual dilution of individual dsRNAs and will

decrease individual dsRNA to protoplast ratios, and, because the gene silencing in protoplasts depends on the dose of transfected dsRNA (Fig. 4), will decrease the potency of RNAi-silencing effects. In addition, cotransfection of two or more dsRNAs imposes a difficulty in accessing the transfection efficiency of cotransfected dsRNAs. To circumvent this, we ligated 3'-UTR sequences by PCR to obtain a single, hybrid template for in vitro dsRNA synthesis (Fig. 7A). We used *HXK1* and *HXK2* genes as model genes, because we have already established that we can interfere with their expression simultaneously and individually (Fig. 6). We transfected protoplasts with 10  $\mu$ g of the hybrid dsRNA<sub>UTRHXK1-UTRHXK2</sub>. RT-PCR analysis revealed that transfection of protoplasts with hybrid dsRNA<sub>UTRHXK1-UTRHXK2</sub> decreased the abundance of *HXK1* and *HXK2* transcripts simultaneously (Fig. 7B). As expected, expression of other family members was not affected (Fig. 7B). Comparison of the level of the suppression of *HXK1* and *HXK2* expression by different sources of dsRNAs (Table 2) demonstrated that the more potent RNAi silencing was achieved when protoplasts were transfected with the linked dsRNA<sub>UTRHXK1-UTRHXK2</sub>. When abundance of *HXK1* and *HXK2* transcripts were normalized to the level of *ACT2*, 1.3- and 2-fold more potent suppression of *HXK1* and *HXK2* expression, respectively, was observed when protoplasts were transfected with the hybrid dsRNA<sub>UTRHXK1-UTRHXK2</sub> than when transfected with dsRNA against sequence that is shared between both family members or, in the case of *HXK1*, when transfected with dsRNA against *HXK1* 3'-UTR (Table 1). These data show that transfection of a hybrid dsRNA against UTRs of several genes is a powerful approach for their simultaneous silencing.

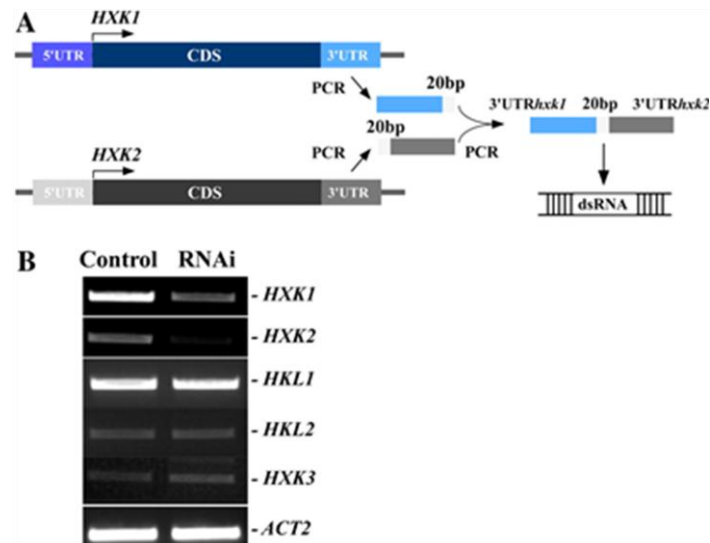


**Figure 7.** Gene-specific and simultaneous interference with the expression of *HXK1* and *HXK2* using PCR-linked UTR regions as dsRNA templates. **A**, DNA fragments corresponding to 3'-UTR regions of *HXK1* and *HXK2* were PCR amplified, and, in the second round of PCR, were linked with a 20-bp linker (20 bp). The resulting PCR product encompassing 3'-UTR regions of both *HXK1* and *HXK2* genes was used as a template for in vitro dsRNA synthesis. **B**, RT-PCR analysis of the members of the *HXK* gene family after RNAi using the hybrid dsRNA, synthesized from a template described in A. Mock-transfected protoplasts (Control) and dsRNA-transfected protoplasts (RNAi) were collected for RT-PCR analysis after 24 h of transfection.

**Table 1.** Comparison of the relative abundance of transcripts in protoplasts after RNAi using different DNA templates. Relative abundance of transcripts after RT-PCR was normalized to the level of actin, *AtACT2*, gene using *GelQuant* software.

DNA templates for dsRNA synthesis	Size of dsRNA	Percentage of depletion of relative transcripts abundance after RNAi	
		<i>AtHXK1</i>	<i>AtHXK2</i>
1 cDNA of <i>AtHXK1</i>	524bp	53	46
2 3'UTR of <i>AtHXK1</i>	281bp	55	0
3 3'UTR of <i>AtHXK2</i>	207bp	0	92
4 3'UTR of <i>AtHXK1</i> +3'UTR of <i>AtHXK2</i>	500bp	73	92

## **RNAi in Protoplasts Is Suitable for Functional Analysis of Plant Genes**

The studies described above have established that the specific or simultaneous depletion of gene transcripts is successfully achieved in protoplasts by transfection of in vitro-synthesized dsRNAs. We also demonstrated that RNAi effects lasted at least 96 h. However, is RNAi depletion of transcripts of endogenous genes accompanied by a decrease in a polypeptide level? Can we use RNAi in protoplasts to study the function of silenced genes? Are RNAi phenotypes in protoplasts comparable with those observed in genetic mutants? To address these questions, we selected an RNAi-targeted gene using the following criteria: (1) the RNAi-targeted gene should be a single-copy gene with the established expression level; (2) antibody for the analysis of the corresponding polypeptide by western-blot analysis should be available; (3) tests for analysis of the functional activity of the encoded polypeptide should be well established and simple; and (4) mutant alleles with well-characterized phenotypes should be available.

Using these criteria, we selected *ECSI* (alias *cad2*) encoding  $\beta$ -glutamylcysteine synthase ( $\beta$ -ECS) as an RNAi target. ECS1 is a key enzyme in biosynthesis of the ubiquitous tripeptide GSH ( $\beta$ -Gly-Cys-Gly). Therefore, its functional activity in RNAi protoplasts can be evaluated by assaying their GSH content (Cobbett et al., 1998). In addition, the expression of *ECSI* has been established, antibodies are commercially available, and the *cad2-1* mutant allele of *ECSI* has been generated (Cobbett et al., 1998). It has also been determined that the decrease in the activity of ECS1 of *cad2-1* is accompanied by a 55% decrease in cellular GSH content (Cobbett et al., 1998).

Because *ECSI* is a single-copy gene, we selected 548 bp of its coding sequence as an RNAi target, PCR amplified it from the *Arabidopsis* cDNA library, synthesized dsRNA<sub>*ECSI*</sub> in vitro, and transfected it into protoplasts. RT-PCR analysis of mock-

and dsRNA<sub>ECSI</sub>-transfected protoplasts after 48 h of transfection established that the abundance of *ECSI* transcript is substantially decreased in RNAi, but not in control, protoplasts (Fig. 8A). Importantly, RNAi in protoplasts not only depleted the abundance of *ECSI* transcript but substantially decreased the level of the corresponding polypeptide (Fig. 8B). As determined by SDS/PAGE and western-blot analysis, a single polypeptide species that reacted with the rabbit polyclonal anti-ECS1 antibody was presented in lysates from control and dsRNA<sub>ECSI</sub>-transfected protoplasts. However, in comparison with control protoplasts, the level of the polyclonal anti-ECS1 antibody-reactive polypeptide was 3-fold lower in dsRNA<sub>ECSI</sub>-transfected protoplasts (Fig. 8B).

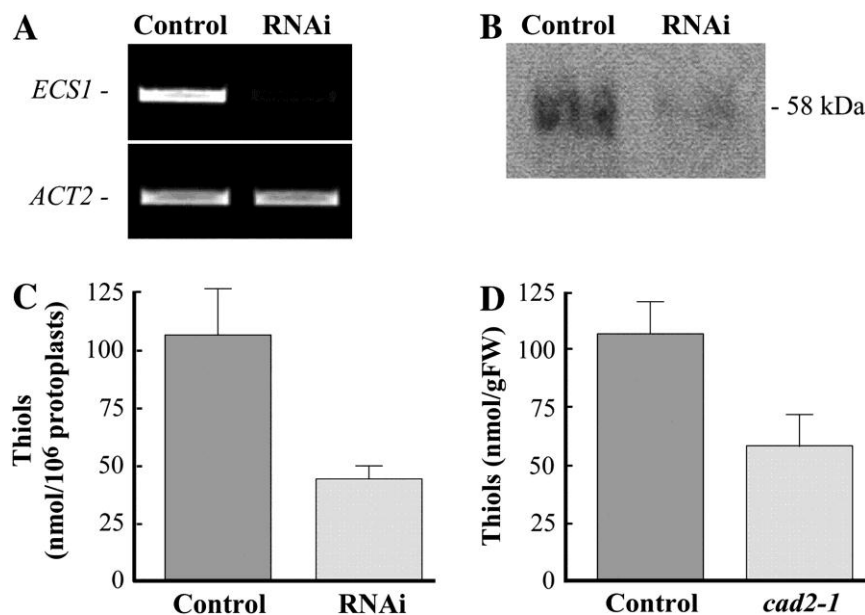


**Figure 8.** RNAi silencing of ECS1 in protoplasts interferes with the expression of *ECSI* RNA and polypeptide, and decreases the ability of protoplasts to accumulate GSH. **A**, RT-PCR analysis of the abundance of *ECSI* in protoplasts transfected with dsRNA<sub>ECSI</sub> (RNAi) or water (Control). **B**, SDS-PAGE and western-blot analysis of ECS1 polypeptide in mock-transfected (Control) or RNAi protoplasts (RNAi). **C**, RP-HPLC analysis of GSH content in protoplasts transfected with water (Control) or with dsRNA<sub>ECSI</sub> (RNAi). Protoplasts were collected and analyzed after 48 h of transfection.



**D**, RP-HPLC analysis of GSH content in wild-type *Arabidopsis* (Control) and *cad2-1* mutants (*cad2-1*). FW, Fresh weight.

We then asked if RNAi against *ECS1* would affect the GSH content of protoplasts. Reverse-phase HPLC (RP-HPLC) analysis of nonprotein thiol compounds in mock-transfected protoplasts revealed a peak of GSH, the chromatographic properties of which were indistinguishable from commercially available GSH standard (Sigma-Aldrich). The aggregate GSH content in control protoplasts was  $106.9 \pm 19.9$  nmol/10<sup>6</sup> protoplasts (Fig. 8C). The GSH content of RNAi protoplasts was 2.5-fold lower and was consistent with the fold-decrease of ECS1 polypeptide (Fig. 8, B and C). These data showed that transfection of dsRNA into protoplasts not only affected the transcript level but also the abundance of the translated polypeptide and, as judged by the decrease in accumulation of the end product of the encoded enzymatic activity of the RNAi targeted gene, interfered with the gene's function.

Importantly, the fold-decrease in the GSH content resulting from RNAi silencing of *ECS1* in protoplasts is comparable with that observed in *cad2-1* mutants bearing a 6-bp deletion in the sixth exon of the *ECS1* gene (Cobbett et al., 1998). The content of GSH in cell-free extracts from *cad2-1* mutants was 1.8-fold lower than in extracts from wild-type *Arabidopsis* (Fig. 8D). Taken together, our data demonstrate that RNAi can be used as a versatile approach to study gene function in protoplasts.

## CONCLUSION AND FUTURE PERSPECTIVES

In this manuscript, we presented data demonstrating that RNAi can be effectively used for functional analysis of genes in protoplasts. We substantiated the results of An et al.

(2003, 2005) by presenting the following findings. First, RNAi-mediated silencing was induced in protoplasts by transfecting in vitro-synthesized dsRNA. This circumvented the necessity to clone dsRNA into expression vectors, which can be time consuming and labor intensive, especially for the genome-wide studies. Second, RNAi effects in protoplasts depended on a dose of transfected dsRNA. Third, RNAi effects in protoplasts lasted at least 96 h, allowing sufficient time for subsequent functional analysis. Fourth, RNAi in protoplasts silenced individual genes as well as multiple members of gene families simultaneously. Fifth, transfecting protoplasts with dsRNAs possessing linked 3'-UTRs of two genes that are members of a multigene subfamily silenced both genes simultaneously, but did not interfere with the expression of other family members. In doing so, we circumvented the necessity to cotransfect protoplasts with two dsRNAs against targeted genes, avoided the inevitable mutual dilution of dsRNAs in the transfection media, a possibility of different transfection efficiencies of two dsRNAs, and thus achieved potent gene silencing of both genes simultaneously. We expect that this approach will be especially valuable for the analysis of interactions among distinct pathways when it will be necessary to silence genes from two (or more) families that share high sequence similarity. Sixth, transfection of dsRNA depleted the abundance not only of the transcript of a targeted gene but also of the corresponding polypeptide. This was a significant finding, because protoplasts are nongrowing cells that have a limited lifespan. Therefore, if the studied gene is not induced under experimental condition, RNAi silencing of its function in protoplasts will be contingent on the turnover rates of the corresponding polypeptide. In the case of ECS1, we achieved a 72% decrease in the level of

polypeptide after 48 h of protoplast transfection with dsRNA<sub>ECS1</sub>, whereas in our assays, protoplasts were viable, and RNAi-depletion of a gene transcript lasted even longer, for 96 h. Therefore, this method should be appropriate for functional studies of even relatively stable proteins and is particularly appropriate for studies of conditionally inducible genes. Seventh, transient RNAi knockdown of *ECS1* in protoplasts led to a loss-of-ECS1 function: protoplasts transfected with dsRNA<sub>ECS1</sub> accumulated 60% less of the end product of ECS1 enzymatic activity, GSH. Eighth, RNAi in protoplasts yields results comparable with those of genetic mutants for the same gene. Ninth, we adapted protoplast isolation protocol to 14-d-old seedlings. Therefore, the described procedure is rapid; 20 d are sufficient for analysis. This time includes growing *Arabidopsis*, isolation of protoplasts, in vitro dsRNA synthesis, transfection of dsRNA into protoplasts, and analysis of phenotypes. Taking together, RNAi can silence gene functions in protoplasts, providing a rapid and a cost-efficient tool for reverse-genetic studies.

Limitations of using RNAi in protoplasts for functional analysis of genes include potential artifacts that might emerge due to the removal of plant cell walls, disruption of cell-to-cell communications, and the artificial protoplast culture conditions. Clearly, phenotypes observed in RNAi protoplasts have to be verified and complemented by studies in planta. Nevertheless, RNAi in protoplasts can be used as a rapid and affordable initial screen for selection of candidate genes for subsequent studies in planta using available resources such as transposon/T-DNA insertion lines or RNAi transgenic plants. While it is unlikely that RNAi in protoplasts will be appropriate for studies of genes involved in developmental processes, it presents an

excellent approach for biochemical characterization of proteins with enzymatic activities (e.g. ECS1; Fig. 8) with many of them having no experimentally assigned functions. This method is particularly suitable for deciphering components of metabolic pathways and establishing of metabolic networks and, perhaps, can be adapted to high-throughput metabolomics. Because protoplasts can be isolated from different sources, this approach can be used to study tissue-specific biochemical processes in *Arabidopsis* and other plant species.

RNAi in protoplasts can be also used as an initial step for identifying genes required for a particular function. For instance, this approach is particularly valuable if gene silencing is anticipated to result in a conditional lethal phenotype (e.g as for genes required for tolerance to xenobiotics, cold, heat). In this case, combining protoplast viability assays using fluorescent vital dyes (e.g. propidium iodide, SYTOX Orange, etc.) with the fluorescence-activated cell sorting analyses will provide a powerful and rapid approach for selecting gene candidates required for tolerance to applied stress.

Another interesting example involves cell wall metabolism. It is well documented in different plant species that protoplasts regenerate their cell walls (Burgess and Fleming, 1974; Wenck and Marton, 1995); hence, RNAi in protoplasts will greatly assist in discovery and analyses of genes involved in cell wall biogenesis.

To conclude, RNAi in protoplasts complements existing approaches for functional analyses of genes as it provides the time-efficient and affordable initial step for selecting of genes of interest for further in depth studies in planta. The recent advances in sequencing of many plant genomes provide information for targeted and systematic screens of genes and gene families, awaiting development of novel

functional genetic approaches, such as presented here. Therefore, adopting RNAi in protoplasts to a high-throughput, genome-wide phenotyping technology will greatly facilitate assigning functions to unknown genes not only in *Arabidopsis* but also in other plant species.

## MATERIALS AND METHODS

### **Plant Material and Growth Conditions**

Wild-type *Arabidopsis thaliana* Columbia ecotype seeds were sterilized in 70% ethanol, 1.8% bleach solution (made up by diluting a household Clorox containing 6% sodium hypochlorite), and 0.1% Tween 20. Seeds were sown on 1/2 Murashige and Skoogmedium, pH 5.7, adjusted with 1 N KOH, supplemented with 1% Sucrose and 0.7% agar and then kept for 24 h at 4 °C in the dark for stratification. Seedlings were germinated and grown in an 8-h-light/16-h-dark photoperiod (at a photosynthetic photon flux density of 250  $\mu\text{mol m}^{-2} \text{s}^{-1}$ ) at a 23 °/19 °C light/dark temperature regime and 75% relative humidity.

### **Isolation of Protoplasts from *Arabidopsis* Seedlings**

Protoplasts were isolated from *Arabidopsis* seedlings using a modified method of Chen and Halkier (2000). Briefly, 2 g of 14-d-old *Arabidopsis* seedlings were sliced with a razor blade to 1-mm strips in 15 mL of filter-sterilized TVL (0.3 M sorbitol, 50 mM  $\text{CaCl}_2$ ) solution. Twenty milliliters of enzyme solution (0.5 M Suc, 10 mM MES-KOH, pH 5.7, 20 mM  $\text{CaCl}_2$ , 40 mM KCl, 1% Cellulase [Onozuka R-10], 1% Macerozyme [R10]) were added to the sliced seedlings, and the mixture was agitated

at 35 rpm in the dark at room temperature. After 16 to 18 h, the released protoplasts were sieved through eight layers of cheesecloth, pre-wet in W5 solution (0.1% [w/v] Glc, 0.08% [w/v] KCl, 0.9% [w/v] NaCl, 1.84% [w/v] CaCl<sub>2</sub>, 2 mM MES-KOH, pH 5.7) and transferred into 50-mL Falcon centrifuge tubes. Protoplasts and plant debris retained on the cheesecloth were gently sieved-through one more time by washing the cloth with 15 mL of W5 solution. Sieved-through protoplasts were combined in a 50-mL Falcon centrifuge tube, overlaid with 10 mL of W5 solution, and centrifuged for 7 min at 100g. Protoplasts were collected at the interface of enzyme and W5 solutions (Fig. 1A). The protoplast yield was evaluated by cell counting with a hemocytometer. Using this procedure, we typically harvested 5 to  $10 \times 10^6$  protoplasts from 1 g of fresh seedlings.

### **In Vitro Synthesis of dsRNA**

DNA templates were synthesized by PCR from *Arabidopsis* cDNA and engineered to contain the minimal T7-RNA polymerase promoter sequence (TAATACGACTCACTATAGGG) on both 5' and 3' ends (Sastry and Ross, 1997). Primers used to amplify DNA of targeted genes are described in Table 2. The PCR conditions were as follows: denaturing step at 94 °C for 3 min followed by 30 cycles of 94 °C for 45 s, 57 °C for 30 s, 72 °C for 45 s, and a final extension at 72 °C for 10 min. dsRNAs were synthesized in vitro using the Ambion MEGAscript T7 kit (Ambion) according to the manufacturer's recommendation with the exception that in vitro transcription was allowed to proceed for at least 6 h. DNA templates were removed with the RNases-free DNase (Invitrogen), dsRNAs were purified with the RNAeasy

kit (Qiagen), reconstituted with deionized, sterile water, and quantified using UV spectrophotometry. The standard output of dsRNA in a 20- $\mu\text{L}$  reaction was between 100 and 200  $\mu\text{g}$ .

### **Transfection of Protoplasts with Plasmid DNA or dsRNAs**

Protoplasts were transfected using a procedure adopted from Yoo et al. (2007). Briefly, protoplasts collected at interface of the enzyme solution and the W5 solution and were washed three times by reconstituting in W5 solution and pelleting at 100g for 2 min. After the third wash, protoplasts were resuspended in MMG solution (4 mM MES-KOH, pH5.7, 0.4 M mannitol, 15 mM  $\text{MgCl}_2$ ) to reach a final concentration of 5 to  $10 \times 10^5$  protoplasts/mL. Aliquots of protoplasts (100  $\mu\text{L}$ ;  $0.5\text{--}1.0 \times 10^5$  protoplasts/ml) were transferred into a 2-mL round-bottom microcentrifuge tube and mixed gently with the plasmid DNA (6  $\mu\text{g}$  in 10  $\mu\text{L}$ ) or with dsRNA (1, 5, or 10  $\mu\text{g}$  in 10  $\mu\text{L}$ ). In control transfections, we omitted DNA or RNA and instead used equivalent volumes of deionized, sterile water (mock-transfection). Transfection was initiated by the addition of 110  $\mu\text{L}$  of PEG-calcium solution (40% PEG-4000, 0.2 M mannitol, 100 mM  $\text{CaCl}_2$ ). Protoplasts were mixed with PEG-calcium solution by gently tapping the tube and incubating for 5 min at room temperature. Transfection was terminated by diluting the mixture with 600  $\mu\text{L}$  of W5 solution. Transfected protoplasts were collected by centrifugation for 2 min at 100g, resuspended in 1 mL of W5 solution, and kept in the dark for the time periods indicated in the figures prior to further analyses.

**Table 2.** List of oligos that were used to amplify DNA templates for *in vitro* dsRNA synthesis.

Gene		Primers (5'-3')
<i>AtPCSI</i>	Forward	GCGCCTAATACGACTCACTATAGGGAGAGAACCTCTGGAAGTAGTGAAGGAA
	Reverse	GCGCCTAATACGACTCACTATAGGGAGACTGTGAACCTACAAGACGAGGAAC
<i>GFP</i>	Forward	GCGCCTAATACGACTCACTATAGGGAGAGCCAACACTTGTCACTACTTTCTC
	Reverse	GCGCCTAATACGACTCACTATAGGGAGACATGTGGTCTCTCTTTTCGTTG
<i>γ-ECSI</i>	Forward	TAATACGACTCACTATAGGGAGATCATGCCAAAGGGGAGATAC
	Reverse	TAATACGACTCACTATAGGGAGACTCTTCAACCGAACCTCTGG
<i>HXK1</i> (CD)	Forward	AAGCTTTAATACGACTCACTATAGGGCTGCTTCCAAAATCAGGAGAAA
	Reverse	GGATCCTAATACGACTCACTATAGGGGTAATGCTCAAACAATCCACCA
<i>HXK1</i> (3'UTR)	Forward	GCGCCTAATACGACTCACTATAGGGAGATCGCTATCAGAAAACGCCTAA
	Reverse	GCGCCTAATACGACTCACTATAGGGAGACTCCAGTGAAGTGAGCTTTGA
<i>HXK2</i> (3'UTR)	Forward	GCGCCTAATACGACTCACTATAGGGAGATTGTTTTGCCGTTAGGGTTT
	Reverse	GCGCCTAATACGACTCACTATAGGGAGAACAACATTGGCTGGTCGTTT
<i>HXK1</i> (3'UTR)+Linker	Forward	GCGCCTAATACGACTCACTATAGGGAGATCGCTATCAGAAAACGCCTAA
	Reverse	GGACCGTCACAATAGTACATAGAGAGGCCTCCAGTGAAGTGAGCTTTGA
<i>HXK2</i> (3'UTR)+Linker	Forward	GCCTCTCTATGTACTATTGTGACGGTCCTTGTGTTTTGCCGTTAGGGTTT
	Reverse	GCGCCTAATACGACTCACTATAGGGAGAACAACATTGGCTGGTCGTTT

### RT-PCR Analysis of Gene Expression in RNAi Protoplasts

RNAi and control protoplasts ( $10^5$  cells/mL) were collected by centrifugation for 2 min at 100g. Total RNA was extracted with TRIzol reagent (Invitrogen, 1 mL/ $10^5$  protoplasts) following the manufacturer's protocol. RNA aliquots (10  $\mu$ L) were subjected to RT with M-MuLV Reverse Transcriptase (New England Biolabs) followed by PCR analysis using GoTag Green Master mix (Promega). PCR conditions were as follows: denaturing at 95 °C for 2 min, followed by 30 cycles of 95 °C for 30 s, 55 °C for 30 s, 72 °C for 60 s, and a final extension at 72 °C for 5 min. Primers that were used for RT-PCR analyses are described in Table 3. The effectiveness of RNAi was



evaluated by analysis of aliquots from RT-PCR reactions on a 1.2% gel and comparing the relative abundance of transcripts of RNAi-targeted genes to the level of the *Arabidopsis* actin gene, *ACT2*, using the *GelQuant* software, version 2.7 (DNR Bio-Imaging Systems).

**Table 3.** List of oligos that were used for RT-PCR analyses.

Genes		Oligos (5'-3')
<i>AtPCS1</i>	Forward	GCTGGATCGAAATAGCCAAG
	Reverse	GCTTCAGGACCACATTCACA
<i>ECS1</i>	Forward	ATTGCCTATCTTGCCTCTGG
	Reverse	ATCCGTTTGGCTTTCCTTCT
<i>HXK1</i>	Forward	GGACGTGTTTTGGCTATCCTC
	Reverse	GAAATCCAGCGTGTGATCAA
<i>HXK2</i>	Forward	GACAGAGTACGACCACTCTCTAGATG
	Reverse	TTAACTTGTTTCAGAGTCATCTTCAAG
<i>HXK3</i>	Forward	AGGAAAACGGGTCCGATTCA
	Reverse	TGCTTCTCCCGCTCGTGAT
<i>HXK4</i>	Forward	GGGCTTTATCCTTTGGACATTT
	Reverse	TCATACGGATGGTATTGTTTGAAC
<i>HXK5</i>	Forward	CCAATTACATCGTGATGTCCG
	Reverse	GCGGAAGAATCTTAGAGAACCC
<i>HXK6</i>	Forward	GAACTATTACTGTTACGTGGGACG
	Reverse	CAGTCTCCCGTTCTTCGGAT

### Western-Blot Analysis of ECS1 in RNAi Protoplasts

RNAi and control protoplasts ( $10^5$  cells/mL) were collected by centrifugation at 100g for 2 min and lysed by resuspension in 10  $\mu$ L of the Laemmli buffer. Protoplast proteins were denatured at 50 °C for 10 min, separated by SDS-PAGE on 10% (w/v) gels, and electrotransferred in Towbin buffer (Towbin et al., 1979) to a nitrocellulose filter. The nitrocellulose blots were probed with the primary rabbit polyclonal anti-ECS antibody (1:1,000 dilution; Agrisera) and with the secondary HP-conjugated anti-rabbit antibody (1:2,500; GE Healthcare). Immunoreactive bands were visualized with

LumiGLO system (KPL).

### **Analysis of GSH Content**

GSH content was analyzed in RNAi and control protoplasts and in plant extracts by a combination of RP-HPLC and thiol quantitation with Ellman's reagent as described (Vatamaniuk et al., 2000). Aliquots of protoplasts corresponding to  $10^6$  cells or cell-free plant extracts (10–20  $\mu\text{g}$  of protein) were made 5% (w/v) with 5-sulfosalicylic acid and centrifuged before aliquots of the supernatant (50  $\mu\text{L}$ ) were loaded onto an Econosphere C18, 150 x 4.6-mm RP-HPLC column (Alltech). The column was developed with a linear gradient of water, 0.05% (v/v) phosphoric acid, and 17% (v/v) acetonitrile, 0.05% (v/v) phosphoric acid at a flow rate of 1 mL/min. For the quantitation of GSH, thiols were estimated spectrophotometrically at 412 nm by reacting aliquots (500  $\mu\text{L}$ ) of the column fractions with 0.8 mM 5,5'-dithiobis(2-nitrobenzoic acid) (500  $\mu\text{L}$ ) dissolved in 250 mM phosphate buffer, pH 7.6 (Ellman, 1959). Commercially available GSH (Sigma) was used as a RP-HPLC standard and for calibration.

### REFERENCES

- Allen RS, Millgate AG, Chitty JA, Thisleton J, Miller JAC, Fist AJ, Gerlach WL, Larkin PJ** (2004) RNAi-mediated replacement of morphine with the nonnarcotic alkaloid reticuline in opium poppy. *Nat Biotechnol* **22**: 1559–1566
- Alonso JM, Stepanova AN, Leisse TJ, Kim CJ, Chen H, Shinn P, Stevenson DK, Zimmerman J, Barajas P, Cheuk R, et al**(2003) Genome-wide insertional mutagenesis of *Arabidopsis thaliana*. *Science* **301**: 653–657

- An CI, Sawada A, Fukusaki E, Kobayashi A** (2003) A transient RNA interference assay system using Arabidopsis protoplasts. *Biosci Biotechnol Biochem* **67**: 2674–2677
- An CI, Sawada A, Kawaguchi Y, Fukusaki E, Kobayashi A** (2005) Transient RNAi induction against endogenous genes in Arabidopsis protoplasts using in vitro-prepared double-stranded RNA. *Biosci Biotechnol Biochem* **69**: 415–418
- Arabidopsis Genomics Initiative** (2000) Analysis of the genome sequence of the flowering plant Arabidopsis thaliana. *Nature* **408**: 796–815
- Bai J, Binari R, Ni JQ, Vijayakanthan M, Li HS, Perrimon N** (2008) RNA interference screening in Drosophila primary cells for genes involved in muscle assembly and maintenance. *Development* **135**: 1439–1449
- Baulcombe D** (2004) RNA silencing in plants. *Nature* **431**: 356–363
- Bernstein E, Caudy AA, Hammond SM, Hannon GJ** (2001) Role for a bidentate ribonuclease in the initiation step of RNA interference. *Nature* **409**: 363–366
- Bezanilla M, Perroud PF, Pan A, Klueh P, Quatrano RS** (2005) An RNAi system in Physcomitrella patens with an internal marker for silencing allows for rapid identification of loss of function phenotypes. *Plant Biol (Stuttg)* **7**: 251–257
- Boutros M, Kiger AA, Armknecht S, Kerr K, Hild M, Koch B, Haas SA, Consortium HFA, Paro R, Perrimon N** (2004) Genome-wide RNAi analysis of growth and viability in Drosophila cells. *Science* **303**: 832–835
- Brodersen P, Sakvarelidze-Achard L, Bruun-Rasmussen M, Dunoyer P, Yamamoto YY, Sieburth L, Voinnet O** (2008) Widespread translational inhibition by plant miRNAs and siRNAs. *Science* **320**: 1185–1190
- Brodersen P, Voinnet O** (2006) The diversity of RNA silencing pathways in plants. *Trends Genet* **22**: 268–280

- Burgess J, Fleming EN** (1974) Ultrastructural observations of cell wall regeneration around isolated tobacco protoplasts. *J Cell Sci* **14**: 439–449
- Chen S, Halkier BA** (2000) Characterization of glucosinolate uptake by leaf protoplasts of *Brassica napus*. *J Biol Chem* **275**: 22955–22960
- Clemens JC, Worby CA, Simonson-Leff N, Muda M, Maehama T, Hemmings BA, Dixon JE** (2000) Use of double-stranded RNA interference in *Drosophila* cell lines to dissect signal transduction pathways. *Proc Natl Acad Sci USA* **97**: 6499–6503
- Cobbett C, Howden R, Rolls B** (1998) The glutathione-deficient, cadmium-sensitive mutant, *cad2-1* of *Arabidopsis thaliana* is deficient in gamma-glutamylcysteine synthetase. *Plant J* **16**: 73–78
- Cocking EC** (1960) A method for the isolation of plant protoplasts and vacuoles. *Nature* **187**: 962–963
- Ellman GL** (1959) Tissue sulfhydryl groups. *Arch Biochem Biophys* **82**: 70–77
- Fire A, Xu S, Montgomery MK, Kostas SA, Driver SE, Mello CC** (1998) Potent and specific genetic interference by double-stranded RNA in *Caenorhabditis elegans*. *Nature* **391**: 806–811
- Hamilton B, Dong Y, Shindo M, Liu W, Odell I, Ruvkun G, Lee SS** (2005) A systematic RNAi screen for longevity genes in *C. elegans*. *Genes Dev* **19**: 1544–1555
- Helliwell CA, Waterhouse PM, David R, Engelke AJJR** (2005) Constructs and methods for hairpin RNA-mediated gene silencing in plants. In DR Engelke, JJ Rossi, eds, *Methods in Enzymology*, Vol 392. Academic Press, San Diego, pp 24–35
- Kamath RS, Fraser AG, Dong Y, Poulin G, Durbin R, Gotta M, Kanapin A, Le Bot N, Moreno S, Sohrmann M, et al** (2003) Systematic functional analysis of the *Caenorhabditis elegans* genome using RNAi. *Nature* **421**: 231–237

- Karve A, Rauh BL, Xia X, Kandasamy M, Meagher RB, Sheen J, Moore BD** (2008) Expression and evolutionary features of the hexokinase gene family in *Arabidopsis*. *Planta* **228**: 411–425
- Kennerdell JR, Carthew RW** (1998) Use of dsRNA-mediated genetic interference to demonstrate that *frizzled* and *frizzled 2* act in the wingless pathway. *Cell* **95**: 1017–1026
- Miki D, Itoh R, Shimamoto K** (2005) RNA silencing of single and multiple members in a gene family of rice. *Plant Physiol* **138**: 1903–1913
- Sastry SS, Ross BM** (1997) Nuclease activity of T7 RNA polymerase and the heterogeneity of transcription elongation complexes. *J Biol Chem* **272**: 8644–8652
- Schwab R, Ossowski S, Riester M, Warthmann N, Weigel D** (2006) Highly specific gene silencing by artificial microRNAs in *Arabidopsis*. *Plant Cell* **18**: 1121–1133
- Smith NA, Singh SP, Wang MB, Stoutjesdijk PA, Green AG, Waterhouse PM** (2000) Gene expression: total silencing by intron-spliced hairpin RNAs. *Nature* **407**:319–320
- Stam M, de Bruin R, Kenter S, van der Hoorn RAL, van Blokland R, Mol JNM, Kooter JM** (1997) Post-transcriptional silencing of chalcone synthase in *Petunia* by inverted transgene repeats. *Plant J* **12**: 63–82
- Towbin H, Staehelin T, Gordon J** (1979) Electrophoretic transfer of proteins from polyacrylamide gels to nitrocellulose sheets: procedure and some applications. *Proc Natl Acad Sci USA* **76**: 4350–4354
- Travella S, Klimm TE, Keller B** (2006) RNA interference-based gene silencing as an efficient tool for functional genomics in hexaploid bread wheat. *Plant Physiol* **142**: 6–20
- Tzfira T, Tian GW, Lacroix B, Vyas S, Li J, Leitner-Dagan Y, Krichevsky A,**

- Taylor T, Vainstein A, Citovsky V** (2005) pSAT vectors: a modular series of plasmids for autofluorescent protein tagging and expression of multiple genes in plants. *Plant Mol Biol* **57**: 503–516
- Vatamaniuk OK, Mari S, Lu YP, Rea PA** (1999) AtPCS1, a phytochelatin synthase from *Arabidopsis*: isolation and in vitro reconstitution. *Proc Natl Acad Sci USA* **96**:7110–7115
- Vatamaniuk OK, Mari S, Lu YP, Rea PA** (2000) Mechanism of heavy metal ion activation of phytochelatin (PC) synthase: blocked thiols are sufficient for PC synthase-catalyzed transpeptidation of glutathione and related thiol peptides. *J Biol Chem* **275**: 31451–31459
- Vidali L, Augustine RC, Kleinman KP, Bezanilla M** (2007) Profilin is essential for tip growth in the moss *Physcomitrella patens*. *Plant Cell* **19**: 3705–22
- Waterhouse PM, Helliwell CA** (2003) Exploring plant genomes by RNA-induced gene silencing. *Nat Rev Genet* **4**: 29–38
- Waterhouse PM, Wang MB, Lough T** (2001) Gene silencing as an adaptive defence against viruses. *Nature* **411**: 834–842
- Wenck AR, Marton L** (1995) Large-scale protoplast isolation and regeneration of *Arabidopsis thaliana*. *Biotechniques* **18**: 640–643
- Wilson JA, Richardson CD** (2003) Induction of RNA interference using short interfering RNA expression vectors in cell culture and animal systems. *Curr Opin Mol Ther* **5**:389–396
- Worby CA, Simonson-Leff N, Dixon JE** (2001) RNA interference of gene expression (RNAi) in cultured *Drosophila* cells. *Sci STKE* **2001**: p11
- Wortman JR, Haas BJ, Hannick LI, Smith RK Jr, Maiti R, Ronning CM, Chan AP, Yu C, Ayele M, Whitelaw CA, et al** (2003) Annotation of the *Arabidopsis* genome. *Plant Physiol* **132**: 461–468

**Yoo SD, Cho YH, Sheen J** (2007) Arabidopsis mesophyll protoplasts: a versatile cell system for transient gene expression analysis. *Nat Protocols* **2**: 1565–1572

Other related publications:

7. **Zhai Z**, Jung HI, Vatamaniuk OK (2009). Isolation of protoplasts from tissues of 14-day-old seedlings of *Arabidopsis thaliana*. *J Vis Exp.*, 17; (30). pii: 1149. doi: 10.3791/1149.
8. Jung HI, **Zhai Z** and Vatamaniuk OK (2011). Direct Transfer of Synthetic Double-Stranded RNA into Protoplasts of *Arabidopsis thaliana*. In Kodama, Hiroaki and Komamine, Atsushi (Eds.), *RNAi and Plant Gene Function Analysis* (Vol.8) New York, U.S.A: Humana Press.